Master's thesis
Submitted: 15.08.2013

Photon gates in atomic ensembles

Ivan Iakoupov
Supervisors: Anders S. Sørensen and Darrick Chang

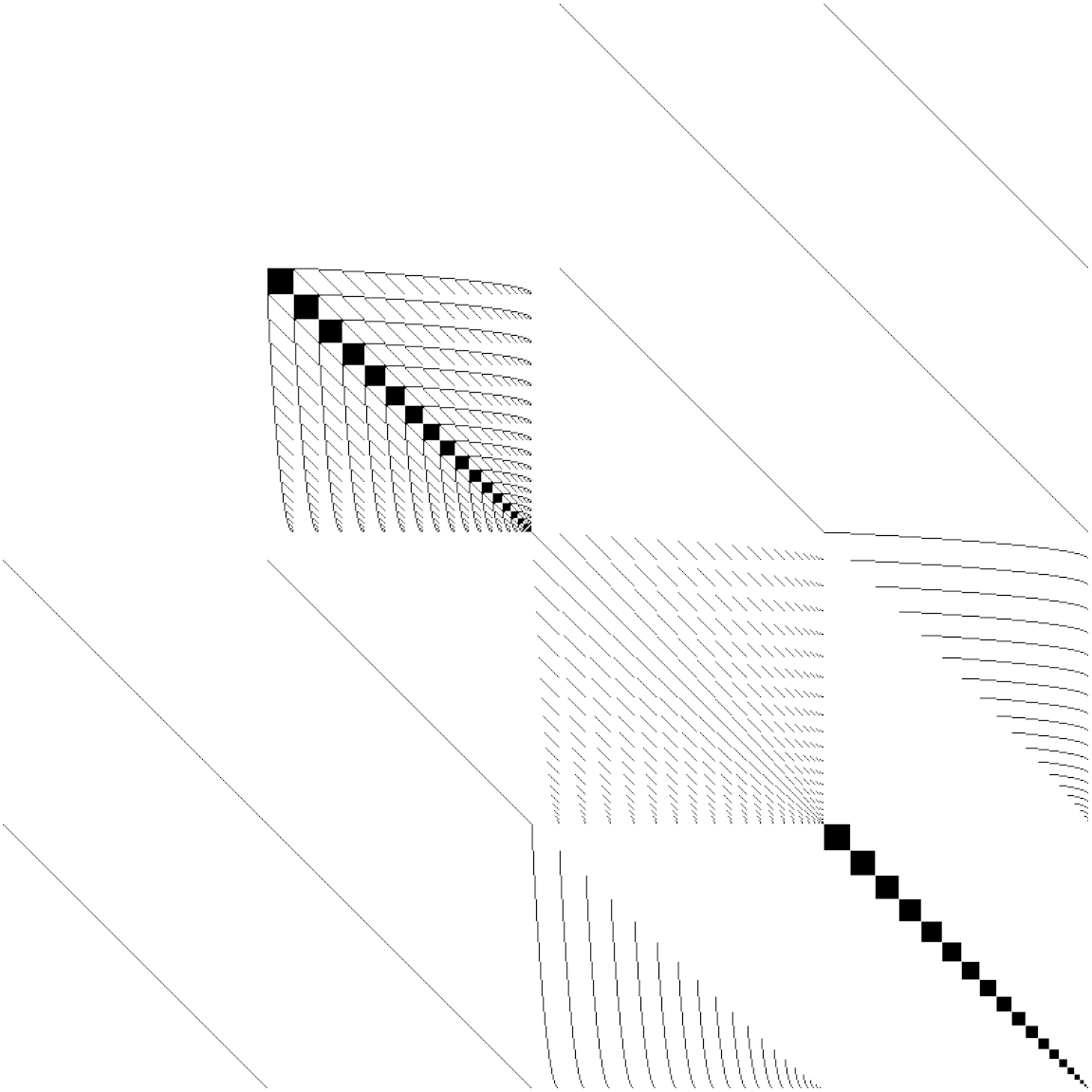

Abstract

Quantum computers operate with qubits, which are entities that can be in the state $|0\rangle$, state $|1\rangle$ or any superposition (linear combination) of those. One of the essential parts of a quantum computer is a controlled two-qubit gate. An example of such gate is the *controlled phase gate*, which imparts a phase of π (i.e. multiplies by -1) to the state, where both qubits are in $|1\rangle$. In this thesis we shall look at three different schemes to implement a controlled phase gate for qubits stored in photons. The photons are special in the sense that they normally do not interact with each other, which makes it hard to make controlled two-qubit gates with them. This is why the usual role of the photons in quantum computing is to carry quantum information over long distances instead of being the registers of a quantum computer that the quantum algorithms are run on directly. However, the single-qubit gates for photons work very well, and if an efficient two-qubit gate was constructed, the photons could also possibly function in the latter role. We are going to use atoms with a certain energy level structure to make an effective interaction between the photons. In the first of the three controlled phase gate schemes, only one such atom will be used. The description of the first scheme consists of an intuitive derivation based on physical arguments which is then verified by running the numerical simulations. Afterwards we look at two modifications that make use of an ensemble of those atoms and the collective enhancement effects that it can give. The second scheme builds upon the analytical results of the first one. The last scheme is treated using a different effective theory of the interaction and under a number of approximations. Hence as the last topic in this thesis we take the first steps towards verifying this effective theory and the other approximations by running the numerical simulations.

Resumé på dansk

Kvantecomputere opererer med qubits, som er enheder, der kan være i tilstanden $|0\rangle$, tilstanden $|1\rangle$ eller en vilkårlig superposition (lineær kombination) af disse. En af de nødvendige dele af en kvantecomputer er en kontrolleret to-qubit gate. Et eksempel af sådan en gate er den *kontrollerede fase gate*, som giver en fase af π (dvs. ganger med -1) til tilstanden, hvor begge qubits er i $|1\rangle$. I denne afhandling skal vi kigge på tre forskellige tilgange til at realisere en kontrolleret fase gate for qubits gemt i fotoner. Fotonerne er specielle i den forstand, at de normalt ikke vekselvirker med hinanden, hvilket gør det svært at lave kontrollerede to-qubit gates med dem. Derfor er fotonernes sædvanlinge rolle i kvantedatabehandling at overføre kvanteinformation over lange afstande i stedet for at være registre i en kvantecomputer, som kvantealgoritmer er kørt på direkte. Fra den anden side virker enkelt-qubit gates for fotoner godt, og hvis en effektiv to-qubit gate var konstrueret, så ville fotoner også kunne fungere i den sidstenævnte rolle. Vi skal bruge atomer med en bestemt energiniveaustruktur for at lave en effektiv vekselvirkning mellem fotoner. I den første af de tre tilgange til at lave en kontrollet fase gate vil kun ét sådant

atom blive brugt. Beskrivelsen af den første tilgang består af en intuitiv udledning baseret på fysiske argumenter, hvilket er dernæst verificeret ved at køre numeriske simulationer. Efterfølgende kigger vi på to modifikationer, som benytter et ensemble af disse atomer og de kollektive forstærkningseffekter, som det kan give. Den anden tilgang går ud fra de analytiske resultater af den første. Den sidste tilgang er behandlet vha. en anden effektiv teori af vekselvirkningen og en række af approksimationer. Derfor som det sidste emne af denne afhandling tager vi de første skridt imod verificering af denne effektive teori og de andre approksimationer ved at køre numeriske simulationer.

Acknowledgements

The work presented in this thesis was done partly in QUANTOP, Danish Quantum Optics center, Copenhagen and partly in ICFO – The Institute of Photonic Sciences, Barcelona (Castelldefels). I want to thank the following people: my supervisors – Anders S. Sørensen (QUANTOP) and Darrick Chang (ICFO) – for giving me exciting ideas to work on; Tommaso Caneva (ICFO) for many helpful discussions about the numerical simulations; Sumanta Das (QUANTOP) for reading the draft version of this thesis and pointing out the typos and opportunities for clarification.

Contents

Chapter 1

Introduction

As the transistors inside the classical computers are manufactured with ever smaller dimensions, it makes it possible to have more of them in a single package. In fact, the increase of the number of transistors with time is well approximated by an exponential. This is the famous prediction of Gordon Moore that was first stated in 1965 [1]. The original observation was that the optimal number of components (in terms of the cost per component) in an integrated circuit was doubling every year and that trend was expected to continue "for at least 10 years". Later the statement was revised to "doubling every two years". The current formulation taken from the 2012 report of the International Technology Roadmap for Semiconductors [2] states that the chip density doubles "on a periodic basis; and the cycle of that period is set by the technological advancement of manufacturing process capability". The last formulation reflects the reasonable doubt that setting any fixed period of doubling will hold true indefinitely.

The difficulty in keeping up a fixed rate of doubling is due in part to the fact that physical objects behave very differently when their sizes become small. Quantum mechanics is the best description we have today of the small-scale phenomena and it predicts such processes as *tunneling*, i.e. a tendency of the quantum particles to leak through any potential barrier (no matter, whether they have the energy to overcome it according to clasical mechanics or not). The conventional computers operate with bits – entities that can be either 0 or 1. The physical states that correspond to those two logical states are respectively absence or presence of electrons at a certain position inside the integrated circuit. As transistors become smaller, they operate on fewer and fewer electrons at a time. For a small number of electrons the difference between one of them tunneling through a potential barrier in a transistor might lead to a change of the logical state from 0 to 1. Such non-deterministic changes are certainly detrimental to most types of classical computation one might want to do: every classical algorithm usually assumes that when a certain bit is set to 0, it stays that way until it is explicitly set to something else later.

Instead of only focusing the attention on mitigating the unwanted effects of quantum

mechanics, another line of thought is to try finding ways to harness the rich variety of the quantum phenomena. Maybe they can help us compute things even faster than before? For example, in this thesis we would need to simulate a physical system. Since nature is inherently quantum mechanical, simulating real physical systems in principle means simulating all of their quantum mechanical degrees of freedom. In many cases it is enough to only do classical simulations, because as the size of the system grows, typically the quantum mechanical side becomes less pronounced and may be completely neglected. In other cases, more sophisticated classical algorithms can account for the important quantum mechanical effects and discard the rest, thus still making the simulation possible. However, sometimes the quantum mechanical effects are so strong that even the best classical algorithms break down. Probably the most prominent example here is high temperature superconductivity. Currently there is no theory that describes this phenomenon completely [3], and it might help if one could simulate reasonably large systems properly accounting for all quantum mechanical interactions [4]. This is exactly the task that a quantum computer would excel at.

If we only wanted to simulate physical systems, a general purpose quantum computer may not be needed. A special purpose one would suffice. Indeed, the field of quantum simulations [4] is thriving right now. Focusing on specific real physical system and building a quantum simulator specifically designed for that task seems to be a promising way to simulate bigger systems with less effort compared to building a general purpose quantum computer. There are some disadvantages to that approach, however. Basically such specialization gains efficiency at the cost of flexibility. Moreover, a general purpose quantum computer will be very useful for certain purely classical problems that are slow (exponential runtime) on classical computers but are theoretically proven to be fast (polynomial runtime) on quantum computers. The usual example here is factoring of large numbers into primes [5]. It can be argued that many such algorithms either do not possess a particularly broad application range or do not yield a big enough speedup to be of much interest. Here one may try to be optimistic and conjecture that given that there exist quantum algorithms at all even without any quantum computer to run them, then certainly a fully functional quantum computer would be a sufficient motivation to invent more and better algorithms.

In this thesis we shall focus on a crucial part of a general purpose quantum computer – a two-qubit controlled phase gate (where the qubits are stored in the states of the photons). The main contributions of this work are:

- Proposal of a single-atom controlled phase gate for photons and a possible modification, which uses an atomic ensemble (chapter 6).
- Detailed fidelity calculations of a different but highly related phase gate based on an atomic ensemble (chapter 7).
- Application of a novel numerical method to simulate linear and nonlinear processes in an atomic ensemble (chapters 4, 6 and 8).
- Transfer matrix analysis of an atomic ensemble with the counterpropagating classical drives (chapter 8).

The thesis outline is:

Chapter 1 is this introduction.

Chapter 2 describes the main parts of a general purpose quantum computer: both the abstract formalism and the concrete implementations.

Chapter 3 discusses the linear properties of the two-level and three-level atoms.

Chapter 4 introduces the theory that we shall use for the numerical simulations and performs a simple benchmark of it.

Chapter 5 discusses two candidates for physical systems, where a controlled phase gate could be implemented.

Chapter 6 describes the single atom phase gate and its possible modification that uses an atomic ensemble.

Chapter 7 considers a different kind of an ensemble phase gate than in chapter 6. For this gate a detailed fidelity calculation is performed.

Chapter 8 contains the transfer matrix analysis of the atomic ensemble that was used in chapter 7.

Chapter 9 discusses possible ways to build upon the results presented in this thesis and concludes this thesis.

Chapter 2

Quantum computer

2.1 DiVincenzo criteria

In [6] there were identified five requirements (which are now often referred to as the "DiVincenzo criteria") that needed to be fulfilled in order to build a general purpose quantum computer. Here we shall restate them and give examples in terms of the concrete proposals for the implementation of quantum computers. In particular we shall consider the ion trap computer [7] and the photon (optical) quantum computer. The former is taken because it is arguably the most complete and experimentally successful, while the latter is chosen since it will be the focus of this thesis. The simplified version of the DiVincenzo criteria is:

1. Qubits
2. Initialization
3. Long decoherence times
4. A "universal" set of quantum gates
5. Measurement

In the next sections we shall go through these criteria. They will help us understand where this thesis fits in the big picture of quantum computing and simultaneously better define the scope of the thesis.

2.2 Qubits

Quantum computers operate on qubits. Contrary to classical bits that can only be in two states – 0 or 1 – qubits can contain an arbitrary *superposition* of those. In quantum

mechanics we usually denote states in *ket* notation, so that logical state 0 is written as the quantum state $|0\rangle$ (a ket), and the logical state 1 is written as the quantum state $|1\rangle$. The quantum mechanical versions have more structure to them. The states $|0\rangle$ and $|1\rangle$ are thought to be elements (vectors) in a certain kind of an inner product space $\mathcal{H}$ – the Hilbert space. We denote inner product of two elements $|\psi\rangle$ and $|\phi\rangle$ of $\mathcal{H}$ by $\langle\psi|\phi\rangle$. To begin with we assume that $\mathcal{H}$ is a two-dimensional space, and we want our states $|0\rangle$ and $|1\rangle$ to form an orthonormal basis of $\mathcal{H}$. Orthonormality of the basis is formally expressed in terms of the inner products between the basis vectors:

$$\begin{aligned}\langle 0|1\rangle &= \langle 1|0\rangle = 0,\\ \langle 0|0\rangle &= \langle 1|1\rangle = 1.\end{aligned}$$

Then the general state of a single qubit $|\psi_{\text{one qubit}}\rangle$ is an element in this inner product space and has the form

$$|\psi_{\text{one qubit}}\rangle = a|0\rangle + b|1\rangle, \tag{2.1}$$

where a and b are complex numbers such that $|a|^2 + |b|^2 = 1$. The last condition together with orthonormality of the basis ensures that the state $|\psi_{\text{one qubit}}\rangle$ is normalized (the inner product with itself equal to 1). We note that here and in the rest of the thesis we shall mostly look at the *pure* quantum states. In general one may need to also consider *mixed* states which are a generalization of the pure states in the sense that a mixed state can be thought of as a collection of pure states, and each of them occurs according to some (classical) probability distribution.

Often more than one qubit is needed. Formally we think that each qubit is an element in its own two-dimensional Hilbert space. Then the state of *all* the qubits is an element in the product of those Hilbert spaces. The state of two isolated qubits is the product of the single qubit states. If the single qubit states are $|\psi_{\text{qubit 1}}\rangle = a_1|0\rangle + b_1|1\rangle$ and $|\psi_{\text{qubit 2}}\rangle = a_2|0\rangle + b_2|1\rangle$, then the two-qubit state is

$$\begin{aligned}|\psi_{\text{two qubits}}\rangle &= |\psi_{\text{qubit 1}}\rangle|\psi_{\text{qubit 2}}\rangle\\ &= a_1a_2|0\rangle|0\rangle + a_1b_2|0\rangle|1\rangle + b_1a_2|1\rangle|0\rangle + b_1b_2|1\rangle|1\rangle\\ &= c_{00}|00\rangle + c_{01}|01\rangle + c_{10}|10\rangle + c_{11}|11\rangle.\end{aligned} \tag{2.2}$$

In the second line we defined $c_{00} = a_1a_2$, $c_{01} = a_1b_2$, $c_{10} = b_1a_2$, $c_{11} = b_1b_2$ and used a shorthand notation for products of two states, i.e. by writing, say, $|01\rangle$ we understand the product state $|0\rangle|1\rangle$. The reason for the new constants here is that when we later look at the evolution of qubits, it is in general not the individual qubits (i.e. the coefficients a_j and b_j) that evolve, but rather it is the whole state $|\psi_{\text{two qubits}}\rangle$ (described by the coefficients c_{ij}) that is changed. Whenever we have a (pure) two-qubit state that cannot be factorized into a product of two one-qubit states we say that these two qubits are *entangled*. This

behaviour is completely different from the classical computers that do not possess anything similar.

Another thing to note here is that we need 4 complex numbers to describe the state of two qubits. The state of N qubits is then described by 2^N complex numbers. In general, any quantum system experiences such exponential growth of the number of the parameters that describe its state. Formally we say that the basis of the Hilbert space grows exponentially with the number of subsystems (particles, qubits, etc.). It is precisely why we wanted to have a quantum computer in the first place. Instead of having to use 2^N complex numbers on a classical computer (where each of those complex numbers is typically represented by 64 or 128 bits), we only need N qubits on a quantum computer. Of course not all quantum mechanical systems of interest can be readily described by a collection of two-level subsystems. In principle, however, if we have M subsystems, each of them having k internal quantum mechanical states, then we need k^M complex numbers to describe them. We see that $N = M \ln(k)/\ln(2)$ (rounded up to an integer) qubits contain the same amount of information. In this way the number of qubits is only weakly (logarithmically) dependent on the number of internal degrees of freedom of the subsystems. Finally we remark that products of quantum states that we used above can describe not only state of several qubits but in general the state of several distinct subsystems. Shortly we shall use products of quantum states to describe the modes of the two optical fibers.

There are a lot of ways to realize the abstract concept of a qubit. Since we are using electrons to represent bits in the typical personal computers, we could simply use superpositions of 0 electrons and 1 electron to represent our qubits. There is another option that is purely quantum mechanical in nature. One can use the *internal* states of the particles. Electrons, for example, are spin 1/2 particles, and can be in a state with spin up $|\uparrow\rangle$ or in a state with spin down $|\downarrow\rangle$. Quantum mechanics also allows the electron to have an internal state that is a superposition of spin up and spin down. Hence if we identify spin down with the logical state 0 and spin up with the logical state 1, we can naturally map the internal state of the electron onto a single qubit.

Atoms have a much more complex internal level structure than electrons. Fortunately, with the advancements of atomic physics one has a gained a thorough understanding of that structure, and many experimental techniques were developed. Most of them involve shining a laser at the atom in such a way that the internal state of the atom changes. The energy (frequency) and polarization of the photons in the laser beam determine whether a transition between a given pair of the internal states of the atom is possible. If we know that the atom is in a particular state, then tuning the laser such that it is possible to transition between that state and only one other state, the atom effectively becomes a "two-level" atom. Formally the internal states of such two-level atom are entirely equivalent to the internal states of an electron, and thus a two-level atom is another example of a physical system that represents a qubit. In the case of the atom, however, it is possible to build upon all the experience of the atomic physics gained throughout the years to manipulate the qubit practically in any way one can think of. But it is not necessary to stop at only

two levels. Later we shall look at three-level atoms and ultimately at four-level atoms.

The ion trap quantum computer [7] is a direct application of the techniques of the atomic physics. As the name suggests, this computer uses ionized atoms that are trapped by a particular (time-varying) configuration of electric fields. The trapping potential makes the atoms form a one-dimensional chain. Since all of them have an overall positive charge, they repel each other. Under sufficiently low temperature the thermal vibrations of the ions become negligible, and they form a crystal. The qubits are stored in the internal atomic energy levels.

The final example of a qubit is the qubit stored in photons. Just like with the electrons above, one can either use the internal states of a photon or superpositions of 0 and 1 photon. Photons can have different polarization. Any polarization state can be expressed as a linear combination of the horizontal and vertical polarization. Thus one can encode a qubit into the polarization state. In this thesis we shall be focusing on the other approach – using states of 0 photons and 1 photon in an optical fiber. However, it turns out that it is better to use *two distinct* optical fibers instead of one – the so-called *dual-rail* representation. In this way changing the state of the qubit from, say, $|1\rangle$ to $|0\rangle$ involves rerouting the photon from one optical fiber to the other. If we call the modes of the two fibers by A and B, then photon being present or absent in the mode A is described by the states $|1\rangle_A$ and $|0\rangle_A$ respectively, and the photon being present or absent in the mode B is described by $|1\rangle_B$ and $|0\rangle_B$ respectively. Using this notation we define the states of our qubit as $|0\rangle = |0\rangle_A|1\rangle_B$ and $|1\rangle = |1\rangle_A|0\rangle_B$. We also note here that conversion between the polarization and dual-rail encodings can be accomplished using polarizing beam splitters and half-wave plates [8].

The formulation of [6] specifically mentions that the collection of the qubits one might want to use should be *scalable*. However, it is probably only the ion trap quantum computer, that is at the stage where it starts to matter. Most of the other concrete proposals have to solve much more basic problems first. In this thesis we shall address one of such basic problems of the photon computer.

The scalability of the ion trap computer is limited by the fact that it is challenging to continue adding more ions to the one-dimensional chain. Even if one could do it, the two-qubit gate speed would decrease [9]. Thus schemes of connecting distinct ion chains are being considered. One possibility is simply using classical shuttling of the ions between different chains. Another way is to establish a quantum link between the two ions belonging to different chains, i.e. *entangle* them. Then this quantum link can be used to *teleport* the qubits from one ion chain to the other and thereby make it possible to perform operations with any pair of qubits from both of the entangled ion chains. The entangling of the ions is performed by having both of them emit a photon and then measuring both photons in a particular way. In this context one might ask that since using photons in an ion trap computer seems to be necessary anyway, then maybe operating on photons directly with photon gates would be better in the end. This thesis is by no means a definitive answer to this question but it can be viewed as a small step in this direction. Also, to accomplish teleportation across big distances (to connect two distant quantum computers), quantum

repeaters [10] are needed. As each repeater node is essentially a small quantum computer itself, it can be of advantage to be able to process qubits stored in photons directly instead of needing to convert them into stationary qubits first.

2.3 Initialization

For the ion trap computer, initialization is performed with a technique called "optical pumping"[11]. Every energy level in an atom has a certain lifetime after which it spontaneously decays into a lower level. Contrary to a transition using a laser, the spontaneous decay is an irreversible process. For optical pumping the goal is to initialize the atom in some long lived state. Usually there are several such long lived states and one wants to single out one of them as a part of the qubit. The wavelengths and polarizations of the applied lasers can be chosen in such a way that all the undesired long lived states get constantly excited to some higher states with short lifetimes and consequently spontaneously decay back to the manifold of the long lived states. If the desired state is the only one that cannot be excited by the lasers but at the same time it is possible to decay into it, then after some time the atom inevitably ends up initialized in this particular state.

The photon quantum computer qubits can be initialized by emitting a photon into one of the two optical fibers that represent the qubit. It is, however, challenging to create single photon states. The most accessible way is to use *weak coherent states*. The coherent states represent the states of a laser. The coherent state is described by the complex number α, which corresponds to the amplitude and the phase of the laser. We can write such a state in the number state basis. If we call the state with n photons by $|n\rangle$ then the coherent state can be written as

$$|\alpha\rangle = e^{-|\alpha|^2/2} \sum_{n=0}^{\infty} \frac{\alpha^n}{\sqrt{n!}} |n\rangle.$$

This state is a superposition of different photon numbers, but the states with higher photon numbers also have a smaller probability of being present. If one chooses sufficiently small $|\alpha|$ then the state $|\alpha\rangle$ is approximately vacuum with a small part of the single photon state. With weak coherent states we can only obtain single photons probabilistically and there is no way to synchronize multiple such sources to produce single photon states simultaneously.

One of the alternatives to the weak coherent states is to use *parametric down-conversion*. This is a process where one photon is converted into two due to nonlinearities in the medium. One of those photons can be sent to a photon detector, so that whenever the detector clicks, it is known for sure that there was also produced another photon. That photon can then be stored in a quantum memory. Synchronizing multiple such sources is possible, since retrieval of the photons from quantum memories can be in principle accomplished deterministically. For this setup the main limiting factor is low efficiency of the quantum memories.

2.4 Long decoherence times

In the context of quantum computation *decoherence* means that after initialization all qubits have a tendency to change their state due to interactions with the environment. Decoherence time is the time for this usually unwanted effect to happen.

In the ion trap computer the qubits are stored in the hyperfine sublevels of the atoms. To be specific we can look at the ions of ytterbium $^{171}Yb^{+}$ that were discussed in [9]. Even though those atoms have a lot of electrons, there are only two of them in the outer shell. After ionizing, only one electron remains. The hyperfine structure then arises from a small energy difference of either aligning or anti-aligning the nuclear magnetic moment and the electronic spin of the lone outer electron. We want to store the qubit in the two ground state sublevels that have the energy difference given by the hyperfine splitting. Since hyperfine sublevels are magnetic they are unaffected by the electric fields used to trap the ions. Furthermore, the natural lifetime of the excited hyperfine state is so big that it is not the limiting factor in the experiments. Instead the decoherence time of the qubits is often limited by the level of vacuum [9] (which gives mean time between the collisions of the other atoms in the chamber with the ions that contain the qubits).

In the photon computer the decoherence time of the qubits is set by decay rate of the optical fibers. The probability of a photon surviving a trip through an optical fiber of a given length decays exponentially with the length. This is a big problem for quantum communication where one wants to transmit qubits over long distances [12]. For our purpose of building an isolated quantum computer we would like to make all the distances inside it as small as possible. We are going to assume that the decoherence due to the qubits flying from one gate (see section 2.5) to another will be negligible compared to the loss due to imperfections in the gates themselves. Here we can also remark that precisely because it is relatively easy to make photons retain their state (since they interact weakly with each other and the environment) it is relatively hard to make gates between them (which require strong interaction). On the other hand, even if photons can fly a comparatively long distance without a significant decoherence, the speed of light is still so big that this translates into rather small decoherence times. Thus for long running computations, efficient single-photon memories will be needed to make the decoherence times longer.

2.5 A "universal" set of quantum gates

In classical computers, any algorithm can in principle be reduced to basic logical operations such as NOT, AND, OR etc. An abstract device that performs those logical operations is called a *gate*. Classical gates operate either on one or two bits at a time and produce a single bit as the output. The NAND logical gate (AND followed by a NOT) is called *universal* in the sense that any logical operations can be implemented in terms of it. Another universal gate is the NOR (OR followed by a NOT).

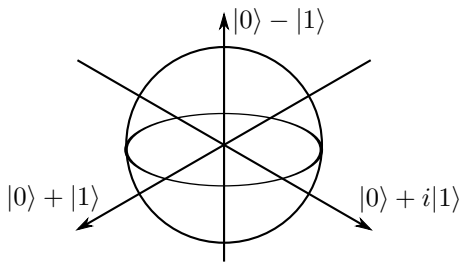

Figure 2.1: The Bloch sphere. Any single-qubit state (2.1) can be represented as a point on its surface.

In a quantum computer we need to obey the laws of quantum mechanics which requires that the evolution of the states (in a closed system) must be *unitary*. Unitarity means that the norm of the states is preserved and that the evolution must be reversible. Thus the classical gates mentioned above that take two inputs and produce one output do not satisfy this condition: they irreversibly destroy information that way. Another complication arises due to the fact that a qubit is a superposition of two logical states. Thus it is not enough to simply be able to do a NOT, i.e. flip $|0\rangle$ to $|1\rangle$ or vice versa. One needs to be able to take any qubit of the form (2.1) with parameters a and b and produce a state with any other parameters a' and b'. We shall call such an operation an *arbitrary rotation*. Calling it a "rotation" refers to the often employed visualization of any state of the form (2.1) as a point on a sphere of unit radius (figure 2.1). The reduction from 2 complex numbers (i.e. 4 real numbers) to 2 real angles is possible if we impose normalization condition $|a|^2+|b|^2 = 1$ and neglect an overall phase of the state. An arbitrary rotation is then described by 3 real numbers which are or can be related to angles of rotation about each of the 3 axes. One can write the general one-qubit unitary operation as

$$U_{\text{qubit}}(\alpha, \beta, \theta) = \begin{pmatrix} e^{i(\alpha+\beta)} \cos\theta & e^{i\alpha} \sin\theta \\ -e^{i\beta} \sin\theta & \cos\theta \end{pmatrix}$$

Here we understand that this matrix operates on a vector

$$|\psi\rangle_{\text{one qubit}} = \begin{pmatrix} a \\ b \end{pmatrix} \tag{2.3}$$

with the coefficients a and b being the same as the ones in (2.1). Thus representations (2.1) and (2.3) are two equivalent ways to describe a one qubit quantum state. A general

two-qubit state can then be written

$$|\psi\rangle_{\text{two qubits}} = \begin{pmatrix} c_{00} \\ c_{01} \\ c_{10} \\ c_{11} \end{pmatrix} \tag{2.4}$$

with the coefficients of (2.2). An example of a two-qubit gate is the controlled NOT

$$U_{\text{CNOT}} = \begin{pmatrix} 1 & 0 & 0 & 0 \\ 0 & 1 & 0 & 0 \\ 0 & 0 & 0 & 1 \\ 0 & 0 & 1 & 0 \end{pmatrix}$$

The gate U_{CNOT} keeps the states $|00\rangle$ and $|01\rangle$, but changes $|10\rangle \to |11\rangle$ and $|11\rangle \to |10\rangle$. Thus it performs the NOT operation (swaps $|0\rangle$ and $|1\rangle$) on one of the qubits only when the other is in the state $|1\rangle$.

The gates U_{qubit} and U_{CNOT} constitute a universal set of gates [13] in the sense that any unitary operation on any number of qubits can be approximated to arbitrary precision using only those two gates. However, arbitrary single qubit rotations are not necessary to have a universal set of gates. If the goal is only to be able to *approximate* any unitary operation then the set consisting of U_{CNOT} together with the gates

$$H = \frac{1}{\sqrt{2}} \begin{pmatrix} 1 & 1 \\ 1 & -1 \end{pmatrix}, \quad \sigma_z^{1/4} = \begin{pmatrix} 1 & 0 \\ 0 & e^{i\pi/4} \end{pmatrix}$$

(a Hadamard gate and a single qubit phase gate) is universal [14].

In practice, both for the ion trap computer and for the photon computer instead of the controlled NOT gate it seems easier to implement the controlled *phase* gate

$$U_{\text{CPHASE}} = \begin{pmatrix} 1 & 0 & 0 & 0 \\ 0 & 1 & 0 & 0 \\ 0 & 0 & 1 & 0 \\ 0 & 0 & 0 & -1 \end{pmatrix}. \tag{2.5}$$

The gate U_{CPHASE} keeps the states $|00\rangle$, $|01\rangle$ and $|10\rangle$ unchanged and imparts a *phase* of π (i.e. a factor of $e^{i\pi} = -1$) to the state $|11\rangle$. In the literature, the controlled π phase gate is sometimes called the controlled *sign* gate. U_{CPHASE} can be related to U_{CNOT} using H. Note that the operation of applying H on the first qubit and keeping the second one as it is, can be written in terms of a Kronecker product of the single qubit identity matrix I

and H:

$$I \otimes H = \frac{1}{\sqrt{2}} \begin{pmatrix} 1 & 1 & 0 & 0 \\ 1 & -1 & 0 & 0 \\ 0 & 0 & 1 & 1 \\ 0 & 0 & 1 & -1 \end{pmatrix}.$$

Then it can be verified that $U_{\mathrm{CNOT}} = (I \otimes H) U_{\mathrm{CPHASE}} (I \otimes H)$.

In the ion trap computer the qubits stored in the hyperfine sublevels are not directly addressable by the visible light lasers. Instead, a pair of lasers can be used to make a transition via a third auxiliary level. By choosing the phase, intensity and the interaction time of the laser pulses one can implement arbitrary rotations U_{qubit} in this way. For the two-qubit gates, the collective vibrational modes of the ion chain are used. Upon absorbing a photon, the ion not only goes from one energy level to another but also starts to vibrate thus causing the other ions to vibrate. Conversely the ion responds differently to the laser light depending on whether it is already vibrating or not. The details of the exact protocol used to implement U_{CPHASE} employing this idea can be found in [7].

For the photon computer, H can be implemented for the polarization encoding as a half-wave plate (a birefringent material) oriented at 22.5°, and for the dual-rail encoding as a beam splitter [8]. The single qubit phase gate $\sigma_z^{1/4}$ can be implemented for polarization encoding as an eighth-wave plate, and for the dual-rail encoding by having the two paths go through media with a different refractive indices, such that one path effectively becomes longer than the other. The implementation of U_{CPHASE} is the main objective of this thesis.

2.6 Measurement

The measurement postulate of quantum mechanics applied to any single qubit state (2.1) says that regardless of what values of a and b the state had, upon measurement one will find the state to be either *exactly* $|0\rangle$ with probability $|a|^2$ or exactly $|1\rangle$ with probability $|b|^2$. Due to this property all the quantum algorithms have the general principle that no matter what quantum transformations of the qubits they employ, in the end they try to evolve the state such that is is mostly classical and the measurement does not introduce much uncertainty. However, even then the measurement can introduce errors due to imperfections of the equipment.

In the ion trap computer the measurement process can in principle be done with 100% efficiency. The procedure [9] is to tune the laser such that only one of the two states $|0\rangle$ and $|1\rangle$ can be transferred to a short-lived excited state. Assume that it is the state $|1\rangle$ for concreteness. If the short-lived excited state also decays back to $|1\rangle$, then experimentally one sees either (almost) nothing if the qubit state was $|0\rangle$ or a lot of emitted light from the ion due to repeated excitations and spontaneous deexcitations if the qubit state was $|1\rangle$.

In the photon computer using the dual-rail encoding one needs to put a photon detector at the end of each of the paths that represent the qubit. Photon detectors have multiple problems though [8]. For example they cannot distinguish between one or more photons and have efficiency of about 70%.

Chapter 3

Two-level and three-level atoms

3.1 Introduction

In the thesis we shall be talking a great deal about two-level and three-level atoms, so it will be helpful to understand some of their general properties before the main objective of this thesis will be discussed. While two energy levels can be positioned relative to each other in only one way (up to relabelling of the states), there is in principle a bit more freedom with three levels. In this thesis we shall mostly look at the so-called Λ-type three-level atoms (figure 3.1).

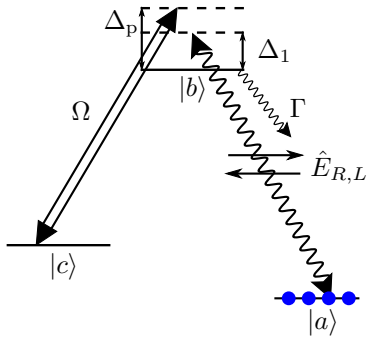

Figure 3.1: A Λ-type three-level atom. The quantum electric field is coupled to the transition $|a\rangle \leftrightarrow |b\rangle$. The shown detuning Δ_1 is the detuning of the carrier (central) frequency ω_{k_0} of the quantum field from the atomic transition frequency ω_{ba}, i.e. $\Delta_1 = \delta_{k_0} = \omega_{k_0} - \omega_{ba}$. The classical electric field (laser) is coupled to the transition $|c\rangle \leftrightarrow |b\rangle$ with the detuning Δ_{p}. The blue dots on the state $|a\rangle$ indicate, that the atom (or the whole ensemble of atoms) is initialized in this state before any storage of the excitations is attempted.

In this section we shall be studying linear properties of the two-level and three-level

atoms. Here by *linear* we understand properties of interaction of the atoms with a *single photon*. The *nonlinear* processes are the interactions with *more than one photon*, and in this thesis "more than one photon" will exclusively mean "two photons".

3.2 Model

As the starting point in this discussion we shall imagine a three-level atom coupled to quantized electric field that represents photons. The electric field is treated in a one-dimensional manner: it only depends on one spatial coordinate z. The physical structure that confines the motion of the photons in one dimension is called a *waveguide*. In this thesis "electric field" will exclusively mean the electric field of the photons and correspondingly the waveguides will be optical waveguides. However, the formalism introduced in this section can also be used to describe other kinds of electric field excitations, e.g. plasmons [15].

The electric field has only two different modes: the left-going and the right-going. We denote those two modes by the operators $\hat{E}_{\mathrm{L}}$ and $\hat{E}_{\mathrm{R}}$ respectively. The electric field operators have commutation relations

$$\begin{aligned}\left[\hat{E}_{\mathrm{L}}(z), \hat{E}_{\mathrm{L}}^{\dagger}(z')\right] &= \left[\hat{E}_{\mathrm{R}}(z), \hat{E}_{\mathrm{R}}^{\dagger}(z')\right] = \delta(z - z'), \\ \left[\hat{E}_{\mathrm{L}}(z), \hat{E}_{\mathrm{R}}^{\dagger}(z')\right] &= \left[\hat{E}_{\mathrm{R}}(z), \hat{E}_{\mathrm{L}}^{\dagger}(z')\right] = 0.\end{aligned} \tag{3.1}$$

The atom is described by operators $\hat{\sigma}_{\alpha\beta} = |\alpha\rangle\langle\beta|$ where α and β can be either a, b or c (one the three states of the atom as in figure 3.1). They have commutation relations

$$\left[\hat{\sigma}_{\alpha\beta}, \hat{\sigma}_{\alpha'\beta'}\right] = \delta_{\beta,\alpha'}\hat{\sigma}_{\alpha\beta'} - \delta_{\beta',\alpha}\hat{\sigma}_{\alpha'\beta}.$$

The Hamiltonian with only energy conserving terms present is

$$\begin{aligned}\hat{H} =& \hbar\omega_{ba}\hat{\sigma}_{bb} + \hbar\omega_{ca}\hat{\sigma}_{cc} - \hbar\Omega\hat{\sigma}_{bc}e^{-i\omega_{\mathrm{p}}t} - \hbar\Omega^{*}\hat{\sigma}_{cb}e^{i\omega_{\mathrm{p}}t} \\ & - \hbar g\sqrt{2\pi}\int \delta(z - z_j)\left\{\hat{\sigma}_{ba}\left[\hat{E}_{\mathrm{R}}(z) + \hat{E}_{\mathrm{L}}(z)\right] + \left[\hat{E}_{\mathrm{R}}^{\dagger}(z) + \hat{E}_{\mathrm{L}}^{\dagger}(z)\right]\hat{\sigma}_{ab}\right\} dz \\ & + i\hbar c\int\left[\hat{E}_{\mathrm{L}}^{\dagger}(z)\,\frac{\partial\hat{E}_{\mathrm{L}}}{\partial z} - \hat{E}_{\mathrm{R}}^{\dagger}(z)\,\frac{\partial\hat{E}_{\mathrm{R}}}{\partial z}\right] dz.\end{aligned}$$

In the first line of the Hamiltonian the first two terms give the energies of being in the states $|b\rangle$ and $|c\rangle$ respectively, while the last two terms describe coupling of the classical drive field (the "pump") with frequency ω_{p} to the transition $|b\rangle \leftrightarrow |c\rangle$. In the second line of the Hamiltonian we have coupling of the quantized electric field to the transition $|a\rangle \leftrightarrow |b\rangle$ (with the coupling constant g). Here we assume that the atom is located at the position $z = z_j$ in the waveguide. The index j is here because later we shall look at an array of

atoms. Since the array is periodic, a lot of knowledge about the linear properties of the whole array can be inferred by studying a single atom at a time. The third line in the Hamiltonian describes the propagation of the left and right going modes of the electric field.

Using the Hamiltonian above we can find Heisenberg equations for the light and for the atoms. For the atoms we shall make the approximation that most of the population is in the state $|a\rangle$. This effectively means that we can approximate the population of the ground state as $\hat{\sigma}_{aa} \approx 1$ and the population of the excited state as $\hat{\sigma}_{bb} \approx 0$. The coherence $\hat{\sigma}_{bc}$ expresses transitions between two very scarcely populated states, thus we also set $\hat{\sigma}_{bc} \approx 0$. With these approximations the equations become linear in the operators. By considering only a single photon and single atomic excitation states we can effectively treat the operators in the equations of motion as complex-valued functions and stop writing the hats.

We arrive at the equations for the electric field:

$$\left(\frac{1}{c}\frac{\partial}{\partial t} + \frac{\partial}{\partial z}\right) E_{\mathrm{R}}(z) = \frac{ig\sqrt{2\pi}}{c}\delta(z - z_j)\sigma_{ab},$$
$$\left(\frac{1}{c}\frac{\partial}{\partial t} - \frac{\partial}{\partial z}\right) E_{\mathrm{L}}(z) = \frac{ig\sqrt{2\pi}}{c}\delta(z - z_j)\sigma_{ab}.$$

Later we shall need to use the integrated versions of these two equations. We integrate both sides from $z_j^- = z_j - \varepsilon$ to $z_j^+ = z_j + \varepsilon$ for some ε that we shall let go to zero at the end of the calculations. If we define $E_{\mathrm{L,in}} = E_{\mathrm{L}}(z_j^+)$ and $E_{\mathrm{R,in}} = E_{\mathrm{R}}(z_j^-)$ then we can write the integrated equations as

$$E_{\mathrm{R}}(z_j^+) = E_{\mathrm{R,in}} + \frac{ig\sqrt{2\pi}}{c}\sigma_{ab}, \tag{3.2}$$
$$E_{\mathrm{L}}(z_j^-) = E_{\mathrm{L,in}} + \frac{ig\sqrt{2\pi}}{c}\sigma_{ab}. \tag{3.3}$$

In the equations of motion for the atoms we include the decay rate Γ' of the state $|b\rangle$ into the modes outside of the waveguide. The state $|c\rangle$ is assumed to be metastable, i.e. it has a spontaneous decay rate that is smaller than all the other rates (inverses of the timescales) we shall consider. The equations for the atoms then become

$$\dot{\sigma}_{ab} = \left(-\frac{\Gamma'}{2} - i\omega_{ba}\right)\sigma_{ab} + i\Omega\sigma_{ac}e^{-i\omega_{\mathrm{p}}t} + ig\sqrt{2\pi}\left[E_{\mathrm{R}}(z_j) + E_{\mathrm{L}}(z_j)\right], \tag{3.4}$$
$$\dot{\sigma}_{ac} = -i\omega_{ca}\sigma_{ac} + i\Omega^*\sigma_{ab}e^{i\omega_{\mathrm{p}}t}. \tag{3.5}$$

Because of the continuity of E_{L} and E_{R} at $z = z_j$ and using equations (3.2) and (3.3)

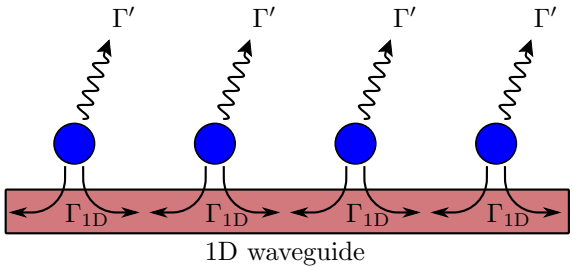

Figure 3.2: An ensemble of atoms (blue circles) coupled to a one-dimensional (1D) waveguide (red rectangle). Two different decay rates are shown: The decay rate into the waveguide Γ_{1D} and the decay rate into all other modes Γ'.

we can write

$$\begin{aligned} E_{\mathrm{R}}(z_j) + E_{\mathrm{L}}(z_j) &= \frac{1}{2}\left(E_{\mathrm{R}}(z_j^-) + E_{\mathrm{R}}(z_j^+)\right) + \frac{1}{2}\left(E_{\mathrm{L}}(z_j^-) + E_{\mathrm{L}}(z_j^+)\right) \\ &= \frac{1}{2}\left(2E_{\mathrm{R,in}} + \frac{ig\sqrt{2\pi}}{c}\sigma_{ab}\right) + \frac{1}{2}\left(2E_{\mathrm{L,in}} + \frac{ig\sqrt{2\pi}}{c}\sigma_{ab}\right) \end{aligned}$$

Upon inserting this expression into (3.4) and defining the decay rate into the waveguide $\Gamma_{1D} = 4\pi g^2/c$ (also see figure 3.2) and the total decay rate $\Gamma = \Gamma_{1D} + \Gamma'$, we obtain

$$\dot{\sigma}_{ab} = \left(-\frac{\Gamma}{2} - i\omega_{ba}\right)\sigma_{ab} + i\Omega\sigma_{ac}e^{-i\omega_{\mathrm{p}}t} + ig\sqrt{2\pi}\left[E_{\mathrm{R,in}} + E_{\mathrm{L,in}}\right]. \tag{3.6}$$

Now we solve the equations of motion by Fourier transform. The idea here is that transition $|a\rangle \leftrightarrow |b\rangle$ is coupled to the quantum field with frequency ω_k (for the different k-vectors), and the transition $|c\rangle \leftrightarrow |b\rangle$ is driven by the classical field with frequency ω_{p}. We also define $\delta_k = \omega_k - \omega_{ba}$. For the electric fields we assume that initially some right-going wave-packet comes from the left ($z < z_j$) and gets scattered on the atom. After scattering there will be some right-going electric field on the right ($z > z_j$) that is multiplied by the transmission coefficient $t(\delta_k)$ and some left-going electric field on the left that is multiplied by the reflection coefficient $r(\delta_k)$. Using above considerations we can write our Fourier components of the atomic coherences and the electric fields as

$$\begin{aligned} \sigma_{ab}(t) &= Ae^{-i\omega_k t} = Ae^{-i(\delta_k+\omega_{ba})t} \\ \sigma_{ac}(t) &= Be^{-i(\omega_k-\omega_{\mathrm{p}})t} = Be^{-i(\delta_k+\omega_{ba}-\omega_{\mathrm{p}})t} \\ E_{\mathrm{R}}(z) &= e^{ik(z-z_j)-i\omega_k t}\left(\theta_{\mathrm{H}}(-z+z_j) + t(\delta_k)\theta_{\mathrm{H}}(z-z_j)\right) \\ E_{\mathrm{L}}(z) &= e^{-ik(z-z_j)-i\omega_k t}r(\delta_k)\theta_{\mathrm{H}}(-z+z_j) \end{aligned}$$

Here θ_{H} is the Heaviside theta function. Note that by continuity of the electric field at $z = z_j$ we have $1 + r(\delta_k) = t(\delta_k)$. We insert the above into (3.2), (3.3), (3.5) and (3.6) and solve the equations. If we define $\Delta_{\mathrm{p}} = \omega_{\mathrm{p}} - (\omega_{ba} - \omega_{ca})$ we can write the reflection and transmission coefficients for a three-level atom as

$$\begin{aligned} r_3(\delta_k) &= -\frac{\Gamma_{1\mathrm{D}}(\delta_k - \Delta_{\mathrm{p}})}{(\Gamma - 2i\delta_k)(\delta_k - \Delta_{\mathrm{p}}) + 2i|\Omega|^2}, \\ t_3(\delta_k) &= \frac{(\Gamma' - 2i\delta_k)(\delta_k - \Delta_{\mathrm{p}}) + 2i|\Omega|^2}{(\Gamma - 2i\delta_k)(\delta_k - \Delta_{\mathrm{p}}) + 2i|\Omega|^2}. \end{aligned} \tag{3.7}$$

From $r_3(\delta_k)$ and $t_3(\delta_k)$ above we can get the reflection and transmission coefficients for the two-level atom by setting $\Omega = 0$. We obtain

$$r_2(\delta_k) = -\frac{1}{1 + (\Gamma' - 2i\delta_k)/\Gamma_{1\mathrm{D}}}, \quad t_2(\delta_k) = \frac{(\Gamma' - 2i\delta_k)/\Gamma_{1\mathrm{D}}}{1 + (\Gamma' - 2i\delta_k)/\Gamma_{1\mathrm{D}}}. \tag{3.8}$$

Comparing (3.7) and (3.8) we see that two-level atoms and three-level atoms behave rather differently. The two-level atoms have a non-zero reflection for all $\Gamma_{1\mathrm{D}} > 0$, i.e. for all cases when the atom is coupled to the waveguide, even if only weakly. In fact, for $\Gamma_{1\mathrm{D}}/(\Gamma' - 2i\delta_k) \to \infty$ we have $r_2(\delta_k) \to -1$, so we have a total reflection and get a factor of -1 (a phase of π) which will be very important for us later. The three-level atoms, on the other hand, can be made completely transparent. We see that for any $\Omega \neq 0$, we have $t_3(\Delta_{\mathrm{p}}) = 1$. This phenomenon is known as electromagnetically induced transparency (EIT).

In figure 3.3 we plot the reflectance $|r(\delta_k)|^2$ and loss $|l(\delta_k)|^2 = 1 - |t(\delta_k)|^2 - |r(\delta_k)|^2$ of two-level and three-level atoms. It highlights the difference between high $\Gamma_{1\mathrm{D}}$ (compared to Γ') regime and low $\Gamma_{1\mathrm{D}}$ regime. In the high $\Gamma_{1\mathrm{D}}$ regime a single two-level atom can reflect most of the light while keeping losses comparatively low, while in the low $\Gamma_{1\mathrm{D}}$ regime the two-level atom transmits most of the light while dissipating a sizable fraction of it into other modes than the waveguide. In both cases we also see that a three-level atom has complete transmission on resonance ($\delta_k = 0$). However, for high enough detuning δ_k the three-level atom essentially behaves as a two-level atom. In fact, for chosen parameters in figure 3.3 this so-called EIT window, where transmission is close to unity, is rather narrow.

3.3 Applications

3.3.1 A cavity made out of atomic mirrors

From the reflection coefficient of the two-level atom (3.8) we have seen that in the limit $\Gamma_{1\mathrm{D}}/(\Gamma' - 2i\delta_k) \to \infty$ we have a complete reflection. Often $\Gamma_{1\mathrm{D}}$ is not big enough to give a significant reflection from a single atom. In that case N atoms can be spaced at the distance of $\lambda/2$ from each other, where $\lambda = \lambda_{k_0}$ is the carrier wavelength of the electric

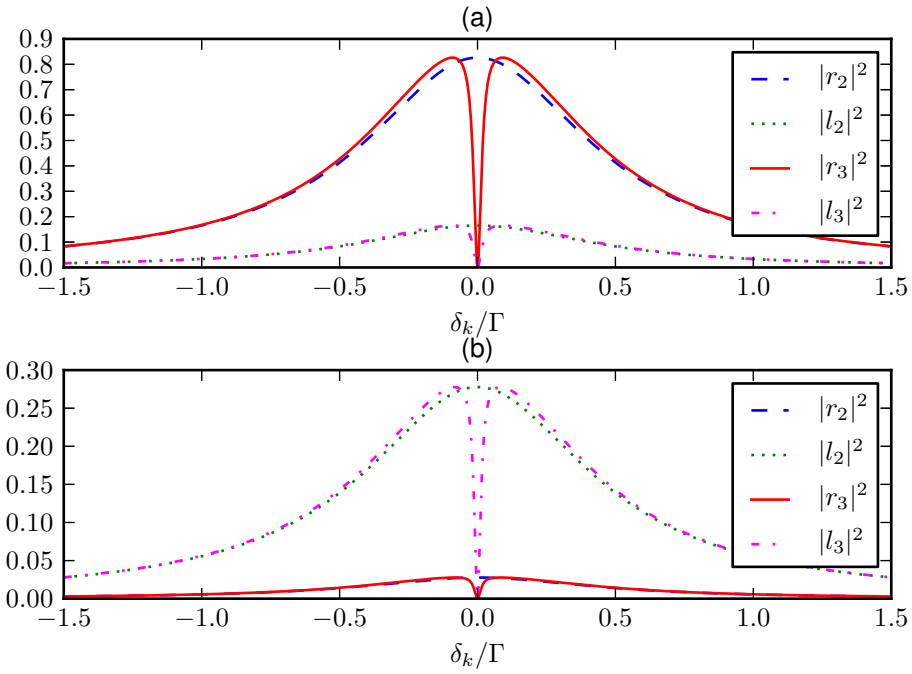

Figure 3.3: Reflectance $|r(\delta_k)|^2$ and loss $|l(\delta_k)|^2 = 1 - |t(\delta_k)|^2 - |r(\delta_k)|^2$ of two-level atoms ($|r_2|^2$, $|l_2|^2$) and three-level atoms ($|r_3|^2$, $|l_3|^2$) plotted as a function of δ_k/Γ with $\Gamma = \Gamma_{1D} + \Gamma'$. (a) $\Gamma_{1D} = 10\Gamma'$, $\Omega = \Gamma'$. (b) $\Gamma_{1D} = 0.2\Gamma'$, $\Omega = 0.1\Gamma'$. For the three-level atom we set $\Delta_p = 0$.

field pulse. In this way the reflected electric field from each consecutive atom will add constructively with the electric field reflected from all the previous atoms. Such a setup was considered in [16]. One of the results was to obtain reflectance $R(\delta_k) = |r(\delta_k)|^2$ and transmittance $T(\delta_k) = |t(\delta_k)|^2$ of the whole array. They were found to be

$$R(\delta_k) = \frac{(N\Gamma_{1D})^2}{(\Gamma' + N\Gamma_{1D})^2 + 4\delta_k^2},$$
$$T(\delta_k) = \frac{\Gamma'^2 + 4\delta_k^2}{(\Gamma' + N\Gamma_{1D})^2 + 4\delta_k^2}.$$

The effect of N atoms arranged in this way is to effectively increase the decay rate into the waveguide Γ_{1D} by a factor of N. In a sense, one can obtain characteristics reminiscent of those shown in figure 3.3(a) even if a single atom behaves like shown in figure 3.3(b). Since such an atomic mirror has a high reflectance for high enough N, one can build a

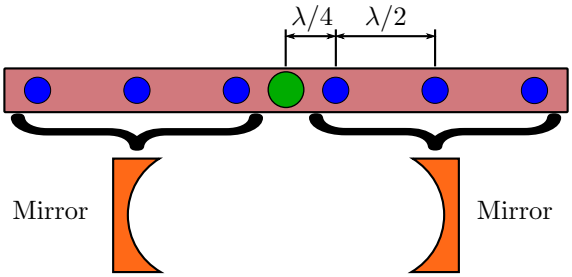

Figure 3.4: Two-level atoms (small blue) and an "impurity" atom (big green) placed in a waveguide (red rectangular background). The two-level atoms are placed with distance $\lambda/2$ from each other and with distance $\lambda/4$ from the impurity atom. The two-level atoms effectively create mirrors around the impurity atom.

cavity around some "impurity" atom [16] by using a pair of these mirrors (figure 3.4). The impurity atom needs to be placed such that its distance from the mirrors is $\lambda/4$, i.e. it is located on the antinode of the field. This way the coupling strength is maximized.

Cavities are often used in quantum optics experiments because (among other things) they can enhance interactions of light and atoms by making photons pass through the atom multiple times. The other often employed technique to enhance the interaction strength is to use atomic ensembles [17] and consider coupling of the light to the collective modes of the atoms. Construction of atomic mirrors can be regarded as a first step in the merger of these two approaches. We shall later look at a setup where this "cavity-ensemble duality" is even more apparent (section 8.2).

3.3.2 Slow light

In section 3.3.1 we have seen, how the reflection from an array of two-level atoms can be enhanced. Here we shall see, how the "transparency" can be enhanced by using an array of three-level atoms. To this end we shall introduce the transfer matrix formalism here, because it will also be used later. The description of EIT here is mostly based on [18], which compared to previous treatments considered EIT in the high Γ_{1D} regime. In terms of parameters of (3.7) we set $\Delta_p = 0$ and assume that the incoming electric field pulse has the carrier frequency on resonance with the transition $|a\rangle \leftrightarrow |b\rangle$, i.e. $\delta_{k_0} = 0$.

In section 3.2 we essentially found the relations

$$E_R(z_j^+) = t(\delta_k)E_R(z_j^-) + r(\delta_k)E_L(z_j^+), \tag{3.9}$$

$$E_L(z_j^-) = t(\delta_k)E_L(z_j^+) + r(\delta_k)E_R(z_j^-). \tag{3.10}$$

Instead we want to find a matrix M such that

$$\begin{pmatrix} E_{\mathrm{R}}(z_j^+) \\ E_{\mathrm{L}}(z_j^+) \end{pmatrix} = M \begin{pmatrix} E_{\mathrm{R}}(z_j^-) \\ E_{\mathrm{L}}(z_j^-) \end{pmatrix}$$

After rewriting (3.9) and (3.10) and defining

$$\beta(\delta_k) = -\frac{r(\delta_k)}{t(\delta_k)}$$

we obtain

$$M(\beta) = \frac{1}{t} \begin{pmatrix} t^2 - r^2 & r \\ -r & 1 \end{pmatrix} = \begin{pmatrix} 1-\beta & -\beta \\ \beta & 1+\beta \end{pmatrix}. \tag{3.11}$$

Free evolution between the scattering processes is described by the transfer matrix

$$M_f(kd) = \begin{pmatrix} e^{ikd} & 0 \\ 0 & e^{-ikd} \end{pmatrix} \tag{3.12}$$

given in terms of the k-vector and distance d.

Using $M(\beta)$ and $M_f(kd)$ one can in principle build any unit cell of a periodic arrangement of two-level or three-level atoms. For the case of EIT as considered in [18] the unit cell consists of a three-level atom and free space propagation. The parameter β for reflection and transmission coefficients of the three-level atom (3.7) is

$$\beta_3(\delta_k) = -\frac{r_3(\delta_k)}{t_3(\delta_k)} = \frac{\Gamma_{1\mathrm{D}}(\delta_k - \Delta_{\mathrm{p}})}{(\Gamma' - 2i\delta_k)(\delta_k - \Delta_{\mathrm{p}}) + 2i|\Omega|^2}. \tag{3.13}$$

The transfer matrix for the unit cell is then $M_{\mathrm{cell}} = M_f(kd)M(\beta_3)$. We also note here that in general, when a transfer matrix

$$T = \begin{pmatrix} T_{11} & T_{12} \\ T_{21} & T_{22} \end{pmatrix} \tag{3.14}$$

for an array of linear optical elements has been computed, we can always recover transmission and reflection coefficients for the whole array. The transmission and reflection coefficients are given by

$$t = \frac{1}{T_{22}}, \quad r = \frac{T_{12}}{T_{22}}.$$

In the high $\Gamma_{1\mathrm{D}}$ regime, reflection can be a significant factor. As we have seen in figure 3.3, reflectance from a three-level atom is only zero on resonance, but for slight deviations from resonance we rapidly approach reflectance of a two-level atom, which is close

to 1 in the high Γ_{1D} limit. Since by the principle of uncertainty of quantum mechanics the pulses of electric field have a certain spread of δ_k, the spacing between the atom is important. Compared with section 3.3.1, where we put atoms $\lambda/2$ apart to *maximize* reflection from the whole array, now we shall put atoms $d = \lambda/4$ apart to *minimize* reflection from the whole array. This was shown in [18] by considering the transfer matrix for two consecutive blocks M_{cell}^2. The physical reason for choosing $d = \lambda/4$ is that reflections from two consecutive cells interfere destructively.

Having decided the spacing between the atoms d, we shall now find the dispersion relation. We do this by obtaining an expression for the Bloch vectors K_b. If we diagonalize the matrix $M_{\text{cell}} = SDS^{-1}$, then the diagonal matrix will have the form

$$D = \begin{pmatrix} e^{iK_b d} & 0 \\ 0 & e^{-iK_b d} \end{pmatrix}. \tag{3.15}$$

For a general transfer matrix (3.14) we can rewrite the characteristic equation $\det(T - e^{\pm iK_b d} I) = 0$ to obtain

$$\det(T) + e^{\pm 2iK_b d} = \text{tr}(T) e^{\pm iK_b d}.$$

Both transfer matrices (3.11) and (3.12) can be verified to have determinant 1, and since T is a product of those, we have $\det(T) = 1$. Using the specific form of the eigenvalues (3.15) we obtain the equation for the Bloch vectors

$$\cos(K_b d) = \frac{1}{2}\text{tr}(T).$$

For the specific transfer matrix $T = M_{\text{cell}}$ that we are considering, the equation above becomes

$$\cos(K_b d) = \cos(kd) - i\beta_3(\delta_k)\sin(kd). \tag{3.16}$$

The sine and cosine on the right hand side come from free space propagation. We shall assume that dispersion due to free space propagation is negligible compared to dispersion due to scattering from the atoms. Thus we approximate $kd = k_0 d + \delta_k d/c \approx k_0 d = \pi/2$.

The left hand side of the equation (3.16) is bounded by unity in absolute value, while there is no such restriction on the right hand side. This implies a band gap, since for some values of δ_k there is no K_b to satisfy the equation. For the case of negligible spontaneous decay Γ' and in the weakly coupled EIT regime ($\Omega < \Gamma_{1D}$), there are band gaps for the values of δ_k from $\pm 2\Omega^2/\Gamma_{1D}$ to $\pm\Gamma_{1D}/2$. Thus the width of the EIT window here is $4\Omega^2/\Gamma_{1D}$. Inside this window, the electric field pulse will experience slow group velocity ("slow light"). This fact can be seen by finding δ_k from (3.16) as a function of K_b. Expanding up to second order we obtain

$$\delta_k(k) \approx v_g(k - k_0) + \frac{1}{2}\alpha(k - k_0)^2. \tag{3.17}$$

with

$$v_{\mathrm{g}} = \frac{2d|\Omega|^2}{\Gamma_{1\mathrm{D}}}, \quad \alpha = -i\frac{4d^2|\Omega|^2\Gamma'}{\Gamma_{1\mathrm{D}}^2} \tag{3.18}$$

being the group velocity and absorption respectively. We see that the group velocity can be controlled by the strength of the classical drive $|\Omega|$ and can in principle be arbitrarily close to zero. The reason for the slow group velocity is that the photons spend a significant fraction of the time as stationary atomic excitations. This property was the motivation for introduction of *dark-state polaritons* [19], which are quasiparticles of the combined excitations of atoms and electric field. They are called "dark-state" because the excitations are stored in the meta-stable states $|c\rangle$ which do not spontaneously radiate light. The excitations stored in the meta-stable states are often referred to as *spinwaves* in the literature.

Using the expansion (3.17) we can find, how a photon propagates inside the ensemble of three-level atoms. We look at the situation when the photon has already completely entered the ensemble. If the number of atoms is big, we can treat them as a continuous medium that has an effective dispersion relation given by (3.17). Suppose that the initial wavefunction of the photon is f, so that the probability of it being at a position z is given by $|f(z)|^2$. Then, if we denote the Fourier transform of f by $\tilde{f}$, the wavefunction after time t is given by

$$f(z,t) = \frac{1}{\sqrt{2\pi}}\int_{-\infty}^{\infty}\tilde{f}(k)e^{ikz-i\delta_k(k)t}dk.$$

For an initial Gaussian wavefunction

$$f(z) = \frac{1}{(2\pi\sigma^2)^{1/4}}\exp\left(-\frac{(z-\mu)^2}{4\sigma^2}\right)e^{ik_0 z}, \tag{3.19}$$

we obtain

$$f(z,t) = \frac{1}{(2\pi\sigma^2)^{1/4}}\sqrt{\frac{1}{1+\frac{i\alpha t}{2\sigma^2}}}\exp\left(-\frac{(z-\mu-v_{\mathrm{g}}t)^2}{4\sigma^2(1+\frac{i\alpha t}{2\sigma^2})}\right)e^{ik_0 z}. \tag{3.20}$$

From the last expression we see that the wavefunction moves with group velocity v_{g} and its shape is preserved if $i\alpha t/\sigma^2 \ll 1$. (Note that $i\alpha$ is real and positive.) The parameter $i\alpha t/\sigma^2$ also appears in the expression for the norm of the final state:

$$\mathcal{N}_{\mathrm{final}}^2 = \int_{-\infty}^{\infty}|f(z,t)|^2dz = \frac{1}{\sqrt{1+\frac{i\alpha t}{2\sigma^2}}} \approx 1 - \frac{i\alpha t}{4\sigma^2}, \tag{3.21}$$

where in the last line we expanded around the limit $i\alpha t/\sigma^2 \ll 1$. Also, here we assumed an infinte ensemble for simplicity.

To pass through the entire ensemble we need to choose $t = L/v_{\mathrm{g}}$. Expressing the spacing between the atoms as $d = L/N$ we have

$$\frac{i\alpha t}{2\sigma^2} = \frac{\Gamma' L^2}{N\Gamma_{1\mathrm{D}}\sigma^2} \tag{3.22}$$

We see that regardless of the values $\Gamma_{1\mathrm{D}}$ and Γ' (which are usually hard to adjust), (3.22) can be made arbitrarily small by using more atoms in the ensemble. Thus it is the parameter $N\Gamma_{1\mathrm{D}}/\Gamma'$ that matters for the linear effects and not any of those quantities separately. The expression (3.22) also suggests that for narrow pulses (L/σ big) it is harder to achieve lossless propagation than for wide pulses.

Chapter 4

"Electric field elimination" theory

4.1 Motivation

In chapter 3 we considered the linear (single photon) properties of the two-level and three-level atoms. In this thesis, however, our ultimate goal is to study nonlinear (two photon) processes. For the nonlinear processes, it is challenging to generalize the techniques that we have used in section 3.2. For the transfer matrix formalism, for example, we have effectively replaced each atom with a simple transmission and reflection coefficient. But it is not always a valid approximation. For instance, a two-level atom that has absorbed a photon and not yet reemitted it, cannot absorb another one immediately. Thus the second photon will have a completely different transmission and reflection coefficient than the first one.

On the other hand, freely propagating photons have for all practical purposes a completely linear behaviour. It is the atoms that make photons behave nonlinearly. It is indeed possible to find effective equations of motion for the photons taking into account the nonlinearities due to the atoms in a perturbative fashion. We shall do that in chapter 7. Even though the resulting equations of motion obtained there are rather simple and have a clear intuitive interpretation, it it not possible to determine from that formalism alone, whether too much information was discarded or not. Taking first steps towards answering that question will be another major topic of this thesis (the first one being the construction of a photon phase gate).

Since it is the atoms that cause the nonlinearities, the main idea of the formalism presented in this chapter is to *focus on the atoms and effectively eliminate the electric field.* This approach may seem counterintuitive at first. After all, our goal is to describe *photon* gates. However, by elimination we do not mean completely discarding the information about the photons. As we shall see, the states of the photons can be exactly and straightforwardly recovered, if the states of the atoms are known. Furthermore, we have noted before that in the case of EIT the photons actually become polaritons (mixed light and

atom excitations), so looking at the atomic excitations (spinwaves) directly will already tell us, how the polaritons propagate through the ensemble. Hence we do not actually need to calculate the states of the electric field.

4.2 Preliminaries

Before we begin the derivation, we shall briefly restate certain facts about the dynamics of open systems. In general, a state is described by a density operator $\hat{\rho}$. The evolution of the density operator is given by

$$\dot{\hat{\rho}} = -\frac{i}{\hbar}[\hat{H}, \hat{\rho}] + \mathcal{L}[\hat{\rho}],$$

where the Hamiltonian $\hat{H}$ describes the unitary evolution, and the Lindblad superoperator $\mathcal{L}$ describes the dissipative processes. The most general form of $\mathcal{L}$ is

$$\mathcal{L}[\hat{\rho}] = -\frac{1}{2}\left(\hat{C}^\dagger\hat{C}\hat{\rho} + \hat{\rho}\hat{C}^\dagger\hat{C} - 2\hat{C}\hat{\rho}\hat{C}^\dagger\right). \tag{4.1}$$

The operators $\hat{C}$ here are arbitrary for the time being. Later, we shall look at a couple of concrete examples. The simplest one is $\hat{C} = \Gamma' \sum_j \hat{\sigma}^j_{ab}$ that describes the decay from the excited state $|b\rangle$ to the ground state $|a\rangle$ for each of the individual atoms in the ensemble with the decay rate Γ'.

In (4.1), we shall call $2\hat{C}\hat{\rho}\hat{C}^\dagger$ the *jump term*. The non-jump terms ($\hat{C}^\dagger\hat{C}\hat{\rho}$ and $\hat{\rho}\hat{C}^\dagger\hat{C}$) can be absorbed into the non-Hermitian Hamiltonian

$$\hat{H}_N = \hat{H} - \frac{i\hbar}{2}\hat{C}^\dagger\hat{C}.$$

Then the evolution of the density matrix is given by the equation

$$\dot{\hat{\rho}} = -\frac{i}{\hbar}\left(\hat{H}_N\hat{\rho} - \hat{\rho}\hat{H}_N^\dagger\right) + \hat{C}\hat{\rho}\hat{C}^\dagger.$$

If the jump term can be neglected, and if the initial state is a pure state $|\psi\rangle$, then there is no need to consider the full density matrix evolution. The pure state itself can be evolved directly by using the non-Hermitian Hamiltonian and solving the Schrödinger equation

$$i\hbar\frac{\partial}{\partial t}|\psi\rangle = \hat{H}_N|\psi\rangle.$$

It has the formal solution $|\psi(t)\rangle = \exp(-i\hat{H}_N t/\hbar)|\psi(0)\rangle$. The jump terms can be taken into account by performing projections into the state $|\psi\rangle_{\text{projected}} = \hat{C}|\psi\rangle$ at discrete times. This is the so-called stochastic wavefunction approach [20].

For the operator $\hat{C} = \Gamma' \sum_j \hat{\sigma}^j_{ab}$ of the example above, the role of the non-jump terms is to take the probability out of the excited states, and the role of the jump term is to put that probability back into the ground states. In the following we shall be distinguishing between the *ground state of a particular atom*, which is the state $|a\rangle$ of that atom, and the *ground state of the ensemble* $|a\rangle^N$, which is the collective state of all the atoms, where each of the N atoms is in the state $|a\rangle$.

The Heisenberg equation of motion for a given operator $\hat{A}$ due to action of the non-Hermitian Hamiltonian is

$$\frac{\mathrm{d}}{\mathrm{d}t}\,\hat{A} = \frac{i}{\hbar}\left(\hat{H}_N^\dagger \hat{A} - \hat{A}\hat{H}_N\right). \tag{4.2}$$

This equation would have reduced to the regular Heisenberg equation, if $\hat{H}_N$ were Hermitian.

4.3 Derivation

Our starting point for the derivation will be the same Hamiltonian as in section 3.2, with the difference that now we explicitly sum over all the atoms in the ensemble. Also assume real Ω for simplicity. We have

$$\begin{aligned}\hat{H} =& \hbar \sum_j \left\{ \omega_{ba}\hat{\sigma}^j_{bb} + \omega_{ca}\hat{\sigma}^j_{cc} - \Omega\left[\hat{\sigma}^j_{bc}e^{-i\omega_\mathrm{p}t} + \hat{\sigma}^j_{cb}e^{i\omega_\mathrm{p}t}\right]\right\} \\ &- \hbar g\sqrt{2\pi}\int \sum_j \delta(z-z_j)\left\{\hat{\sigma}^j_{ba}\left[\hat{E}_\mathrm{R}(z)+\hat{E}_\mathrm{L}(z)\right] + \left[\hat{E}^\dagger_\mathrm{R}(z)+\hat{E}^\dagger_\mathrm{L}(z)\right]\hat{\sigma}^j_{ab}\right\} dz \\ &+ i\hbar c\int\left[\hat{E}^\dagger_\mathrm{L}(z)\,\frac{\partial \hat{E}_\mathrm{L}}{\partial z} - \hat{E}^\dagger_\mathrm{R}(z)\,\frac{\partial \hat{E}_\mathrm{R}}{\partial z}\right] dz.\end{aligned}$$

The decay to modes outside of the waveguide with the rate Γ' is described by the Lindblad superoperator

$$\mathcal{L}[\hat{\rho}] = -\frac{\Gamma'}{2}\sum_j\left(\hat{\sigma}^j_{ba}\hat{\sigma}^j_{ab}\hat{\rho} + \hat{\rho}\hat{\sigma}^j_{ba}\hat{\sigma}^j_{ab} - 2\hat{\sigma}^j_{ab}\hat{\rho}\hat{\sigma}^j_{ba}\right).$$

Heisenberg equations for the atoms are

$$\begin{aligned}\dot{\hat{\sigma}}^j_{ab} &= -i\omega_{ba}\hat{\sigma}^j_{ab} + i\Omega\hat{\sigma}^j_{ac}e^{-i\omega_\mathrm{p}t} - ig\sqrt{2\pi}(\hat{\sigma}^j_{bb}-\hat{\sigma}^j_{aa})\left[\hat{E}_\mathrm{R}(z_j)+\hat{E}_\mathrm{L}(z_j)\right], \\ \dot{\hat{\sigma}}^j_{ac} &= -i\omega_{ca}\hat{\sigma}^j_{ac} + i\Omega\hat{\sigma}^j_{ab}e^{i\omega_\mathrm{p}t} - ig\sqrt{2\pi}\hat{\sigma}^j_{bc}\left[\hat{E}_\mathrm{R}(z_j)+\hat{E}_\mathrm{L}(z_j)\right], \\ \dot{\hat{\sigma}}^j_{bc} &= i(\omega_{ba}-\omega_{ca})\hat{\sigma}^j_{bc} - i\Omega(\hat{\sigma}^j_{cc}-\hat{\sigma}^j_{bb})e^{i\omega_\mathrm{p}t} - ig\sqrt{2\pi}\left[\hat{E}^\dagger_\mathrm{R}(z_j)+\hat{E}^\dagger_\mathrm{L}(z_j)\right]\hat{\sigma}^j_{ac}.\end{aligned}$$

These are not all the equations for the atoms. We are missing the populations $\hat{\sigma}^j_{aa}$, $\hat{\sigma}^j_{bb}$ and $\hat{\sigma}^j_{cc}$, while equations for the other coherences $\hat{\sigma}^j_{ab}$, $\hat{\sigma}^j_{ca}$ and $\hat{\sigma}^j_{bc}$ can be obtained by the Hermitian conjugation. Our final goal in this derivation is to obtain an effective Hamiltonian that will give the Heisenberg equations of motion for the atoms (with the electric field eliminated). In that sense the equations of motion above will serve as examples to check, whether the effective Hamiltonian is the correct one. We could have written down the equations for the populations and the rest of the coherences and applied the same transformations, as we are going to use on the equations for $\hat{\sigma}^j_{ba}$, $\hat{\sigma}^j_{ac}$ and $\hat{\sigma}^j_{cb}$, but for the sake of brevity we shall not do so.

We continue with the first step towards elimination of the electric field from the above equations. Heisenberg equations for the fields are

$$\left(\frac{1}{c}\frac{\partial}{\partial t}+\frac{\partial}{\partial z}\right)\hat{E}_{\mathrm{R}}(z)=\frac{ig\sqrt{2\pi}}{c}\sum_j\delta(z-z_j)\hat{\sigma}^j_{ab},$$
$$\left(\frac{1}{c}\frac{\partial}{\partial t}-\frac{\partial}{\partial z}\right)\hat{E}_{\mathrm{L}}(z)=\frac{ig\sqrt{2\pi}}{c}\sum_j\delta(z-z_j)\hat{\sigma}^j_{ab}.$$

These can be solved exactly. The general solutions are

$$\hat{E}_{\mathrm{R}}(z,t)=\hat{E}_{\mathrm{R,in}}(z-ct)+\frac{ig\sqrt{2\pi}}{c}\sum_j\theta_{\mathrm{H}}(z-z_j)\hat{\sigma}^j_{ab}\left(t-\frac{z-z_j}{c}\right),$$
$$\hat{E}_{\mathrm{L}}(z,t)=\hat{E}_{\mathrm{L,in}}(z+ct)+\frac{ig\sqrt{2\pi}}{c}\sum_j\theta_{\mathrm{H}}(z_j-z)\hat{\sigma}^j_{ab}\left(t-\frac{z_j-z}{c}\right),$$

where $\hat{E}_{\mathrm{R,in}}$ and $\hat{E}_{\mathrm{L,in}}$ are arbitrary operators which represent the free propagation of the input modes of the electric field. We shall assume here that there's no input light in the waveguide, so we set $\hat{E}_{\mathrm{R,in}}(z-ct)=\hat{E}_{\mathrm{L,in}}(z+ct)=0$. Setting these operators equal to zero makes $\hat{E}_{\mathrm{R}}$ and $\hat{E}_{\mathrm{L}}$ no longer commute with $\hat{\sigma}^j_{ab}$ and $\hat{\sigma}^j_{ac}$. Since we want to insert the expressions for $\hat{E}_{\mathrm{R}}$ and $\hat{E}_{\mathrm{L}}$ into the equations for the atoms, we need to choose a definite position of $\hat{E}_{\mathrm{R}}$ and $\hat{E}_{\mathrm{L}}$ with respect to $\hat{\sigma}^j_{ab}$ and $\hat{\sigma}^j_{ac}$ and stick with it in all the following calculations. We choose the positions such that the expectation value of the ground state of the ensemble is zero. With such choice of the ordering we obtain

$$\dot{\hat{\sigma}}^j_{ab}=-i\omega_{ba}\hat{\sigma}^j_{ab}+i\Omega\hat{\sigma}^j_{ac}e^{-i\omega_{\mathrm{p}}t}+\frac{2\pi g^2}{c}(\hat{\sigma}^j_{bb}-\hat{\sigma}^j_{aa})\sum_k\hat{\sigma}^k_{ab}\left(t-\frac{|z_j-z_k|}{c}\right),$$
$$\dot{\hat{\sigma}}^j_{ac}=-i\omega_{ca}\hat{\sigma}^j_{ac}+i\Omega\hat{\sigma}^j_{ab}e^{i\omega_{\mathrm{p}}t}+\frac{2\pi g^2}{c}\hat{\sigma}^j_{bc}\sum_k\hat{\sigma}^k_{ab}\left(t-\frac{|z_j-z_k|}{c}\right),$$
$$\dot{\hat{\sigma}}^j_{bc}=i(\omega_{ba}-\omega_{ca})\hat{\sigma}^j_{bc}-i\Omega(\hat{\sigma}^j_{cc}-\hat{\sigma}^j_{bb})e^{i\omega_{\mathrm{p}}t}-\frac{2\pi g^2}{c}\sum_k\hat{\sigma}^k_{ba}\left(t-\frac{|z_j-z_k|}{c}\right)\hat{\sigma}^j_{ac}.$$

Until now we were only doing the exact transformations. Even though the equations above no longer depend on the electric field, they are also non-local, i.e. the evolution of one coherence depends on the values of all the other coherences at previous times which are set by how long it took the photon to carry the information between the sites. Thus the approximation that we are going to employ here is to explicitly *make the equations local*. This amounts to saying that we actually *know*, what the coherences were at the previous times – they simply differ by a phase that was accumulated while the photon was travelling from one site to another. In other words this is the limit where the time it takes for one photon to completely get out of an atom $\sim 1/\Gamma_{1\mathrm{D}}$ is much bigger than the time it takes for it to reach any other atom in the ensemble $\sim L/c$, so it is the limit of very long photons and very short ensembles.

Formally the above idea is expressed by defining new slowly varying coherences $\hat{S}^j_{ab}$, $\hat{S}^j_{ac}$ and $\hat{S}^j_{bc}$. If the carrier frequency of the quantum light is ω_{k_0}, and the frequency of the classical light is ω_p, then these new coherences can be related to the old ones by $\hat{\sigma}^j_{ab}(t) = \hat{S}^j_{ab}(t)e^{-i\omega_{k_0}t}$, $\hat{\sigma}^j_{ac}(t) = \hat{S}^j_{ac}(t)e^{-i(\omega_{k_0}-\omega_\mathrm{p})t}$ and $\hat{\sigma}^j_{bc}(t) = \hat{S}^j_{bc}(t)e^{i\omega_\mathrm{p}t}$. For the equations below we define $k_0 = \omega_{k_0}/c$, $\Delta_1 = \omega_{k_0} - \omega_{ba}$ and $\Delta_\mathrm{p} = \omega_\mathrm{p} - (\omega_{ba} - \omega_{ca})$. We shall assume that $\hat{S}^j_{ab}\left(t - |z_j - z_k|/c\right) \approx \hat{S}^j_{ab}(t)$ and likewise for the other slowly varying quantities. Also, just as before we recognize the decay rate into the waveguide $\Gamma_{1\mathrm{D}} = 4\pi g^2/c$. The equations for the slowly varying quantities are

$$\begin{aligned}
\dot{\hat{S}}^j_{ab} &= i\Delta_1\hat{S}^j_{ab} + i\Omega\hat{S}^j_{ac} + \frac{\Gamma_{1\mathrm{D}}}{2}\sum_k(\hat{\sigma}^j_{bb} - \hat{\sigma}^j_{aa})\hat{S}^k_{ab}e^{ik_0|z_j-z_k|},\\
\dot{\hat{S}}^j_{ac} &= i(\Delta_1 - \Delta_\mathrm{p})\hat{S}^j_{ac} + i\Omega\hat{S}^j_{ab} + \frac{\Gamma_{1\mathrm{D}}}{2}\sum_k\hat{S}^j_{bc}\hat{S}^k_{ab}e^{ik_0|z_j-z_k|},\\
\dot{\hat{S}}^j_{bc} &= i\Delta_\mathrm{p}\hat{S}^j_{bc} - i\Omega(\hat{\sigma}^j_{cc} - \hat{\sigma}^j_{bb}) - \frac{\Gamma_{1\mathrm{D}}}{2}\sum_k\hat{S}^k_{ba}\hat{S}^j_{ac}e^{-ik_0|z_j-z_k|}.
\end{aligned} \tag{4.3}$$

The evolution described by these equations is caused by the effective Hamiltonian

$$\begin{aligned}
\hat{H} = &-\hbar\sum_j(\Delta_1\hat{\sigma}^j_{bb} + (\Delta_1 - \Delta_\mathrm{p})\hat{\sigma}^j_{cc}) - \hbar\sum_j\Omega(\hat{S}^j_{bc} + \hat{S}^j_{cb})\\
&+\hbar\sum_{j,k}\frac{\Gamma_{1\mathrm{D}}}{2}\sin(k_0|z_j - z_k|)\hat{S}^j_{ba}\hat{S}^k_{ab}
\end{aligned}$$

and the Lindblad superoperator

$$\begin{aligned}
\mathcal{L}[\hat{\rho}] = &-\frac{\Gamma'}{2}\sum_j\left(\hat{S}^j_{ba}\hat{S}^j_{ab}\hat{\rho} + \hat{\rho}\hat{S}^j_{ba}\hat{S}^j_{ab} - 2\hat{S}^j_{ab}\hat{\rho}\hat{S}^j_{ba}\right)\\
&-\frac{\Gamma_{1\mathrm{D}}}{2}\sum_{j,k}\left[\cos(k_0|z_j - z_k|)\left(\hat{S}^j_{ba}\hat{S}^k_{ab}\hat{\rho} + \hat{\rho}\hat{S}^j_{ba}\hat{S}^k_{ab} - 2\hat{S}^k_{ab}\hat{\rho}\hat{S}^j_{ba}\right)\right].
\end{aligned}$$

Alternatively if the jump terms in $\mathcal{L}[\hat{\rho}]$ can be neglected, the evolution is described by the non-Hermitian Hamiltonian

$$\begin{aligned}\hat{H}_N = &-\hbar\sum_j\left[(\Delta_1+i\Gamma'/2)\hat{\sigma}^j_{bb}+(\Delta_1-\Delta_\mathrm{p})\hat{\sigma}^j_{cc}\right]-\hbar\sum_j\Omega(\hat{S}^j_{bc}+\hat{S}^j_{cb})\\ &-i\hbar\sum_{j,k}\frac{\Gamma_{1\mathrm{D}}}{2}e^{ik_0|z_j-z_k|}\hat{S}^j_{ba}\hat{S}^k_{ab}\end{aligned} \tag{4.4}$$

The intuitive explanation of the interaction terms $\frac{\hbar\Gamma_{1\mathrm{D}}}{2}e^{ik_0|z_j-z_k|}\hat{S}^j_{ba}\hat{S}^k_{ab}$ is that from the point of view of the atoms, whenever any one of them decays by emitting a photon into the waveguide mode, each of the other ones can become excited due to that. The new excitation will differ by the phase $e^{ik_0|z_j-z_k|}$ that is determined by how long the photon travelled before it got reabsorbed. For the two-level atoms (set $\Omega=0$ in $\hat{H}_N$), an example of such a process can be seen in figure 4.1.

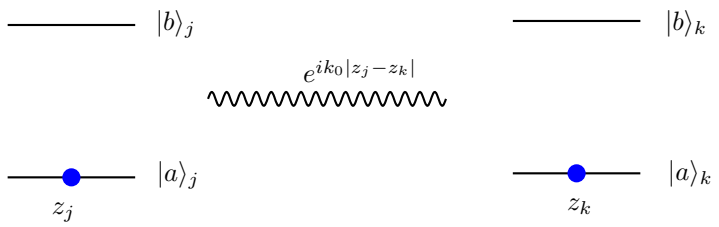

Figure 4.1: A snapshot of a possible interaction process between two atoms (at positions z_j and z_k in the ensemble). One of them has decayed from the excited state $|b\rangle_j$ to the ground state $|a\rangle_j$ by emitting a photon into the waveguide mode. When the other will go from the ground state $|a\rangle_k$ to the excited state $|b\rangle_k$ by absorbing the photon, the new excitation will have a phase difference with respect to the old one.

For the purposes that we want to use this formalism, the non-Hermitian Hamiltonian $\hat{H}_N$ and its generalizations are sufficient. In a typical setup, we shall consider (see an example later in section 4.5), we shall initialize the atomic coherences of the atoms such that they collectively contain one or two excitations. These excitations will then propagate through the ensemble and some part of them will decay to the ground state of the ensemble or go from the double excitation manifold to the single excitation manifold. In the end we want to calculate fidelities, i.e. project the final state onto some superposition of the excited states (in the same manifold, that the initial state was in). For those kinds of calculations the probability that went to a lower excitation manifold or ended up in the ground state of the ensemble (that we neglect by using $\hat{H}_N$) is unimportant. Some issues may arise, if we tried to consider initial state that was in a superposition of the double and

single excitation manifolds. Then the single excitation part of it will get influenced by the decay from the double excitation manifold. This influence will be unaccounted for by only considering $\hat{H}_N$.

Note that if one tries to use the non-Hermitian Hamiltonian (4.4) to obtain the equations (4.3) using (4.2), some discrepancies in the non-Hermitian part of the equations will be observed. Those are caused by the fact that we *do* indeed discard some information about the dissipative part of the evolution when we use the non-Hermitian Hamiltonian.

4.4 Application to numerical simulations

Even though the formalism described in this chapter can be used to obtain analytical results, we shall focus on its application to the numerical simulations. Compared to the transfer matrix theory of section 3.2 we did not do any linearization of the equations of motion. Neither did we convert them into equations of complex-valued functions instead of operators. All the operator properties are still retained in the effective Hamiltonian $\hat{H}_N$. Because of that we can in principle find, how an arbitrary initial state of the ensemble $|\psi_{\text{initial}}\rangle$ evolves. The final state is then given by

$$|\psi_{\text{final}}(t)\rangle = \exp(-i\hat{H}_N t/\hbar)|\psi_{\text{initial}}\rangle. \tag{4.5}$$

The general state of an ensemble of N three-level atoms contains 3^N complex numbers which makes computation of its evolution intractable. As a reminder, this is why we wanted to build a quantum computer: such ensembles of many atoms cannot be simulated on classical computers because of the exponential growth of the Hilbert space. For our purposes we do not need to simulate the general case. Since we wanted to consider the states with at most two incoming photons, then only those states of the ensemble will be excited, that have at most two atomic excitations. Let us introduce the notation that we are going to use in the following. We shall call the state, where the atom with index j is in state $|b\rangle$, and the rest are in the states $|a\rangle$, by $|b_j a\rangle = \hat{S}^j_{ba}|a\rangle^N$. Likewise, $|c_j a\rangle = \hat{S}^j_{ca}|a\rangle^N$ is the state, where the atom j is in $|c\rangle$, and the rest are in $|a\rangle$. For the double excitations we do a straightforward generalization of this notation. For example, the state $|b_j c_k a\rangle = \hat{S}^j_{ba}\hat{S}^k_{ca}|a\rangle^N$ is the state with atom j in $|b\rangle$, atom k in $|c\rangle$ and the rest in $|a\rangle$. In this way it is clear that there are N states $|b_j a\rangle$ and N states $|c_j a\rangle$. Hence the basis for the Hilbert space of the single excitations has the size $2N$. For the double excitations, the number of states $|b_j b_k a\rangle$ and $|c_j c_k a\rangle$ is the same and is equal to the number of ways one can choose two excitations among N states, i.e. the binomial coefficient

$$\binom{N}{2} = \frac{N!}{2!(N-2)!} = \frac{N(N-1)}{2}.$$

Additionally there are $N^2 - N$ states of the form $|b_j c_k a\rangle$ (we subtract N, since states $|b_j c_j a\rangle$ are unphysical). Adding them all together results in $2N^2 - 2N$ as the size of the double excitation basis.

Thus we have shown that, if we only consider states with up to two excitations, the basis of the Hilbert space will grow at most quadratically instead of exponentially, which will allow us to simulate much bigger ensembles.

4.5 A simple benchmark

Before we apply the formalism derived here to systems with nonlinear behaviour, we can check its validity on something simpler first. EIT is a linear phenomenon and is a good test case, since it generalizes to a collective effect of many atoms, and in section 3.2 we have already derived, how a Gaussian pulse will propagate in an ensemble with three-level atoms.

In this benchmark we shall start out with the initial state of N atoms

$$|\psi_{\text{initial}}\rangle = \sum_{j=0}^{N} f(z_j)\sqrt{d}|c_j a\rangle, \tag{4.6}$$

where d is the distance between the atoms, and $f(z)$ is given by (3.19). Then we find the final state using a projection of (4.5) onto the single excitation basis: $|b_j a\rangle$ and $|c_j a\rangle$. The final state found numerically is compared to the analytical final state

$$|\psi_{\text{final,analytical}}(t)\rangle = \sum_{j=0}^{N} f(z_j, t)\sqrt{d}|c_j a\rangle, \tag{4.7}$$

where $f(z,t)$ is given by (3.20).

The comparison of the numerical and analytical results can be seen in figure 4.2. From those results we see that the numerical and the analytical results converge towards each other in the limit where losses given by (3.22) become small, and if the wavepackets are well localized inside the ensemble. In the figure we increased Γ_{1D}/Γ' from 0.1 to 0.2, but instead we could have increased number of atoms from $N = 500$ to $N = 1000$ and obtained identical results.

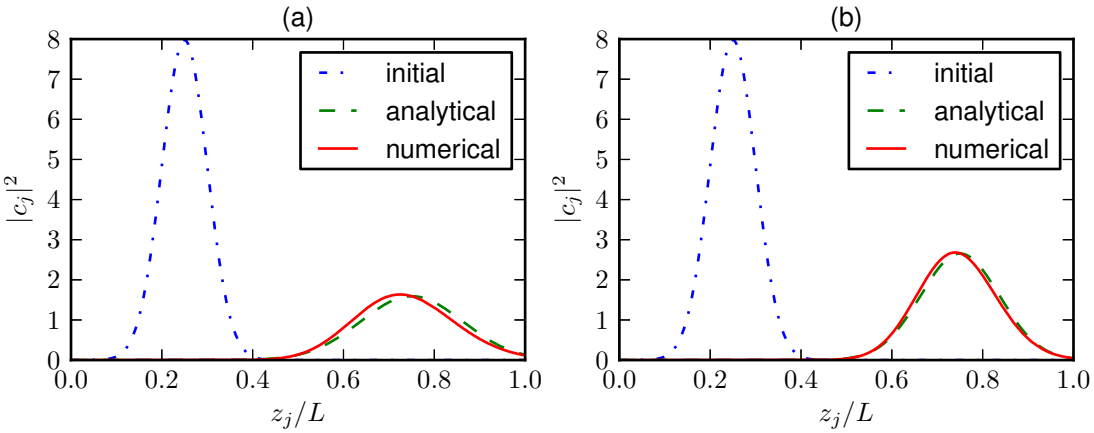

Figure 4.2: An initial Gaussian spinwave (given by the state (4.6)) with width $\sigma = L/20$ and mean $\mu = L/4$ is propagated through the ensemble numerically. For both plots we use the number of atoms $N = 500$ and the strength of the classical drive $\Omega = 0.1(\Gamma' + \Gamma_{1D})$. In (a) we set $\Gamma_{1D} = 0.1\Gamma'$, and in (b) we set $\Gamma_{1D} = 0.2\Gamma'$. The evolution time was chosen such that $v_g t = L/2$. The numerical result is compared to the analytical one given by (4.7). The spinwaves in the plots are normalized such that their norm is given by their integral (instead of their sum). In other words they are *not* multiplied by $\sqrt{d}$ as in (4.6) and (4.7).

Chapter 5

Choosing a physical system for a phase gate

5.1 General principles

We have defined the operation of the controlled phase gate by the matrix (2.5). We want to make a physical device that performs that abstract operation. Our plan is to use atoms (either single atoms or ensembles of atoms) to mediate interactions between the photons. In section 3.2 we have shown that with right parameters three-level atoms can be made transparent, and two-level atoms behave as mirrors that reflect pulses and impart them a phase of π. We want to use this phase to make a controlled phase gate with. Since that phase shift results from reflections, we need to effectively collide photons with each other.

Let us define the basis first. Ultimately we shall consider two-photon processes, which means that we need to use the two-qubit states (2.2). We shall implicitly assume dual-rail encoding, so when we say a photon is absent, we mean that it is absent from the mode that represents the state $|1\rangle$ and instead is in the mode that represents the state $|0\rangle$. Thus $|00\rangle$ is the state with no photons present. The basis states $|01\rangle$ and $|10\rangle$ are the physical states with one photon moving to the right and to the left respectively. We define our basis as being time dependent so that $|01\rangle$ and $|10\rangle$ move with the photons (or in general polaritons) to the respective direction with the speed of light (or the group velocity of the polaritons). For example the basis state $|01\rangle(t = 0)$ is a right-moving photon that is to the left of the interaction area (see figure 5.1) and the same basis state at a later time $|01\rangle(t = t_f)$ is a right-moving photon that has already passed the interaction area and is to the right of it. Similarly, the basis state $|10\rangle$ is a left-moving photon, which starts out as being to the right of the interaction area and eventually moves to the left of the interaction area. The basis state $|11\rangle$ is the state with both photons present, which move in their respective directions.

Now we determine what type of atoms will give us the desired properties. Essentially

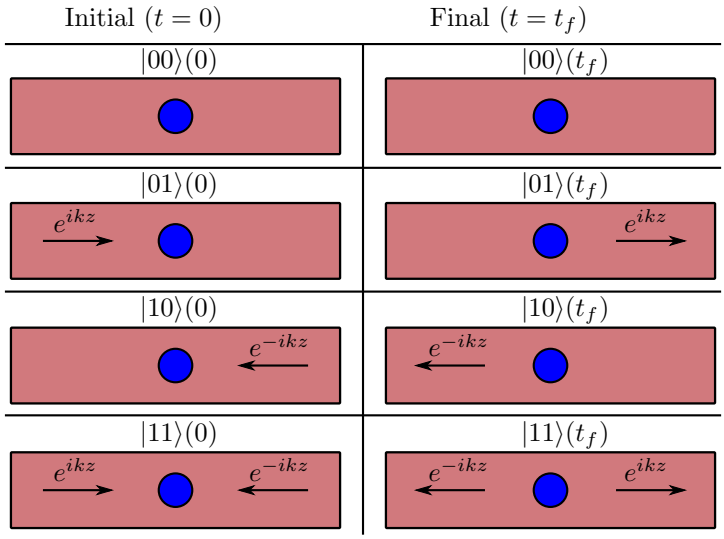

Figure 5.1: A graphical representation of the two-qubit photon basis. The dual-rail encoding is assumed but the second mode is not shown here. The red rectangles represent the waveguide and the blue circles represent the interaction area (either a single atom or an ensemble of atoms).

what we want different processes to happen for one and for two incident photons. Whenever we send only one photon from either side, it should pass through unaffected. When two photons are sent simultaneously, their two-particle state should get multiplied by -1. Thus the general idea that describes all the types of atoms and ensembles with nonlinear properties that are considered in this thesis is the following: we *need something that behaves as a three-level atom for the first photon and as a two-level atom for the second photon.* Here we also briefly note that given two indistinguishable photons that arrive at the atom at the same time, it is fundamentally not determined which photon is the "first" and which photon is the "second". In fact this indistinguishability will give rather peculiar quantum mechanical effects and ultimately it is also what will make our gates work.

5.2 Two candidates

The first candidate that fulfills the general principle stated above is the atom with level structure shown in figure 5.2. Compared to the Λ-type system considered before (figure 3.1) there was added a fourth level $|d\rangle$. The important part here is that the transitions $|a\rangle \leftrightarrow |b\rangle$ and $|c\rangle \leftrightarrow |d\rangle$ couple to the *same* quantum electric field. In this way the atom behaves

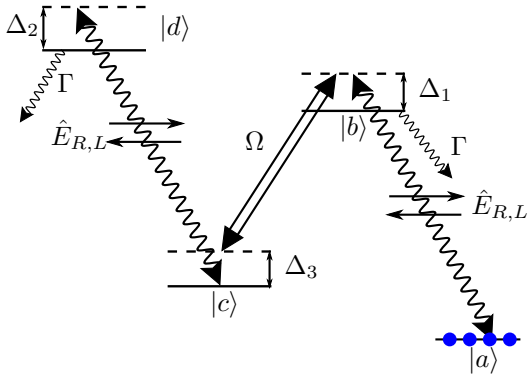

Figure 5.2: The level diagram of an atom with nonlinear properties.

nonlinearly, i.e. differently for different number of photons. The scenario we shall be considering is when the atom is initialized in the state $|a\rangle$. Then the first photon will be temporarily stored in the state $|c\rangle$ as it passes the atom. If the second photon arrives, while the first is still in the state $|c\rangle$, the second one will see the two-level atom transition $|c\rangle \leftrightarrow |d\rangle$. This type of atoms is the one that we shall focus on in this thesis.

Another possible candidate could be Rydberg atoms [21]. Those atoms have a level structure as in figure 3.1, but the state $|c\rangle$ is energetically above the state $|b\rangle$. The state $|c\rangle$ is a Rydberg state with a high principal quantum number which has a big dipole moment. The spontaneous decay from the Rydberg state can be made small enough, so that an ensemble of such atoms will support EIT propagation. However, due to the dipole-dipole interactions of the Rydberg states of the different atoms, the ensemble as a whole has nonlinear properties. Consider two atoms in such an ensemble sitting next to each other. Whenever the first atom has an excitation stored in its Rydberg state $|c\rangle_1$, the Rydberg state of the second atom $|c\rangle_2$ experiences an energy shift. If this shift is bigger than the width of the EIT window, then the second atom effectively becomes a two-level atom.

5.3 Values of Γ_{1D}

As mentioned earlier, Γ_{1D} is usually small. The reason is that optical photons have much bigger transverse cross-sections than single atoms. In [18], Γ_{1D} was big due to the fact that it considered optomechanical systems that behaved like three-level atoms instead of actual three-level atoms. The artificial atoms are physically bigger and thus could couple better to the light. Recently there was some progress towards building structures (photonic crystals) that can confine the light to one dimension and make it interact with the trapped atoms such that decay rates $\Gamma_{1D} \gtrsim 10\Gamma'$ could be achieved [22]. However, until such structures

can be produced, we need to work with significantly lower values of Γ_{1D}. Because of that, in this thesis we shall devote a lot of attention to the use of the collective enhancement effects (i.e. many atoms) to compensate for the low values of Γ_{1D}.

For the four-level atoms shown in figure 5.2 we shall do a more detailed treatment of collective enhancement later. For the Rydberg atoms we can briefly outline the main idea here. The dipole-dipole interactions for those atoms are actually long range. That implies that in the example of section 5.2 we could just as well use N atoms instead of only two. If the atom in the center has an excitation in the Rydberg state, and if the interaction is strong enough to shift the rest of the atoms out of the EIT window, the second excitation will be scattered from $\sim N/2$ two-level atoms. As we have seen in section 3.3.1, two-level atoms can be set up to reflect constructively and thus here we obtain an effective increase in Γ_{1D} that we desired. The caveat here is that ensembles with Rydberg interactions are often gasses, and this makes the analysis of section 3.3.1 (which assumed the ensemble to be a crystal) inapplicable.

Chapter 6

Single atom phase gate

6.1 Analytical treatment

Before we look at the phase gates in ensembles of atoms, we consider a single atom phase gate first. The gate uses an atom with the energy level structure as shown in figure 5.2. We assume that if there comes a single photon from either side, it simply goes through the atom due to EIT. Thus the states $|00\rangle$, $|01\rangle$ and $|10\rangle$ (see figure 5.1) behave as they should for a phase gate, i.e. are unchanged. The state $|11\rangle$, however, corresponds to a photon coming from each side and arriving at the atom at the same time. There are two processes that can happen:

1. The *right* photon gets temporarily stored into the state $|c\rangle$, and the *left* photon sees a two-level atom on transition $|c\rangle \leftrightarrow |d\rangle$ and gets scattered.

2. The *left* photon gets temporarily stored into the state $|c\rangle$, and the *right* photon sees a two-level atom on transition $|c\rangle \leftrightarrow |d\rangle$ and gets scattered.

Because the photons are indistinguishable and because they arrive at the same time, we now claim that *both these processes happen*. This results in both photons being scattered from each other. Based on the knowledge of the scattering properties of the two-level atoms in section 3.2 we can now come up with a quantitative expression for what the state $|11\rangle$ evolves into. For the sake of simplicity we consider plane waves first. For the plane wave it does not make sense to talk about definite positions and consequently about how much time it takes to go through the atom. However, once we make normalized wavepackets out of these plane waves, they will have some finite group velocity, and then these questions become well defined. Thus whenever we have a plane wave with some wavenumber k, we can think of a wavepacket that is centered around k and is narrow enough in k-space that it can be approximately treated as a plane wave.

Because of the two equivalent processes discussed above, the final state will be the sum of those (see figure 6.1). The photon that came from the left, results in a right-going

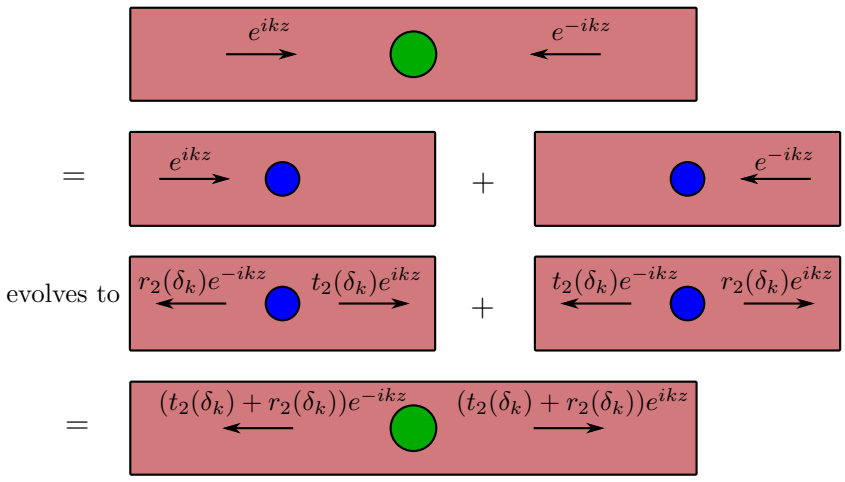

Figure 6.1: Pictorial representation of the scattering process with two incident photons. Here the waveguide is the red rectangular background, four-level atoms are big green circles, and two-level atoms are small blue circles. The scattering of two photons by a four-level atom (first line) can be decomposed into two single-photon scattering processes by a two-level atom (second line). Each of these two single-photon processes results in a transmitted part and a reflected part (third line). Finally, the transmitted and reflected parts of both processes are added together (fourth line).

photon on the right multiplied by the transmission coefficient $t_2(\delta_k)$ given by (3.8), and a left-going photon on the left multiplied by the reflection coefficient $r_2(\delta_k)$. Likewise, the photon that came from the right, results in a left-going photon on the left multiplied by $t_2(\delta_k)$, and a right-going photon on the right multiplied by $r_2(\delta_k)$. The sum of these is a left-going photon on the left and a right-going photon on the right, both multiplied by

$$t_2(\delta_k) + r_2(\delta_k) = \frac{\Gamma' - 2i\delta_k - \Gamma_{1D}}{\Gamma' - 2i\delta_k + \Gamma_{1D}}. \tag{6.1}$$

We see that for $\Gamma_{1D}/(\Gamma' - 2i\delta_k) \to \infty$, $t_2(\delta_k) + r_2(\delta_k) \to -1$. In this limit it is the reflection coefficient that gives this -1, while transmission coefficient goes to zero. Thus also the state $|11\rangle$ behaves as it should for the phase gate.

The transmission coefficient cannot be neglected for the case when Γ_{1D} is close to Γ' or below. For example, for $\delta_k = 0$ and $\Gamma_{1D} = \Gamma'$, we have $t_2(0) + r_2(0) = 0$, i.e. everything goes out of the waveguide and into the other modes. Also we note here that δ_k in (6.1) corresponds to the detuning Δ_2 in four-level atom in figure 5.2.

6.2 Numerical treatment

The intuitive justification of the factor (6.1) is supported by the results of the numerical simulations using the method described in chapter 4. Compared to the situation discussed above, where two photons hit a single four-level atom, we shall make a slight modification. Instead of photons we shall be considering polaritons inside an ensemble of four-level atoms. As we shall see, the ensemble will not alter the scattering properties of a single atom in this case. Until two polaritons begin overlapping, the only thing the ensemble will do is to provide a highly transparent medium, where the polaritons can propagate.

We can follow the procedure of chapter 4 and do a straightforward generalization of the non-Hermitian Hamiltonian (4.4) to the case the four-level atoms considered here. We find

$$\begin{aligned}\hat{H}_N = &-\hbar\sum_j\left[(\Delta_1+i\Gamma'/2)\hat{\sigma}^j_{bb}+\Delta_3\hat{\sigma}^j_{cc}+(\Delta_2+\Delta_3+i\Gamma'/2)\hat{\sigma}^j_{dd}\right]\\ &-\hbar\sum_j\left(\Omega\hat{S}^j_{bc}+\Omega^*\hat{S}^j_{cb}\right)-i\hbar\sum_{j,k}\frac{\Gamma_{1\mathrm{D}}}{2}e^{ik_0|z_j-z_k|}\left(\hat{S}^j_{ba}+\hat{S}^j_{dc}\right)\left(\hat{S}^k_{ab}+\hat{S}^k_{cd}\right).\end{aligned} \tag{6.2}$$

Here the detunings are $\Delta_1 = \omega_{k_0} - \omega_{ba}$, $\Delta_2 = \omega_{k_0} - \omega_{dc}$ and $\Delta_3 = \omega_{k_0} - \omega_{\mathrm{p}} - \omega_{ca}$ given in terms of the carrier frequency of the quantum field ω_{k_0} and the frequency of the classical drive ω_{p} (also see figure 5.2). The main difference of this Hamiltonian from (4.4) is accounting for the fact, that the quantum field couples to both transitions $|a\rangle \leftrightarrow |b\rangle$ and $|c\rangle \leftrightarrow |d\rangle$. This is what the terms $(\hat{S}^j_{ba}+\hat{S}^j_{dc})(\hat{S}^k_{ab}+\hat{S}^k_{cd})$ encapsulate.

To perform the numerical simulations we find all the matrix elements of the Hamiltonian (6.2) for the states of the ensemble that contain up to two excitations. In figure 6.2 the coupling diagram of these states is shown. Depending on the initial state (either $|c_k a\rangle$ or $|c_k c_m a\rangle$), the Hamiltonian (6.2) only makes the transitions in one of the two isolated circuits. For single excitations the matrix is dense enough (the $\langle b_{k'}a|\hat{H}_N|b_k a\rangle$ block is dense) so that we use ordinary matrix exponentiation using Padé approximants to find the final state. This way we can simulate around 1000 atoms within a time frame of several minutes. For the case of double excitations, the resulting matrix becomes too big to simply store its every element in memory for the number of atoms bigger than about 50. Since the double excitation states are rather weakly coupled (figure 6.2), the resulting Hamiltonian matrix is sparse. Hence, if we only store the non-zero elements, this limitation is removed. For the sparse matrices we use the fourth-order Runge-Kutta algorithm to compute the final state. Compared to Padé approximants it does not require computing the whole matrix $\exp(-i\hat{H}_N t/\hbar)$ (which would be dense even though $\hat{H}_N$ is sparse) but only products of $\hat{H}_N$ with the state vector. In this way we are able to simulate up to about 100 atoms within the same time frame of several minutes.

In the simulations we initialize the spinwaves of the atoms such that we have two Gaussians, one with mean $\mu_1 = L/4$ and carrier k-vector $k_0 = \pi/(2d)$ and the other with

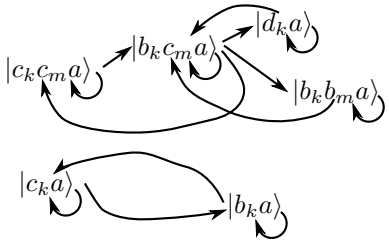

Figure 6.2: The coupling diagram of the ensemble basis with at most two excitations under action of the non-Hermitian Hamiltonian (6.2). The transitions between some of the states have additional requirements on the indices that are not shown in the diagram. The states $|b_k d_m a\rangle$, $|d_k d_m a\rangle$, $|c_k d_m a\rangle$ are inaccessible from the initial states $|c_k a\rangle$ or $|c_k c_m a\rangle$. The ground state of the ensemble (with all atoms in $|a\rangle$) is not shown, as it is only coupled to the other states through the jump terms, which we neglect.

mean $\mu_2 = 3L/4$ and carrier k-vector $-k_0$. The single-excitation states that correspond to those are

$$|\psi_{\text{initial},1}\rangle = \sum_j f_1(z_j)\sqrt{d}|c_j a\rangle, \tag{6.3}$$

$$|\psi_{\text{initial},2}\rangle = \sum_k f_2(z_k)\sqrt{d}|c_k a\rangle; \tag{6.4}$$

with

$$f_1(z) = \frac{1}{(2\pi\sigma^2)^{1/4}} \exp\left(-\frac{(z-\mu_1)^2}{4\sigma^2}\right) e^{ik_0 z},$$

$$f_2(z) = \frac{1}{(2\pi\sigma^2)^{1/4}} \exp\left(-\frac{(z-\mu_2)^2}{4\sigma^2}\right) e^{-ik_0 z}.$$

The state, where both those Gaussians are present is a product of (6.3) and (6.4). We can express it in the two-excitation basis as

$$|\psi_{\text{initial}}\rangle = |\psi_{\text{initial},1}\rangle|\psi_{\text{initial},2}\rangle = \sum_{j,k} f_1(z_j) f_2(z_k) d|c_j c_k a\rangle. \tag{6.5}$$

Note that in (6.5), the sum runs over all j and k from 0 to N. There are two remarks that need to be made. First, we use the convention $|c_j c_j a\rangle = 0$, since these states are unphysical. Second, due to indistinguishability of individual atoms, the states $|c_j c_k a\rangle$ and $|c_k c_j a\rangle$ are the same. This means that (6.5) adds a contribution to the coefficient of a given

basis state $|c_j c_k a\rangle$ twice. We can rewrite (6.5) to explicitly show, what coefficients every basis state ends up with:

$$|\psi_{\text{initial}}\rangle = \sum_j \sum_{\substack{k \\ k>j}} c_{j,k} d|c_j c_k a\rangle, \tag{6.6}$$

with $c_{j,k} = f_1(z_j)f_2(z_k) + f_1(z_k)f_2(z_j)$. Then we evolve the state (6.6) using the Hamiltonian (6.2) for the time $t = L/(2v_{\text{g}})$, i.e. such that the pulses interchange places. The final interacting state is given by

$$|\psi_{\text{final,interacting}}\rangle = \exp(-i\hat{H}_N t/\hbar)|\psi_{\text{initial}}\rangle. \tag{6.7}$$

We want to compare this state to the one, where both of the single-excitation initial states (6.3) and (6.4) are separately evolved by the Hamiltonian (6.2), and then those two are used to construct the final two-excitation state. The non-interacting state can be written as

$$|\psi_{\text{final,non-interacting}}\rangle = \left(\exp(-i\hat{H}_N t/\hbar)|\psi_{\text{initial,1}}\rangle\right)\left(\exp(-i\hat{H}_N t/\hbar)|\psi_{\text{initial,2}}\rangle\right). \tag{6.8}$$

Both these final states will in general *not* have the form (6.6). They will also have some non-zero coefficients of the other basis states, such as $|b_j b_k a\rangle$ or $|b_j c_k a\rangle$. We shall discard those coefficients in our calculations, since in the limit, where EIT propagation works best, the photons should spend most of their time inside the states $|c_j c_k a\rangle$ and only briefly transition to the other states to be able to move from one atom to another. Thus the norm of the states will be the sum of the coefficients of the basis states $|c_j c_k a\rangle$.

If the fourth level $|d\rangle$ were not present, $|\psi_{\text{final,interacting}}\rangle$ and $|\psi_{\text{final,non-interacting}}\rangle$ would be largely the same. Some differences could occur due to boundary effects being different for the one-excitation and two-excitation case. With the fourth-level present, we find that on resonance ($\Delta_2 = 0$) there is phase shift of π between the interacting and non-interacting case, when $\Gamma_{1\text{D}}$ is bigger than Γ' (see figure 6.3 (a) and (b)). For the threshold value $\Gamma_{1\text{D}} = \Gamma'$ (figure 6.3 (c)) the transmission and reflection coefficient of the two-level atom are equal, which results in the state with practically zero norm. Below this value (figure 6.3 (d)), there is no phase shift and only a smaller norm in the interacting case due to partial cancellation of the transmission coefficient.

6.3 Possible modification

To understand, how we can make the gate work at $\Gamma_{1\text{D}} = \Gamma'$ or below, we can look at, what happens if we take a non-zero Δ_2. This is what we have done in figure 6.4. This figure shows that numerical simulations follow very closely the analytical formula (6.1). The only significant deviation is for $\Gamma_{1\text{D}} = \Gamma'$ (figure 6.4 (c)), which is the threshold value

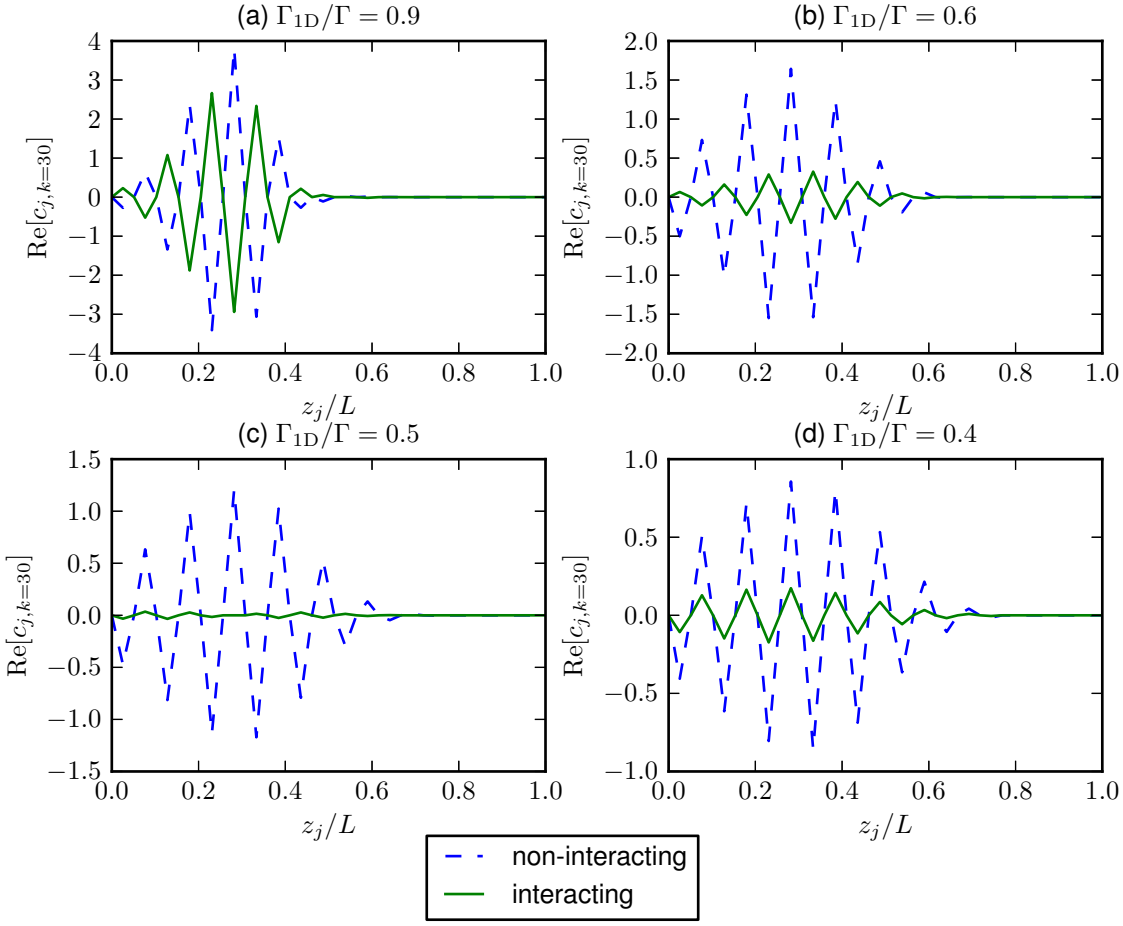

Figure 6.3: This is the two-excitation version of the figure 4.2. Set $\Gamma = \Gamma_{1D} + \Gamma'$. We choose number of atoms $N = 40$, strength of the classical drive $\Omega = 0.1\Gamma$ and detunings $\Delta_1 = \Delta_2 = \Delta_3 = 0$. The value of Γ_{1D} is written in the title of the subplots. The ensemble is initialized in the state (6.6). That state is two Gaussian atomic excitations centered around $\mu_1 = L/4$ and $\mu_2 = 3L/4$ respectively. For their two particle state, the highest probability is concentrated around the coefficient $c_{j=10,k=30}$ ($z_{10} \approx L/4$ and $z_{30} \approx 3L/4$). We let the simulation run for the time $t = L/(2v_g)$ such that the two Gaussians interchange places. Thus we fix $k = 30$ and plot $\mathrm{Re}[c_{j,k=30}]$ of the state $|\psi_{\text{final,non-interacting}}\rangle$ and $|\psi_{\text{final,interacting}}\rangle$ as a function of z_j. As discussed in the text, we chose to write our states in the way, where values $j \geq k$ are considered unphysical. For those values we set $\mathrm{Re}[c_{j,k=30}] = 0$.

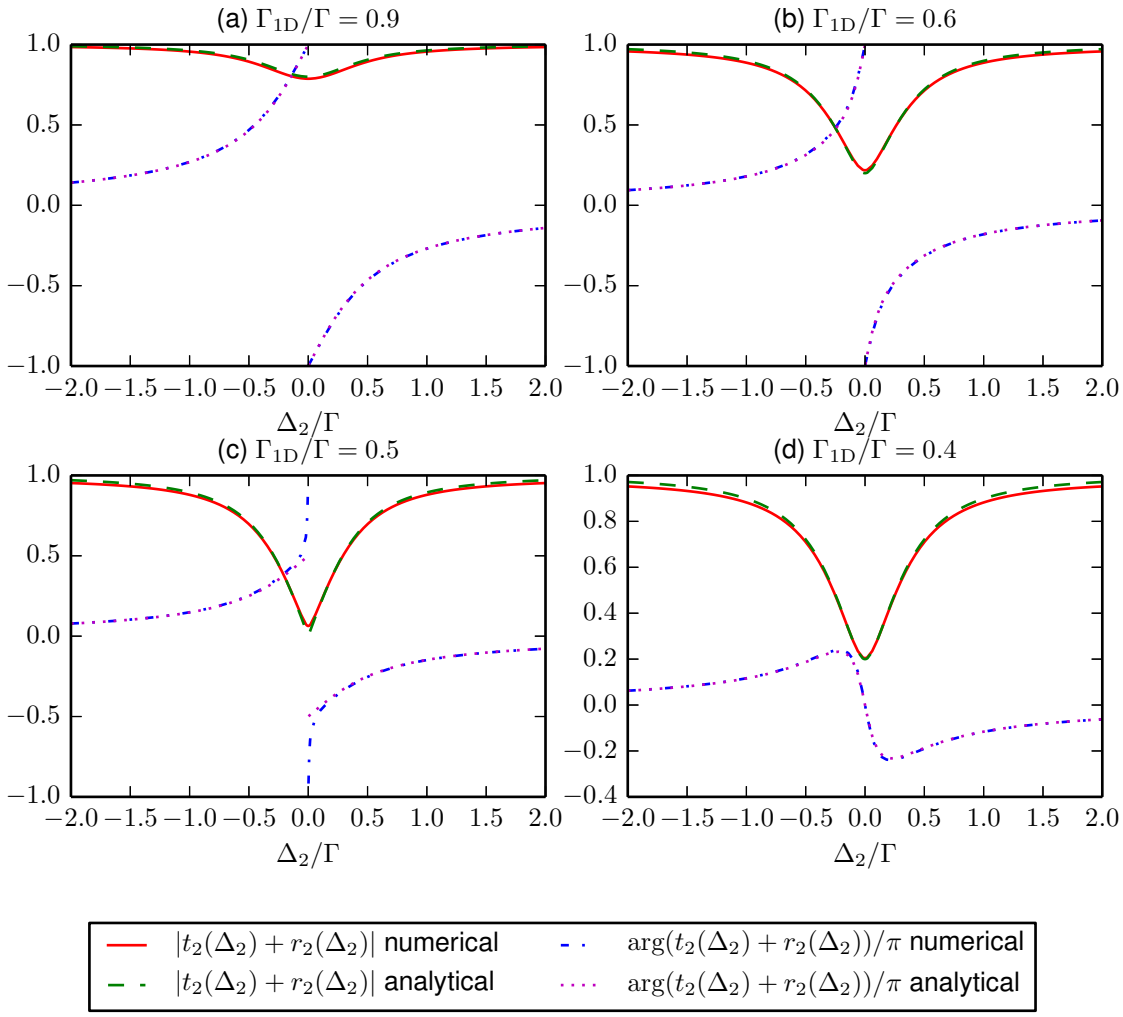

Figure 6.4: The four subplots here correspond to the subplots of figure 6.3. All the parameters are the same as there, except for Δ_2. Instead of setting $\Delta_2 = 0$, here we vary it and plot $|t_2(\Delta_2) + r_2(\Delta_2)|$ and $\arg(t_2(\Delta_2) + r_2(\Delta_2))/\pi$ both numerically and analytically. The analytical plots are found directly from (6.1). For the numerical plots $|t_2(\Delta_2) + r_2(\Delta_2)|$ is found as the ratio of the norms $\left(\langle\psi_{\text{final,interacting}}|\psi_{\text{final,interacting}}\rangle/\langle\psi_{\text{final,non-interacting}}|\psi_{\text{final,non-interacting}}\rangle\right)^{1/2}$. In this sense it is the average of $|t_2(\Delta_2) + r_2(\Delta_2)|$ over all spatial coordinates. Similarly, an average of $\arg(t_2(\Delta_2) + r_2(\Delta_2))/\pi$ is found numerically as $\arg(\langle\psi_{\text{final,non-interacting}}|\psi_{\text{final,interacting}}\rangle)/\pi$.

for the analytical values with $|t_2(0) + r_2(0)| = 0$ and $\arg(t_2(\Delta_2) + r_2(\Delta_2)) \to \mp\pi/2$ for $\Delta \to 0^{\pm}$ (0^+ is the limit from above, and 0^- is the limit from below). For the numerical simulations, $\Gamma_{1D} = \Gamma'$ does not seem to be the threshold value and behaves the same as for $\Gamma_{1D} > \Gamma'$, i.e. numerically $\arg(t_2(\Delta_2) + r_2(\Delta_2)) \to \mp\pi$ for $\Delta \to 0^{\pm}$.

From figure 6.4 we see that the argument goes to zero slower than the norm approaches unity. Indeed, analytically for large Δ_2 we can approximate the norm and the argument as

$$|t_2(\Delta_2) + r_2(\Delta_2)| \approx 1 - \frac{\Gamma_{1D}\Gamma'}{2\Delta_2^2}, \tag{6.9}$$

$$\arg(t_2(\Delta_2) + r_2(\Delta_2)) \approx -\frac{\Gamma_{1D}}{\Delta_2}. \tag{6.10}$$

Thus we can choose Δ_2 big enough that the norm will differ from unity by a much smaller amount than the phase will differ from 0. In this way we can get a small but still significant phase in one scattering process. From section 3.3.2 we know that given enough atoms, we can make losses due to propagation in an EIT medium arbitrarily small. Then we can send the pulses through the EIT medium repeatedly and in that way acquire the desired phase of π. To make this argument more quantitative, we can find a rough estimate of the losses. Formally one can do it by calculating fidelity, as we shall do in section 7.6 for a different kind of a phase gate. For now we simply calculate the norm of the final state. For a phase gate we require that the argument of the final state is shifted by π. From (6.10) we see that we need $M = \pi\Delta_2/\Gamma_{1D}$ scattering events (and M passages through the EIT medium) to obtain it. Thus, using (3.21), (3.22) and (6.9), the norm of the final state in the limit, where the errors are small (so the cross terms can be neglected) is

$$\mathcal{N}_{\text{final}} \approx 1 - M\frac{\Gamma' L^2}{4N\Gamma_{1D}\sigma^2} - M\frac{\Gamma_{1D}\Gamma'}{2\Delta_2^2} = 1 - \frac{\pi\Delta_2\Gamma' L^2}{4N\Gamma_{1D}^2\sigma^2} - \frac{\pi\Gamma'}{2\Delta_2}.$$

Here the first error terms is due to M EIT propagations and the second is due to M scattering events. This expression reaches its maximum for $\Delta_2 = \sqrt{2N}\Gamma_{1D}\sigma/L$ and attains the value

$$\mathcal{N}_{\text{final}} \approx 1 - \pi\frac{L}{\sigma}\frac{\Gamma'}{\sqrt{2N}\Gamma_{1D}}. \tag{6.11}$$

Here L/σ will be determined by balancing this error term with error terms caused by the finite size of the ensemble that we did not account for here, but the approach is similar to the one we shall do in section 7.6.

The collective enhancement phenomena such as this one are usually described in terms of optical depth d^{opt}. This is a quantity that is used to express, how well an ensemble of atoms absorbs light. In the low Γ_{1D} limit, one finds that if a laser is shone at an ensemble and is on resonance with the atomic transitions, then the output intensity I_{out}

that is measured at the other end of the ensemble is related to the input intensity $I_{\rm in}$ of the laser by $I_{\rm out} = \exp(-d^{\rm opt})I_{\rm in}$. The argument of the exponential is the optical depth $d^{\rm opt} = 2N\Gamma_{\rm 1D}/\Gamma$. In the low $\Gamma_{\rm 1D}$ limit that we are considering, $\Gamma \approx \Gamma'$, so we could have written either Γ or Γ' there. In the high $\Gamma_{\rm 1D}$ limit one needs to be careful with this distinction. In this thesis we shall adopt the conventional definition of the optical depth that is given in terms of the total decay rate Γ, but also mention, when the parameter $2N\Gamma_{\rm 1D}/\Gamma'$ would have been more apropriate.

Assuming the low $\Gamma_{\rm 1D}$ limit we can approximate Γ' by Γ in (6.11) and express it in terms of optical depth

$$\mathcal{N}_{\rm final} \approx 1 - \pi\frac{L}{\sigma}\frac{1}{\sqrt{d^{\rm opt}\Gamma_{\rm 1D}/\Gamma}}. \tag{6.12}$$

Usually linear errors only depend on optical depth $d^{\rm opt}$ alone (as for example in (3.22)). However, here it is multiplied by $\Gamma_{\rm 1D}/\Gamma$, which means that achieving better couplings of the atom to the waveguide have bigger impact than increasing the number of atoms. On the other hand, this result also shows that at least in theory one *can* compensate for low values of $\Gamma_{\rm 1D}/\Gamma$ by using the collective enhancement effects (i.e. high $d^{\rm opt}$).

Chapter 7

Phase gate in an atomic ensemble

7.1 Introduction

In chapter 6 we discussed the possibility of making the single atom phase gate work for arbitrary value of Γ_{1D} by using multiple scatterings. In this section we shall look at a system that has this multiple scattering "integrated". In other words, we want to have en ensemble of atoms, where a single passage through it will effectively be the same as multiple passages through the EIT medium discussed earlier.

In EIT, the classical ("pump") drive Ω can be either constant (as in figures 3.1 and 5.2) or *copropagating*. The difference between these two is mostly just the phase of the atomic excitations. The constant classical drive is usually the one that comes from the side and it does not have any difference in the phase for different atoms. In this case, the atomic excitations retain the information about the k-vector of the photons that created them. This is why, for instance, we had to explicitly include a phase in f_1 and f_2 of (6.3) and (6.4). If the classical drive is copropagating, it means that it has the same direction as the electric field of the single photons, and has a spatially-dependent phase $e^{ik_{\mathrm{p}}z}$. The k-vectors of the classical drive and the quantum electric field of the single photons are usually not the same, since the frequency separation can help to distinguish the photons of those two fields. However, the difference is rather small ($|a\rangle$ and $|c\rangle$ are usually separated by a hyperfine splitting) and conceptually we can set those k-vectors to be equal. Then the k-vector, that the photon imparts to the atom under transition $|a\rangle \to |b\rangle$ is immediately removed by the classical drive under the transition $|b\rangle \to |c\rangle$. As a result the stored atomic excitation does not have a phase factor. This makes it possible to apply the classical drive going in the other direction (with an opposite k-vector) to make the stored excitation produce the photon that will fly in the reversed direction compared to the one, that was stored.

For the polaritons, the above idea results in the possibility to reverse their direction of propagation through the ensemble in a controlled fashion. Combined with the idea to

scatter two such polaritons with each other multiple times, we see that it is not even needed to let those polaritons leave the ensemble after the first scattering – we can simply reverse the direction of the classical drive and let them be scattered with each other in the opposite direction. Then we can take one step further and consider, what would happen when *both* classical drives – the one that makes the polaritons go forward and the one, that makes the polaritons go backward – are turned on at the *same time* (figure 7.1). We shall see that we can arrange for polaritons to have a small "bias" k-vector, such that they move backward and forward due to the two classical drives, but still move more in one direction than the other. Such "3 steps forward and 2 steps back" motion will cause two polaritons moving towards each other to scatter multiple times – this is exactly the effect we were looking for.

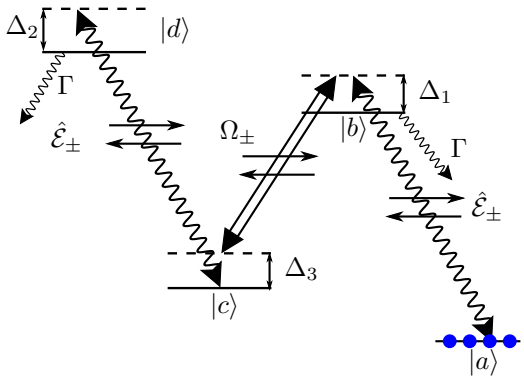

Figure 7.1: A four-level atom, where on the transition $|b\rangle \leftrightarrow |c\rangle$ the counterpropagating classical drives with the strengths Ω_+ and Ω_- are applied.

7.2 Model

Here we shall analyze the system shown in the figure 7.1 using the effective model of [23]. The final equations of motion of that model are comparatively simple, which is very useful in the analytical calculations. In this model atoms are treated as a continuous background rather than discrete point scatterers. To perform this continuum limit we first split the length of ensemble L into K equal parts. If the total number of atoms N is uniformly distributed in the whole length of the ensemble, then in each such part there are $N_z = N/K$ atoms. For each such part we can define the averaged operators

$$\hat{\sigma}_{\alpha\beta}(z) = \frac{1}{N_z} \sum_{i=1}^{N_z} |\alpha\rangle_i \langle\beta|_i.$$

Then we let $K \to \infty$ and make the operators above defined for any real position z. Operators obtained after taking this limit have commutation relations

$$[\hat{\sigma}_{\alpha\beta}(z), \hat{\sigma}_{\alpha'\beta'}(z')] = \frac{L}{N}\delta(z-z')\left(\delta_{\beta,\alpha'}\hat{\sigma}_{\alpha\beta'}(z) - \delta_{\beta',\alpha}\hat{\sigma}_{\alpha'\beta}(z)\right).$$

We shall denote the right-going and left-going electric field operators by $\hat{\mathcal{E}}_+$ and $\hat{\mathcal{E}}_-$ respectively. These are the slowly varying versions of the electric field operators in section 3.2, i.e they are related by

$$\hat{E}_{\mathrm{R}}(z) = \hat{\mathcal{E}}_+(z)e^{ik_0 z - i\omega_{k_0}t},$$
$$\hat{E}_{\mathrm{L}}(z) = \hat{\mathcal{E}}_-(z)e^{-ik_0 z - i\omega_{k_0}t}.$$

The commutation relations are the same as (3.1), but with $\hat{E}$ replaced by $\hat{\mathcal{E}}$.

Using these operators we can write the Hamiltonian in the interaction picture and rotating wave approximation as

$$\begin{aligned}\hat{H} = -\hbar\frac{N}{L}\int\Big\{&[\hat{\sigma}_{bc}(z)(\Omega_+ e^{ik_{\mathrm{p}}z} + \Omega_- e^{-ik_{\mathrm{p}}z}) + \mathrm{H.c.}]\\ &+ g\sqrt{2\pi}[\hat{\sigma}_{ba}(z)(\hat{\mathcal{E}}_+ e^{ik_0 z} + \hat{\mathcal{E}}_- e^{-ik_0 z}) + \mathrm{H.c.}]\\ &+ g\sqrt{2\pi}[\hat{\sigma}_{dc}(z)(\hat{\mathcal{E}}_+ e^{ik_0 z} + \hat{\mathcal{E}}_- e^{-ik_0 z}) + \mathrm{H.c.}]\\ &+\Delta_1\hat{\sigma}_{bb}(z) + \Delta_3\hat{\sigma}_{cc}(z) + (\Delta_2+\Delta_3)\hat{\sigma}_{dd}(z)\Big\}dz.\end{aligned}$$

Here $g = \wp\sqrt{\omega_{k_0}/(4\pi\hbar\varepsilon_0 A)}$, $\wp$ is the dipole moment for transitions $|a\rangle \leftrightarrow |b\rangle$ and $|c\rangle \leftrightarrow |d\rangle$ (assumed to be the same), and A is the effective area of the waveguide modes. Compared to the Hamiltonians we have considered before, where the interactions with the individual atoms at the discrete positions z_j were expressed by delta function terms $\delta(z-z_j)$, this Hamiltonian takes the approximation that interaction of the field and the atoms happens at *every* position z, no matter, whether there is an atom there or not. If we set $\Omega_+ = \Omega$, $\Omega_- = 0$ and remove the fourth level $|d\rangle$, then this Hamiltonian reduces to the one considered in [19]. There, EIT was described in terms of the dark-state polaritons. If we define an angle θ_Ω, that fulfills

$$\cos(\theta_\Omega) = \frac{\Omega}{\sqrt{\Omega^2 + g^2(2\pi)N/L}},$$
$$\sin(\theta_\Omega) = \frac{g\sqrt{2\pi N/L}}{\sqrt{\Omega^2 + g^2(2\pi)N/L}},$$

then the dark-state polaritons are given by

$$\hat{\Psi}_\pm(z,t) = \hat{\mathcal{E}}_\pm(z,t)\cos(\theta_\Omega) - \sqrt{\frac{N}{L}}\hat{\sigma}_{ac}(z,t)e^{-i(\omega_{k_0}-\omega_{\mathrm{c}})t}\sin(\theta_\Omega). \tag{7.1}$$

In general, Ω and hence θ_Ω can be time dependent. However, we shall assume them to be constant. The polaritons have the group velocity

$$v_{\rm g} = c\cos^2(\theta_\Omega) = \frac{c}{1+\frac{2\pi g^2 N}{\Omega^2 L}}.$$

We are interested in the limit $v_{\rm g} \ll c$. This condition is equivalent to $\Omega \ll g\sqrt{2\pi N/L}$. Defining as before $\Gamma_{1\rm D} = 4\pi g^2/c$, in this limit the group velocity is approximately $v_{\rm g} \approx 2\Omega^2 L/(N\Gamma_{1\rm D})$. This expression is the same as (3.18). In the derivation, we are going to eliminate atoms and hence we approximate polaritons to only have the electric field part. In the limit of the low group velocity we have

$$\hat{\Psi}_\pm(z,t) \approx \frac{g\sqrt{2\pi N/L}}{\Omega_\pm}\hat{\mathcal{E}}_\pm. \tag{7.2}$$

With this definition we can perform the adiabatic elimination of the atoms (see appendix A) and obtain effective equations of motion for the polaritons. Defining the total decay rate $\Gamma = \Gamma_{1\rm D} + \Gamma'$ and the constants $\xi = (c\Gamma_{1\rm D}N/L)/(-2i\Delta_1 + \Gamma)$ and $\Delta_n = \pi g^2/(2\Delta_2 + i\Gamma)$, we can write the equations

$$\begin{aligned}\left(\frac{\partial}{\partial t} + c\,\frac{\partial}{\partial z}\right)\hat{\Psi}_+ =& -\frac{\xi}{2}(\hat{\Psi}_+ - \hat{\Psi}_-) - \frac{c}{4v_{\rm g}}\,\frac{\partial}{\partial t}\,(\hat{\Psi}_+ + \hat{\Psi}_-)\\ &- i\Delta_n[(\hat{\Psi}_+^\dagger\hat{\Psi}_+ + \hat{\Psi}_-^\dagger\hat{\Psi}_-)(\hat{\Psi}_+ + \hat{\Psi}_-)\\ &+ (\hat{\Psi}_+^\dagger + \hat{\Psi}_-^\dagger)(\hat{\Psi}_+ + \hat{\Psi}_-)\hat{\Psi}_+]\end{aligned} \tag{7.3}$$

$$\begin{aligned}\left(\frac{\partial}{\partial t} - c\,\frac{\partial}{\partial z}\right)\hat{\Psi}_- =& +\frac{\xi}{2}(\hat{\Psi}_+ - \hat{\Psi}_-) - \frac{c}{4v_{\rm g}}\,\frac{\partial}{\partial t}\,(\hat{\Psi}_+ + \hat{\Psi}_-)\\ &- i\Delta_n[(\hat{\Psi}_+^\dagger\hat{\Psi}_+ + \hat{\Psi}_-^\dagger\hat{\Psi}_-)(\hat{\Psi}_+ + \hat{\Psi}_-)\\ &+ (\hat{\Psi}_+^\dagger + \hat{\Psi}_-^\dagger)(\hat{\Psi}_+ + \hat{\Psi}_-)\hat{\Psi}_-]\end{aligned} \tag{7.4}$$

To simplify these two equations we define the symmetric and antisymmetric modes: $\hat{S} = (\hat{\Psi}_+ + \hat{\Psi}_-)/\sqrt{2}$ and $\hat{A} = (\hat{\Psi}_+ - \hat{\Psi}_-)/\sqrt{2}$. Subtracting (7.4) from (7.3), we get

$$\frac{\partial}{\partial t}\,\hat{A} + c\,\frac{\partial}{\partial z}\,\hat{S} = -\xi\hat{A} - 2i\Delta_n\hat{S}^\dagger\hat{S}\hat{A}.$$

If ξ is large compared to the inverses of the time scales, that we shall consider (e.g. the time it takes for the pulse to travel through the ensemble), we can approximate the above equation by

$$\hat{A} \approx -\frac{c}{\xi}\,\frac{\partial}{\partial z}\,\hat{S}, \tag{7.5}$$

which means that the antisymmetric mode adiabatically follows the symmetric mode. For the symmetric mode, we add (7.3) and (7.4) and get

$$\frac{\partial}{\partial t}\,\hat{S} + c\,\frac{\partial}{\partial z}\,\hat{A} = -\frac{c}{2v_{\rm g}}\,\frac{\partial}{\partial t}\,\hat{S} - i\Delta_n\left(\left((\hat{S}^\dagger + \hat{A}^\dagger)(\hat{S}+\hat{A}) + (\hat{S}^\dagger - \hat{A}^\dagger)(\hat{S}-\hat{A})\right)\hat{S} + 2\hat{S}^\dagger\hat{S}^2\right)$$

We discard the second order terms $\hat{A}^\dagger\hat{A}$ and use the approximate solution (7.5) for the remaining operator $\hat{A}$. Also, by assumption $c \gg v_{\rm g}$, the $\frac{\partial}{\partial t}\hat{S}$ term on the right hand side is much bigger than the one on the left hand side, so we discard the latter. With these changes we can write the above equation as

$$\frac{c}{2v_{\rm g}}\,\frac{\partial}{\partial t}\,\hat{S} = -\frac{c^2}{\xi}\,\frac{\partial^2}{\partial z^2}\,\hat{S} - 4i\Delta_n\hat{S}^\dagger\hat{S}^2.$$

Defining the dimensionless operator $\tilde{S} = \sqrt{L}\hat{S}$ with the commutation relation

$$[\tilde{S}(z), \tilde{S}^\dagger(z')] = L\delta(z-z'),$$

we can write this equation as the nonlinear Schrödinger equation (NLSE)

$$i\,\frac{\partial}{\partial t}\,\tilde{S} = -\frac{1}{2m}\,\frac{\partial^2}{\partial z^2}\,\tilde{S} + 2\frac{\kappa}{L}\tilde{S}^\dagger\tilde{S}^2 \tag{7.6}$$

with the mass

$$m = -\frac{\Gamma_{\rm 1D}^2}{8\Omega^2(L/N)^2(2\Delta_1 + i\Gamma)}, \tag{7.7}$$

and the nonlinearity constant

$$\kappa = \frac{\Omega^2 L}{N(\Delta_2 + i\Gamma/2)}. \tag{7.8}$$

We shall truncate the Hilbert space, so that it only contains states with up to two excitations. The general form of such states is

$$|\psi(t)\rangle = \iint \phi(z_1,z_2,t)\tilde{S}^\dagger(z_1)\tilde{S}^\dagger(z_2)|0\rangle dz_1 dz_2 + \int \theta(z,t)\tilde{S}^\dagger(z)|0\rangle dz + \varepsilon|0\rangle. \tag{7.9}$$

Note that we have a choice here with respect to the symmetrization of ϕ. We can either assume that it is not symmetrized, and that the integrals with respect to the spatial variables z_1 and z_2 go over the whole length of the ensemble; or, alternatively, we can assume that ϕ is symmetrized as $\phi_{\rm sym}(z_1,z_2,t) = \phi(z_1,z_2,t) + \phi(z_2,z_1,t)$, and that the integration area is the triangle, where $z_2 > z_1$. The difference between these two ways of writing the state is the same as the difference between (6.5) and (6.6) for the discrete

atom model. Even if keep ϕ in a non-symmetrized form, we shall still find $\phi_{\rm sym}$ when we calculate the coefficient of the basis state $\tilde{S}^\dagger(z_1)\tilde{S}^\dagger(z_2)|0\rangle$ by taking the inner product with (7.9). Using the identity

$$\langle 0|\tilde{S}(z_1)\tilde{S}(z_2)\tilde{S}^\dagger(z_1')\tilde{S}^\dagger(z_2')|0\rangle = L^2\left(\delta(z_1-z_1')\delta(z_2-z_2')+\delta(z_1-z_2')\delta(z_2-z_1')\right) \quad (7.10)$$

we calculate the coefficient as

$$\frac{1}{L^2}\langle 0|\tilde{S}(z_1)\tilde{S}(z_2)|\psi(t)\rangle = \phi_{\rm sym}(z_1,z_2,t).$$

We want to use the operator equation (7.6) to obtain the evolution equations for the coefficients of (7.9). To do this we first write the Hamiltonian that gives (7.6) as the Heisenberg equation for the operator $\tilde{S}$. This Hamiltonian is

$$\hat{H}_{\rm NLSE} = \frac{\hbar}{L}\int\left(\frac{1}{2m}\tilde{S}^\dagger(z)\,\frac{\partial^2\tilde{S}(z)}{\partial z^2}+\frac{\kappa}{L}(\tilde{S}^\dagger(z))^2(\tilde{S}(z))^2\right)dz \quad (7.11)$$

The Schrödinger equation for the state (7.9) is then

$$i\,\frac{\partial}{\partial t}\,|\psi(t)\rangle = \frac{1}{\hbar}\hat{H}_{\rm NLSE}|\psi(t)\rangle \quad (7.12)$$

Inserting the Hamiltonian (7.11) into (7.12) and taking the inner products to obtain coefficients of (7.12) we finally find the equations of motion for the coefficients

$$\begin{aligned} i\,\frac{\partial}{\partial t}\,\phi_{\rm sym}(z_1,z_2,t) = &-\frac{1}{2m}\left(\frac{\partial^2}{\partial z_1^2}+\frac{\partial^2}{\partial z_2^2}\right)\phi_{\rm sym}(z_1,z_2,t) \\ &+2\kappa\phi_{\rm sym}(z_1,z_2,t)\delta(z_1-z_2) \end{aligned} \quad (7.13)$$

$$i\,\frac{\partial}{\partial t}\,\theta(z,t) = -\frac{1}{2m}\,\frac{\partial^2}{\partial z^2}\,\theta(z,t) \quad (7.14)$$

Even though (7.13) is expressed in terms of the symmetrized ϕ, we shall for the sake of brevity do some of the calculations in the following with the non-symmetrized one. Since in the end we shall need to find fidelity, which is the inner product of two states, the symmetrization will be applied anyway by virtue of the identity (7.10).

7.3 Linear effects

Here and in the following we shall assume that we were able to store the photons inside the ensemble as the excitations of the symmetric mode $\tilde{S}$. Then we can focus on the interaction

of these excitations inside the ensemble. First we define the creation operators

$$\hat{a}_1^\dagger(t) = \frac{1}{\sqrt{\mathcal{N}_1(t)}} \int \theta_1(z,t)\tilde{S}^\dagger(z)dz, \tag{7.15}$$

$$\hat{a}_2^\dagger(t) = \frac{1}{\sqrt{\mathcal{N}_2(t)}} \int \theta_2(z,t)\tilde{S}^\dagger(z)dz, \tag{7.16}$$

where θ_1 and θ_2 are different single-excitation coefficients of the state (7.9) corresponding to distinct (initially non-overlapping) wavepackets. In general, due to $\mathrm{Im}[m] \neq 0$ and the finite size effects we need to include the (time dependent) normalization factors $\mathcal{N}_1(t) = \int |\theta_1(z,t)|^2 dz$ and $\mathcal{N}_2(t) = \int |\theta_2(z,t)|^2 dz$. In terms of the creation operators (7.15) and (7.16), the single excitation states are $|01\rangle(t) = \hat{a}_1^\dagger(t)|00\rangle$ and $|10\rangle(t) = \hat{a}_2^\dagger(t)|00\rangle$. Here and in the following we shall use two equivalent ways to write the vacuum state: $|00\rangle$ and $|0\rangle$. The first one is going to be used for the qubit operators $\hat{a}_1^\dagger$ and $\hat{a}_2^\dagger$ and emphasizes the discrete nature of the two qubits, while the second one is going to be used for the symmetric mode operators $\tilde{S}^\dagger(z)$, as there is an infinite number of positions z, where the excitation can be created.

We are going to consider the initial atomic excitations of the form

$$\theta_1(z, t=0) = \lambda_1(z_1)e^{ik_\mathrm{w}z_1}, \tag{7.17}$$

$$\theta_2(z, t=0) = \lambda_2(z_2)e^{-ik_\mathrm{w}z_2}, \tag{7.18}$$

where k_w is the central momentum of the wavepacket (different from the central momentum k_0 of the quantum field itself); λ_1 and λ_2 can be taken to be Gaussians (3.19) for concreteness, with λ_1 being centered on $-\mu$ and λ_2 being centered on μ. The boundaries of the ensemble itself are $-L/2$ to $L/2$, so we need $\mu < L/2$. In the following we shall take it to be $\mu = L/4$.

The evolution of the states $|01\rangle$ and $|10\rangle$ obeys the free-particle Schrödinger equation (7.14) with dispersion relation $\omega(k) = k^2/(2m)$. The expansion of the dispersion relation around k_w gives

$$\omega(k) = \omega(k_\mathrm{w}) + v_\mathrm{g}(k - k_\mathrm{w}) + \frac{1}{2}\alpha(k - k_\mathrm{w})^2 \tag{7.19}$$

with $\omega(k_\mathrm{w}) = k_\mathrm{w}^2/(2m)$, $v_\mathrm{g} = k_\mathrm{w}/m$ and $\alpha = 1/m$. Thus θ_1 moves in the positive direction with the group velocity v_g, and θ_2 moves in the negative direction with the same group velocity. By substituting the above values of v_g and α into (3.20), adding a factor of $e^{-i\omega(k_\mathrm{w})t}$ (for the zeroth order term) and replacing k_0 by k_w we get

$$\theta_1(z,t) = \frac{1}{(2\pi\sigma^2)^{1/4}} \sqrt{\frac{1}{1+\frac{it}{2m\sigma^2}}} \exp\left(-\frac{(z+\mu-k_\mathrm{w}t/m)^2}{4(\sigma^2+it/(2m))}\right) e^{-i\frac{k_\mathrm{w}^2 t}{2m}} e^{ik_\mathrm{w}z}, \tag{7.20}$$

$$\theta_2(z,t) = \frac{1}{(2\pi\sigma^2)^{1/4}} \sqrt{\frac{1}{1+\frac{it}{2m\sigma^2}}} \exp\left(-\frac{(z-\mu+k_\mathrm{w}t/m)^2}{4(\sigma^2+it/(2m))}\right) e^{-i\frac{k_\mathrm{w}^2 t}{2m}} e^{-ik_\mathrm{w}z}. \tag{7.21}$$

For the double excitation state, we start with defining its value for $t = 0$:

$$|11\rangle(t=0) = \hat{a}_1^\dagger(0)\hat{a}_2^\dagger(0)|00\rangle = \iint \theta_1(z_1, t=0)\theta_2(z_2, t=0)\tilde{S}^\dagger(z_1)\tilde{S}^\dagger(z_2)|0\rangle dz_1 dz_2.$$

At later times the state $|11\rangle$ evolves according to the equation (7.13) with the initial condition $\phi(z_1, z_2, t=0) = \theta_1(z_1, t=0)\theta_2(z_2, t=0)$. That evolution can be understood by studying the scattering properties of the delta function potential.

7.4 Scattering

Just like we had looked at scattering from a two-level atom in section 3.2, we can consider scattering from a delta function potential. The derivation can be found for instance in [24]. However, in [24] only the single particle case was covered. We can reduce (7.13) to two independent single particle equations by assuming that the ensemble is infinite (so we don't have any boundary conditions) and going to the center of mass and relative coordinates

$$z_\mathrm{c} = \frac{1}{2}(z_1 + z_2), \quad z_\mathrm{r} = \frac{1}{2}(z_1 - z_2). \tag{7.22}$$

In these coordinates (and without symmetrization), we can write (7.13) as

$$i\,\frac{\partial}{\partial t}\,\phi(z_\mathrm{c}, z_\mathrm{r}, t) = -\frac{1}{4m}\left(\frac{\partial^2}{\partial z_\mathrm{c}^2} + \frac{\partial^2}{\partial z_\mathrm{r}^2}\right)\phi(z_\mathrm{c}, z_\mathrm{r}, t) + \kappa\phi(z_\mathrm{c}, z_\mathrm{r}, t)\delta(z_\mathrm{r})$$

This equation can be solved by separation of the variables. Start with the assumption $\phi(z_\mathrm{c}, z_\mathrm{r}, t) = Z_\mathrm{C}(z_\mathrm{c})Z_\mathrm{R}(z_\mathrm{r})T(t)$. Then we find that the center of mass coordinate evolves according to the free particle equation $Z_\mathrm{C}''(z_\mathrm{c}) = -k_\mathrm{c}^2 Z_\mathrm{C}(z_\mathrm{c})$, and the relative coordinate evolves according to the single particle Schrödinger equation with a delta potential

$$Z_\mathrm{R}''(z_\mathrm{r}) = -k_\mathrm{r}^2 Z_\mathrm{R}(z_\mathrm{r}) + 4m\kappa\delta(z_\mathrm{r})Z_\mathrm{R}(z_\mathrm{r}). \tag{7.23}$$

The time evolution $T'(t) = -iET(t)$ with $E = k_\mathrm{c}^2/(4m) + k_\mathrm{r}^2/(4m)$ results in a phase factor of $\exp(-iEt)$ on each Fourier component (for each k_c and k_r). Then we can apply the analysis of [24] on (7.23) and find the transmission and reflection coefficients

$$t(k_\mathrm{r}) = \frac{1}{1 + 2im\kappa/k_\mathrm{r}}, \quad r(k_\mathrm{r}) = \frac{-2im\kappa/k_\mathrm{r}}{1 + 2im\kappa/k_\mathrm{r}}. \tag{7.24}$$

We see that if $|m\kappa|/k_\mathrm{r} \to \infty$ then $r(k_\mathrm{r}) \to -1$. This is the desired factor of -1, that we shall use for the phase gate. Using (7.7) and (7.8) we can write

$$\frac{m\kappa}{k_\mathrm{r}} = -\frac{\Gamma_\mathrm{1D}^2 N}{4k_\mathrm{r}(2\Delta_1 + i\Gamma)(2\Delta_2 + i\Gamma)L}. \tag{7.25}$$

This expression highlights a very important feature of this whole setup with the counter-propagating classical drives. Compared to the single atom phase gate before, where we essentially needed the parameter $\Gamma_\mathrm{1D}/(\Gamma' - 2i\delta_k)$ to be big (see (6.1)), here it is possible to make the equivalent parameter $|m\kappa|/k_\mathrm{r}$ big by using more atoms.

7.5 Requirements for an efficient phase gate

Before we do the detailed calculations of the fidelity of a phase gate, we can list all the requirements, that we can directly understand from knowledge of the linear effects and transmission and reflection coefficients (7.24) for the plane waves.

We need to have pulses of small spatial width so that they are mostly localized inside the ensemble. Hence we require

$$\sigma \ll L. \tag{7.26}$$

We need our wave packets to be sharply peaked about their central momentum value in the Fourier space, i.e.

$$k_{\mathrm{w}}\sigma \gg 1. \tag{7.27}$$

These two requirements are going to compete with each other, since pulses that are spatially narrow, are also the pulses that have a wide momentum distribution.

We need big ξ to be able to make the necessary approximations and get an NLSE (7.6). The optical depth d has a simple relation to ξ, when $\Delta_1 = 0$. In this case, $d^{\mathrm{opt}} = 2\xi L/c$. Hence this requirement can be written as

$$d^{\mathrm{opt}} \gg 1. \tag{7.28}$$

We need the mass m to be mostly real. The time evolution of the Fourier components gives the factors

$$\exp\left(-i\frac{k_{\mathrm{w}}^2 t}{2(\mathrm{Re}[m] + i\,\mathrm{Im}[m])}\right) = \exp\left(-i\frac{k_{\mathrm{w}}^2 t\,\mathrm{Re}[m]}{2|m|^2}\right)\exp\left(-\frac{k_{\mathrm{w}}^2 t\,\mathrm{Im}[m]}{2|m|^2}\right).$$

Here $\exp\left(-(k_{\mathrm{w}}^2 t\,\mathrm{Im}[m])/(2|m|^2)\right)$ represents the loss due to the imaginary part of m. Hence we require

$$\mathrm{Im}[m] \ll \mathrm{Re}[m]. \tag{7.29}$$

The reflection coefficient for scattering from a delta function barrier (7.24) approaches -1 in the limit

$$\left|\frac{m\kappa}{k_{\mathrm{w}}}\right| \gg 1. \tag{7.30}$$

If we write the requirement (7.29) using (7.7), then we get

$$\frac{\mathrm{Im}[m]}{\mathrm{Re}[m]} = -\frac{\Gamma}{2\Delta_1} \ll 1.$$

We see here that requirements (7.29) and (7.30) will compete, since (7.29) needs small Γ/Δ_1 and (7.30) (see the alternative form (7.25)) needs large Γ/Δ_1.

7.6 Fidelity

We would like to optimize the operation of our phase gate. If we start with an initial state

$$|\psi_{\text{initial}}\rangle = \frac{1}{\sqrt{2}}(|00\rangle + |11\rangle) \tag{7.31}$$

then we want to end up in the state

$$|\psi_{\text{desired}}\rangle = \frac{1}{\sqrt{2}}(|00\rangle - |11\rangle).$$

Instead, we have a state $|\psi_{\text{final}}\rangle$ and want to know, how well it approximates $|\psi_{\text{desired}}\rangle$. This is what fidelity

$$F = |\langle\psi_{\text{final}}|\psi_{\text{desired}}\rangle|^2 \tag{7.32}$$

calculates. The states are assumed to be normalized, so if $|\psi_{\text{final}}\rangle$ is the same as $|\psi_{\text{desired}}\rangle$, then $F = 1$. Since we now have a measure of how well the gate performs, all we need is to find the functional expression for F and do a standard function maximization to find the optimal parameters.

Note that fidelity depends on the state that we choose to start with. For example, for an input vacuum state we shall always expect to find $F = 1$. We did not choose the initial state to be the completely general two-qubit state (2.2) to focus only on the two-excitation state effects. On the other hand we did not choose the initial state to be simply $|11\rangle$, since then we would not be able to tell, whether the sign was changed or not – the absolute value would still be the same. In this sense, the chosen initial state (7.31) will correctly "detect" the sign change, since $\langle\psi_{\text{initial}}|\psi_{\text{desired}}\rangle = 0$, so $F = 1$ cannot be obtained by simply doing nothing as it would be the case with the initial state $|11\rangle$. For the practical applications, the fidelity for some other input states may be more interesting, or alternatively the worst case fidelity, if arbitrary input states were allowed. For simplicity we shall concentrate on the input state (7.31) in this analysis.

In the detailed derivation here our goal is to find a comparatively simple expression for the fidelity of the form

$$F = 1 - E_1 - E_2 - E_3 - \ldots$$

where E_j terms are errors due the parameters in the requirements (7.26), (7.27), (7.28), (7.29) and (7.30) all having finite values instead of evaluated at a limit. To reach the simple expression we shall apply expansions along the way in such a way that the error due to each requirement will be found in the limit where all the other requirements are satisfied perfectly.

With the above in mind we begin our calculations. To calculate fidelity (7.32) we need to find the states

$$|\psi_{\text{final}}\rangle = \frac{1}{\sqrt{2}}\left(1 + \iint \phi(z_1, z_2, t)\tilde{S}^\dagger(z_1)\tilde{S}^\dagger(z_2)dz_1dz_2\right)|0\rangle, \tag{7.33}$$

$$|\psi_{\text{desired}}\rangle = \frac{1}{\sqrt{2}}\left(1 - \hat{a}_1^\dagger(t)\hat{a}_2^\dagger(t)\right)|00\rangle, \tag{7.34}$$

where the time t is chosen such that the interaction has happened. The group velocity is $v_{\text{g}} = k_{\text{w}}/m$ (m assumed to be real here), and in the following we shall assume that the time t fulfills $v_{\text{g}}t = L/2 = 2\mu$. With this choice of time the wavepackets (7.20) and (7.21) will exactly interchange places.

Using (7.10), (7.33) and (7.34) we can write fidelity (7.32) as

$$F = \left|\frac{1}{2} - \frac{1}{\sqrt{\mathcal{N}_1\mathcal{N}_2}}\frac{1}{2}I_1\right|^2 \tag{7.35}$$

with the integral

$$I_1 = \int_{-L/2}^{L/2}\int_{-L/2}^{L/2}\phi^*_{\text{sym}}(z_1, z_2, t)\theta_1(z_1, t)\theta_2(z_2, t)dz_1dz_2. \tag{7.36}$$

Now we begin the calculation to find $\phi(z_1, z_2, t)$ for arbitrary time t. The initial value is $\phi(z_1, z_2, t = 0) = \theta_1(z_1, t = 0)\theta_2(z_2, t = 0)$. To be able to use the transmission and reflection coefficients (7.24), we need to write ϕ in the center of mass and relative coordinates. It becomes

$$\phi(z_{\text{c}}, z_{\text{r}}, t = 0) = \frac{1}{\sqrt{2\pi\sigma^2}}\exp\left(\frac{z_{\text{c}}^2}{2\sigma^2}\right)\exp\left(-\frac{(z_{\text{r}} + \mu)^2}{2\sigma^2}\right)e^{2ik_{\text{w}}z_{\text{r}}}. \tag{7.37}$$

The corresponding symmetrized state is

$$\phi_{\text{sym}}(z_{\text{c}}, z_{\text{r}}, t = 0) = \phi(z_{\text{c}}, z_{\text{r}}, t = 0) + \phi(z_{\text{c}}, -z_{\text{r}}, t = 0). \tag{7.38}$$

The first correction term that we find is due to the finite ensemble. The initial state $\phi(z_1, z_2, t = 0)$ is normalized according to $\int_{-\infty}^{\infty}\int_{-\infty}^{\infty}|\phi(z_1, z_2, t = 0)|^2dz_1dz_2 = 1$. Due to the way we defined our center of mass and relative coordinates (7.22), this corresponds to the normalization condition $\int_{-\infty}^{\infty}\int_{-\infty}^{\infty}2|\phi(z_{\text{c}}, z_{\text{r}}, t = 0)|^2dz_{\text{c}}dz_{\text{r}} = 1$ (note the factor of two). For the finite ensemble we have a choice of either treating the probability that is outside of it as an error caused by the imperfect loading or assuming that loading process was perfect and normalizing ϕ such that the integral of its norm squared on the finite ensemble is 1. Formally these two options correspond to multiplying ϕ by $1/\sqrt{\mathcal{N}_\phi}$, where $\mathcal{N}_\phi$ can be respectively either 1 or

$$\mathcal{N}_\phi = \int_{-L/2}^{L/2}\int_{z_1}^{L/2}|\phi_{\text{sym}}(z_1, z_2, t = 0)|^2dz_2dz_1.$$

Even though the above integral can be carried out explicitly, as the next step we shall need to take the Fourier transform of (7.37) in the center of mass and relative coordinates. For that step integrating over the triangle $z_2 > z_1$ (suitably expressed in the coordinates z_c and z_r) will make the expressions complicated. Instead we integrate over the set shown in figure 7.2. Then, if we also neglect the second term in (7.38) we can approximate the normalization constant as

$$\mathcal{N}_\phi \approx \int_{-L/4-aL/4}^{0} \int_{-aL/4}^{aL/4} 2|\phi(z_c, z_r, t=0)|^2 dz_c dz_r.$$

If the width of the Gaussians σ in (7.37) is much smaller than the length of the ensemble L (requirement (7.26)), then the approximated integral is very close to the original one. The values of the constant a here can be chosen $1/2$ to be conservative, i.e. the approximate integration set is completely contained in the original one.

Similarly, we shall approximate I_1 (7.36) with the goal that it should be easy to integrate in the center of mass and relative coordinates. As shown in the figure 7.2, the initial product state $\theta_1(z_1, t=0)\theta_2(z_2, t=0)$ has the probability concentrated around the maximum at $(z_1, z_2) = (-L/4, L/4)$ (the center of the blue circle). We picked the final time t such that the maximum of the product state $\theta_1(z_1, t)\theta_2(z_2, t)$ has moved to $(z_1, z_2) = (L/4, -L/4)$ (the center of the dashed circle in figure 7.2). Thus to include the error due to the finite size of the ensemble we shall integrate over the mirror of the green area in figure 7.2, so we approximate

$$I_1 \approx 2 \int_{0}^{L/4+aL/4} \int_{-aL/4}^{aL/4} \phi^*_{\mathrm{sym}}(z_c, z_r, t)\theta_1(z_c + z_r, t)\theta_2(z_c - z_r, t) dz_c dz_r. \tag{7.39}$$

Since we want to consider each error term in the limit, where the others are satisfied perfectly, the integration of the correction terms (denoted by C_j below) will be done with infinite integration limits in (7.39).

The Fourier transform of the initial wavefunction taken on a finite ensemble is

$$\tilde{\phi}(k_c, k_r, t=0) = \tilde{\lambda}(k_c, k_r - 2k_w), \tag{7.40}$$

where

$$\tilde{\lambda}(k_c, k_r) = \frac{1}{\sqrt{\mathcal{N}_\phi}} \int_{-L/4-aL/4}^{0} \int_{-aL/4}^{aL/4} 2\phi(z_c, z_r, t=0) e^{-ik_c z_c - ik_r z_r} dz_c dz_r.$$

Carrying out the integral we obtain

$$\tilde{\lambda}(k_c, k_r) = \frac{1}{\sqrt{\mathcal{N}_\phi}} \frac{\sigma}{\sqrt{2\pi}} e^{-i\sigma^2 k_c^2/2} e^{-\sigma^2 k_r^2/2 - i\mu k_r} C_1 C_2(k_r)$$

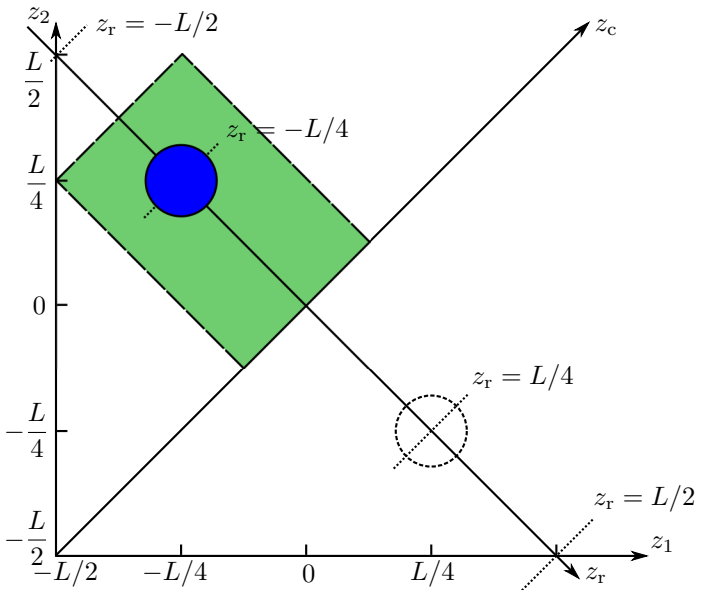

Figure 7.2: A schematic representation of the initial state (7.37). Both the original coordinate system (z_1, z_2) and the center of mass relative coordinate system (7.22) are drawn. The blue circle at $(z_1, z_2) = (-L/4, L/4)$ (or $(z_{\rm c}, z_{\rm r}) = (0, -L/4)$) shows, where the probability for the initial state is concentrated. The initial symmetrized state (7.38) also has another maximum at $(z_1, z_2) = (L/4, -L/4)$ (center of the dotted circle). This will only give a negligible contribution, when integrating on the upper triangle, where $z_2 > z_1$. In the text, instead of integrating over the whole upper triangle, we integrate over the set, where $-aL/4 \leq z_{\rm c} \leq aL/4$ and $-L/4 - aL/4 \leq z_{\rm r} \leq 0$. This set is shown for $a = 1/2$ as a green rectangle enclosed in dashed lines.

with

$$C_1 = \frac{1}{2}\left(\mathrm{erf}\left(\frac{aL + 4ik_{\rm c}\sigma^2}{4\sqrt{2}\sigma}\right) + \mathrm{erf}\left(\frac{aL - 4ik_{\rm c}\sigma^2}{4\sqrt{2}\sigma}\right)\right),$$

$$C_2(k_{\rm r}) = \frac{1}{2}\left(\mathrm{erf}\left(\frac{\mu + ik_{\rm r}\sigma^2}{\sqrt{2}\sigma}\right) + \mathrm{erf}\left(\frac{(1+a)L - 4(\mu + ik_{\rm r}\sigma^2)}{4\sqrt{2}\sigma}\right)\right).$$

Setting $\mu = L/2$ and expanding the above around the limit $L/\sigma \gg 1$ we get $C_1 \approx 1 - C_3$

and $C_2(k_\mathrm{r}) \approx 1 - C_4(k_\mathrm{r})$ with

$$C_3 = \sqrt{\frac{2}{\pi}}\frac{2\sigma}{aL}\left(\exp\left(-(aL/\sigma + 4ik_\mathrm{c}\sigma)^2/32\right) + \exp\left(-(aL/\sigma - 4ik_\mathrm{c}\sigma)^2/32\right)\right),$$
$$C_4(k_\mathrm{r}) = \sqrt{\frac{2}{\pi}}\frac{2\sigma}{L}\left(\frac{1}{a}\exp\left(-(aL/\sigma + 4ik_\mathrm{r}\sigma)^2/32\right) + \exp\left(-(L/\sigma - 4ik_\mathrm{r}\sigma)^2/32\right)\right).$$

We can write the final state in terms of the Fourier transform of the initial state and the Heaviside theta function θ_H:

$$\begin{aligned}\phi(z_\mathrm{c}, z_\mathrm{r}, t) = \theta_\mathrm{H}(-z_\mathrm{r})(\phi_\mathrm{incident}(z_\mathrm{c}, z_\mathrm{r}, t) + \phi_\mathrm{reflected}(z_\mathrm{c}, z_\mathrm{r}, t)) \\ + \theta_\mathrm{H}(z_\mathrm{r})\phi_\mathrm{transmitted}(z_\mathrm{c}, z_\mathrm{r}, t)\end{aligned} \tag{7.41}$$

with

$$\phi_\mathrm{incident}(z_\mathrm{c}, z_\mathrm{r}, t) = \frac{1}{2\pi}\int_0^\infty\int_{-\infty}^\infty \tilde{\phi}(k_\mathrm{c}, k_\mathrm{r}, t=0)e^{-i\frac{k_\mathrm{c}^2}{4m}t}e^{-i\frac{k_\mathrm{r}^2}{4m}t}e^{ik_\mathrm{c}z_\mathrm{c}}e^{ik_\mathrm{r}z_\mathrm{r}}dk_\mathrm{c}dk_\mathrm{r},$$
$$\phi_\mathrm{reflected}(z_\mathrm{c}, z_\mathrm{r}, t) = \frac{1}{2\pi}\int_0^\infty\int_{-\infty}^\infty r(k_\mathrm{r})\tilde{\phi}(k_\mathrm{c}, k_\mathrm{r}, t=0)e^{-i\frac{k_\mathrm{c}^2}{4m}t}e^{-i\frac{k_\mathrm{r}^2}{4m}t}e^{ik_\mathrm{c}z_\mathrm{c}}e^{-ik_\mathrm{r}z_\mathrm{r}}dk_\mathrm{c}dk_\mathrm{r},$$
$$\phi_\mathrm{transmitted}(z_\mathrm{c}, z_\mathrm{r}, t) = \frac{1}{2\pi}\int_0^\infty\int_{-\infty}^\infty t(k_\mathrm{r})\tilde{\phi}(k_\mathrm{c}, k_\mathrm{r}, t=0)e^{-i\frac{k_\mathrm{c}^2}{4m}t}e^{-i\frac{k_\mathrm{r}^2}{4m}t}e^{ik_\mathrm{c}z_\mathrm{c}}e^{ik_\mathrm{r}z_\mathrm{r}}dk_\mathrm{c}dk_\mathrm{r}.$$

To obtain a high fidelity we need the Fourier transform of the initial state (7.40) to be a distribution with mostly positive k_r. This is the case in the limit $k_\mathrm{w}\sigma \gg 1$ (requirement (7.27)). Realistically the distribution of the k-vectors will also have some part with negative k_r. That part moves in the "wrong" direction and is not able to be scattered. To account for this error, the integration over k_r in the above expressions for ϕ_incident, $\phi_\mathrm{reflected}$ and $\phi_\mathrm{transmitted}$ only goes over positive k_r. The part $\phi_\mathrm{reflected}$ is actually an integral over negative k-vectors, and this is expressed by the phase factor $e^{-ik_\mathrm{r}z_\mathrm{r}}$ in the integrand. The solution (7.41) does not describe all the complicated processes *during* the scattering, nor do we need it to. It it, however, accurate for the times that are small enough, that the initial wave packet is still far from the interaction potential, or for the times that are big enough, that the interaction has already happened and the resulting pulses moved away from the interaction potential. It is the latter case that we are interested in. For long times we can neglect ϕ_incident since by then it has already been almost completely transformed into $\phi_\mathrm{reflected}$ and $\phi_\mathrm{transmitted}$. In our approximative solution (7.41) this formally looks like ϕ_incident has moved into the region with big positive z_r such that it does not contribute in the part, where $z_\mathrm{r} < 0$.

We note that we completely disregard the boundary conditions. Thus we treat the evolution, as if it happened in the infinite ensemble, and then obtain corrections for the finite ensemble by discarding the probability outside of the ensemble. Realistically, some of the pulse will be reflected at the boundaries, which will cause the resulting pulse to be

the sum of the incident and reflected parts and hence be distorted compared to the original one (see the simulations in chapter 8).

The symmetrized state is

$$\phi_{\rm sym}(z_{\rm c}, z_{\rm r}, t) = \frac{1}{\sqrt{\mathcal{N}_\phi}} \frac{1}{2\pi} \phi_c(z_{\rm c}, t)(\theta_{\rm H}(-z_{\rm r})I_2 + \theta_{\rm H}(z_{\rm r})I_3)$$

with

$$\begin{aligned}
\phi_c(z_{\rm c}, t) &= \frac{\sigma}{\sqrt{2\pi}} \int_{-\infty}^{\infty} e^{-i\sigma^2 k_{\rm c}^2/2} C_1 e^{-i\frac{k_{\rm c}^2}{4m}t} e^{ik_{\rm c}z_{\rm c}} dk_{\rm c}, \\
I_2 &= \int_0^{\infty} (t(k_{\rm r}) + r(k_{\rm r})) e^{-\sigma^2(k_{\rm r}-2k_{\rm w})^2/2 - i\mu(k_{\rm r}-2k_{\rm w})} C_2(k_{\rm r}-2k_{\rm w}) e^{-i\frac{k_{\rm r}^2}{4m}t} e^{-ik_{\rm r}z_{\rm r}}, \\
I_3 &= \int_0^{\infty} (t(k_{\rm r}) + r(k_{\rm r})) e^{-\sigma^2(k_{\rm r}-2k_{\rm w})^2/2 - i\mu(k_{\rm r}-2k_{\rm w})} C_2(k_{\rm r}-2k_{\rm w}) e^{-i\frac{k_{\rm r}^2}{4m}t} e^{ik_{\rm r}z_{\rm r}}.
\end{aligned}$$

The center of mass part is $\phi_c(z_{\rm c}, t) = \phi_{c,0}(z_{\rm c}, t) - C_5$ with

$$\begin{aligned}
\phi_{c,0}(z_{\rm c}, t) &= \frac{1}{1 + \frac{it}{2m\sigma^2}} \exp\left(-\frac{z_{\rm c}^2}{2(\sigma^2 + it/(2m))}\right), \\
C_5 &= \frac{2\sqrt{2}\sigma}{aL} \sqrt{\frac{4m}{it}} \exp\left(-\frac{a^2L^2}{32\sigma^2}\right) \left(\exp\left(-\frac{(z_{\rm c} - aL/4)^2}{it/m}\right) \exp\left(-\frac{(z_{\rm c} + aL/4)^2}{it/m}\right)\right).
\end{aligned}$$

In the integrands of I_2 and I_3 we can approximate the coefficient $t(k_{\rm r}) + r(k_{\rm r})$ by simply taking its value at $k_{\rm r} = 2k_{\rm w}$ since that is where the Gaussian is centered on. We could expand $t(k_{\rm r}) + r(k_{\rm r})$ around $k_{\rm r} = 2k_{\rm w}$ to first or second order but we shall not do so. The first order expansion will integrate to zero due to symmetry of the Gaussian in the limit $k_{\rm w}\sigma \gg 1$ (requirement (7.27)). The second order term will not integrate to zero, but it is much smaller compared to the zeroth order term, and we shall assume that it can be discarded. Due to the $k_{\rm r}$ cutoff in I_2 and I_3 we shall obtain the next correction terms. We have $I_2 = (t(2k_{\rm w}) + r(2k_{\rm w}))(I_4 - I_5)$ and $I_3 = (t(2k_{\rm w}) + r(2k_{\rm w}))(I_6 - I_7)$ with

$$\begin{aligned}
I_4 &= \int_{-2k_{\rm w}}^{\infty} e^{-\sigma^2 q^2/2 - i\mu q} e^{-i\frac{(q+2k_{\rm w})^2}{4m}t} e^{-i(q+2k_{\rm w})z_{\rm r}} dq, \\
I_5 &= \int_{-\infty}^{\infty} e^{-\sigma^2 q^2/2 - i\mu q} C_4(q) e^{-i\frac{(q+2k_{\rm w})^2}{4m}t} e^{-i(q+2k_{\rm w})z_{\rm r}} dq, \\
I_6 &= \int_{-2k_{\rm w}}^{\infty} e^{-\sigma^2 q^2/2 - i\mu q} e^{-i\frac{(q+2k_{\rm w})^2}{4m}t} e^{i(q+2k_{\rm w})z_{\rm r}} dq, \\
I_7 &= \int_{-\infty}^{\infty} e^{-\sigma^2 q^2/2 - i\mu q} C_4(q) e^{-i\frac{(q+2k_{\rm w})^2}{4m}t} e^{i(q+2k_{\rm w})z_{\rm r}} dq.
\end{aligned}$$

Here we have made a substitution $q = k_\mathrm{r} - 2k_\mathrm{w}$. The lower limit was extended to $-\infty$ in I_5 and I_7 to approximate the finite size ensemble corrections C_4 in the limit $k_\mathrm{w}\sigma \gg 1$. We evaluate I_4 and I_6 and find $I_4 = I_8 C_6$, $I_6 = I_9 C_7$ with

$$I_8 = e^{-i\frac{k_\mathrm{w}^2 t}{m}} e^{-2ik_\mathrm{w} z_\mathrm{r}} \frac{\sqrt{2\pi}}{\sigma} \sqrt{\frac{1}{1+\frac{it}{2m\sigma^2}}} \exp\left(\frac{\left(z_\mathrm{r} + k_\mathrm{w} t/m - \mu\right)^2}{2\sigma^2 + it/m}\right),$$

$$I_9 = e^{-i\frac{k_\mathrm{w}^2 t}{m}} e^{2ik_\mathrm{w} z_\mathrm{r}} \frac{\sqrt{2\pi}}{\sigma} \sqrt{\frac{1}{1+\frac{it}{2m\sigma^2}}} \exp\left(\frac{\left(z_\mathrm{r} - k_\mathrm{w} t/m + \mu\right)^2}{2\sigma^2 + it/m}\right),$$

$$C_6 = \frac{1}{2}\left(1 + \mathrm{erf}\left(-i\frac{z_\mathrm{r} + k_\mathrm{w} t/m - \mu}{\sqrt{2\sigma^2 + it/m}} + k_\mathrm{w}\sigma\sqrt{2 + it/(m\sigma^2)}\right)\right),$$

$$C_7 = \frac{1}{2}\left(1 + \mathrm{erf}\left(i\frac{z_\mathrm{r} - k_\mathrm{w} t/m + \mu}{\sqrt{2\sigma^2 + it/m}} + k_\mathrm{w}\sigma\sqrt{2 + it/(m\sigma^2)}\right)\right).$$

We can expand C_6 and C_7 in the limit $k_\mathrm{w}\sigma \gg 1$ and obtain $C_6 = 1 - C_8$ and $C_7 = 1 - C_9$ with

$$C_8 = \exp\left(\left(-i\frac{z_\mathrm{r} + k_\mathrm{w} t/m - \mu}{\sqrt{2\sigma^2 + it/m}} + k_\mathrm{w}\sigma\sqrt{2 + it/(m\sigma^2)}\right)^2\right) \frac{1}{k_\mathrm{w}\sigma\sqrt{\pi}\sqrt{2 + it/(m\sigma^2)}},$$

$$C_9 = \exp\left(\left(i\frac{z_\mathrm{r} - k_\mathrm{w} t/m + \mu}{\sqrt{2\sigma^2 + it/m}} + k_\mathrm{w}\sigma\sqrt{2 + it/(m\sigma^2)}\right)^2\right) \frac{1}{k_\mathrm{w}\sigma\sqrt{\pi}\sqrt{2 + it/(m\sigma^2)}}.$$

For the remaining integrals we find

$$I_5 = e^{-i\frac{k_\mathrm{w}^2 t}{m}} e^{-2ik_\mathrm{w} z_\mathrm{r}} \sqrt{2}\frac{2\sigma}{L}\sqrt{\frac{4m}{it}} \left(e^{-L^2/(32\sigma^2)} \exp\left(-\frac{(z_\mathrm{r} + k_\mathrm{w} t/m - \mu - L/4)^2}{it/m}\right) + \frac{e^{-a^2 L^2/(32\sigma^2)}}{a} \exp\left(-\frac{(z_\mathrm{r} + k_\mathrm{w} t/m - \mu + aL/4)^2}{it/m}\right)\right),$$

$$I_7 = e^{-i\frac{k_\mathrm{w}^2 t}{m}} e^{2ik_\mathrm{w} z_\mathrm{r}} \sqrt{2}\frac{2\sigma}{L}\sqrt{\frac{4m}{it}} \left(e^{-L^2/(32\sigma^2)} \exp\left(-\frac{(z_\mathrm{r} - k_\mathrm{w} t/m + \mu + L/4)^2}{it/m}\right) + \frac{e^{-a^2 L^2/(32\sigma^2)}}{a} \exp\left(-\frac{(z_\mathrm{r} - k_\mathrm{w} t/m + \mu - aL/4)^2}{it/m}\right)\right).$$

Using the above definitions we can write the integral (7.39) as

$$\begin{aligned} I_1 =& \frac{2}{\sqrt{\mathcal{N}_\phi}} \frac{1}{2\pi} (t(2k_\mathrm{w}) + r(2k_\mathrm{w}))^* \\ & \times \int_0^{L/4+aL/4} \int_{-aL/4}^{aL/4} (\phi^*_{c,0}(z_\mathrm{c}, t) - C^*_5) \\ & \qquad \times (\theta_\mathrm{H}(-z_\mathrm{r})(I^*_8(1 - C^*_8) - I^*_5) + \theta_\mathrm{H}(z_\mathrm{r})(I^*_9(1 - C^*_9) - I^*_7)) \\ & \qquad \times \theta_1(z_\mathrm{c} + z_\mathrm{r}, t)\theta_2(z_\mathrm{c} - z_\mathrm{r}, t) dz_\mathrm{c} dz_\mathrm{r}. \end{aligned}$$

Here C_5, I_5 and I_7 are expressions for the correction to the initial state caused by the finite size of the ensemble; C_8 and C_9 are expressions for the correction due to a cutoff in k_r-space. The limits of integration in I_1 also express corrections caused by the finite size of the ensemble – now for the *final* state. Expanding I_1 such that cross terms involving more than one correction are discarded, we can write

$$I_1 \approx I_{10} + I_{11} + I_{12} + I_{13}$$

with

$$\begin{aligned} I_{10} =& \frac{2}{\sqrt{\mathcal{N}_\phi}} \frac{1}{2\pi} (t(2k_\mathrm{w}) + r(2k_\mathrm{w}))^* \int_0^{L/4+aL/4} \int_{-aL/4}^{aL/4} \phi^*_{c,0}(z_\mathrm{c}, t)(\theta_\mathrm{H}(-z_\mathrm{r})I^*_8 + \theta_\mathrm{H}(z_\mathrm{r})I^*_9) \\ & \qquad \times \theta_1(z_\mathrm{c} + z_\mathrm{r}, t)\theta_2(z_\mathrm{c} - z_\mathrm{r}, t) dz_\mathrm{c} dz_\mathrm{r}, \\ I_{11} =& \frac{2}{\sqrt{\mathcal{N}_\phi}} \frac{1}{2\pi} \int_\infty^\infty \int_{-\infty}^\infty C^*_5(\theta_\mathrm{H}(-z_\mathrm{r})I^*_8 + \theta_\mathrm{H}(z_\mathrm{r})I^*_9)\theta_1(z_\mathrm{c} + z_\mathrm{r}, t)\theta_2(z_\mathrm{c} - z_\mathrm{r}, t) dz_\mathrm{c} dz_\mathrm{r}. \\ I_{12} =& \frac{2}{\sqrt{\mathcal{N}_\phi}} \frac{1}{2\pi} \int_\infty^\infty \int_{-\infty}^\infty \phi^*_{c,0}(z_\mathrm{c}, t)(\theta_\mathrm{H}(-z_\mathrm{r})I^*_5 + \theta_\mathrm{H}(z_\mathrm{r})I^*_7)\theta_1(z_\mathrm{c} + z_\mathrm{r}, t)\theta_2(z_\mathrm{c} - z_\mathrm{r}, t) dz_\mathrm{c} dz_\mathrm{r}, \\ I_{13} =& \frac{2}{\sqrt{\mathcal{N}_\phi}} \frac{1}{2\pi} \int_\infty^\infty \int_{-\infty}^\infty \phi^*_{c,0}(z_\mathrm{c}, t)(\theta_\mathrm{H}(-z_\mathrm{r})I^*_8 C^*_8 + \theta_\mathrm{H}(z_\mathrm{r})I^*_9 C^*_9) \\ & \qquad \times \theta_1(z_\mathrm{c} + z_\mathrm{r}, t)\theta_2(z_\mathrm{c} - z_\mathrm{r}, t) dz_\mathrm{c} dz_\mathrm{r}. \end{aligned}$$

In I_{11}, I_{12} and I_{13} we have approximated $(t(2k_\mathrm{w}) + r(2k_\mathrm{w})) \approx -1$ (to assume perfect scattering) and extended the limits of integration to $\pm\infty$ (to neglect the finite ensemble size corrections for the final state). We shall also assume the mass m to be real in I_{11}, I_{12} and I_{13}. In I_{10}, the only place, where we shall use the imaginary part of m is in the factor

$$e^{i\frac{k_\mathrm{w}^2 t}{m^*}} e^{-i\frac{k_\mathrm{w}^2 t}{m}} = \exp\left(2k_\mathrm{w}^2 t \,\mathrm{Im}\left[1/m\right]\right) = \exp\left(2k_\mathrm{w}\mu\Gamma/\Delta_1\right).$$

In the last equality above we set $t = 2\mu m/\left(k_\mathrm{w}\,\mathrm{Re}[1/m]\right)$ (or equivalently $\mathrm{Re}[v_\mathrm{g}]t = L/2 = 2\mu$).

Using the expressions (7.20) and (7.21) we can write the θ product state in the center of mass and relative coordinates as

$$\begin{aligned}&\theta_1(z_\mathrm{c}+z_\mathrm{r},t)\theta_2(z_\mathrm{c}-z_\mathrm{r},t)\\&=\frac{1}{\sqrt{2\pi\sigma^2}}\frac{1}{1+it/(2m\sigma^2)}\exp\left(-\frac{z_\mathrm{c}^2}{2\sigma^2+it/m}\right)\exp\left(-\frac{(z_\mathrm{r}-\mu)^2}{2\sigma^2+it/m}\right)e^{2ik_\mathrm{w}z_\mathrm{r}}.\end{aligned}$$

Now we evaluate the integral I_{10}. For the chosen value of t, the Gaussian in I_8 is centered on $z_\mathrm{r}=-\mu$ and does not have a significant overlap with $\theta_1(z_\mathrm{c}+z_\mathrm{r},t)\theta_2(z_\mathrm{c}-z_\mathrm{r},t)$; hence we can neglect it. The Gaussian in the integral I_9, however, is centered on $z_\mathrm{r}=\mu$, just like $\theta_1(z_\mathrm{c}+z_\mathrm{r},t)\theta_2(z_\mathrm{c}-z_\mathrm{r},t)$ and thus it will give a significant contribution. As before, when integrating on a finite ensemble we shall expand the resulting error functions around the limit $L/\sigma\gg1$. Under these approximations we find

$$\begin{aligned}I_{10}=&\frac{1}{\sqrt{\mathcal{N}_\phi}}\frac{1+i\kappa^*m^*/k_\mathrm{w}}{1-i\kappa^*m^*/k_\mathrm{w}}\exp\left(k_\mathrm{w}L\Gamma/(2\Delta_1)\right)\\&\times\left(1-\frac{6\exp\left(a^2(L/\sigma)^2/16\right)}{\sqrt{\pi}a(L/\sigma)}-\frac{2\exp\left((L/\sigma)^2/16\right)}{\sqrt{\pi}(L/\sigma)}\right).\end{aligned}$$

Similarly,

$$I_{11}=\frac{1}{\sqrt{\mathcal{N}_\phi}}\frac{4\sqrt{2}}{\sqrt{\pi}a(L/\sigma)}\exp\left(-\left(\frac{1}{32}+\frac{1}{512}\right)a^2(L/\sigma)^2\right)\exp\left(i\frac{1}{8}a^2k_\mathrm{w}L\right),$$

$$\begin{aligned}I_{12}=&\frac{1}{\sqrt{\mathcal{N}_\phi}}\frac{4}{L/\sigma}\left[\exp\left(-\left(\frac{1}{32}+\frac{1+a^2}{512}\right)(L/\sigma)^2\right)\exp\left(i\left(\frac{1}{8}+\frac{1+a^2}{128}\right)k_\mathrm{w}L\right)\right.\\&\left.+\frac{1}{a}\exp\left(-\left(\frac{a^2}{32}+\frac{1+a^2}{512}\right)(L/\sigma)^2\right)\exp\left(i\left(\frac{a^2}{8}+\frac{1+a^2}{128}\right)k_\mathrm{w}L\right)\right],\end{aligned}$$

$$\begin{aligned}I_{13}=&\frac{1}{\sqrt{\mathcal{N}_\phi}}\frac{1}{2\sqrt{\pi}k_\mathrm{w}}\sqrt{\mathrm{Re}\left[\frac{1}{\sigma^2+i\mu/k_\mathrm{w}}\right]}\sqrt{\frac{\sigma^2+i\mu/k_\mathrm{w}}{\sigma^2-i\mu/k_\mathrm{w}}}\\&\times\exp\left(-(2k_\mathrm{w}^2\sigma^2-2ik_\mathrm{w}\mu)\left(\frac{\sigma^2+i\mu/k_\mathrm{w}}{\sigma^2-i\mu/k_\mathrm{w}}+1\right)\right).\end{aligned}$$

Using (7.25) we can write the scattering factor in I_{10} as

$$\frac{1-i\kappa m/k_\mathrm{w}}{1+i\kappa m/k_\mathrm{w}}=\frac{1+i\Gamma_{1\mathrm{D}}^2N/\left(4k_\mathrm{w}L(2\Delta_1+i\Gamma)(2\Delta_2+i\Gamma)\right)}{1-i\Gamma_{1\mathrm{D}}^2N/\left(4k_\mathrm{w}L(2\Delta_1+i\Gamma)(2\Delta_2+i\Gamma)\right)}\tag{7.42}$$

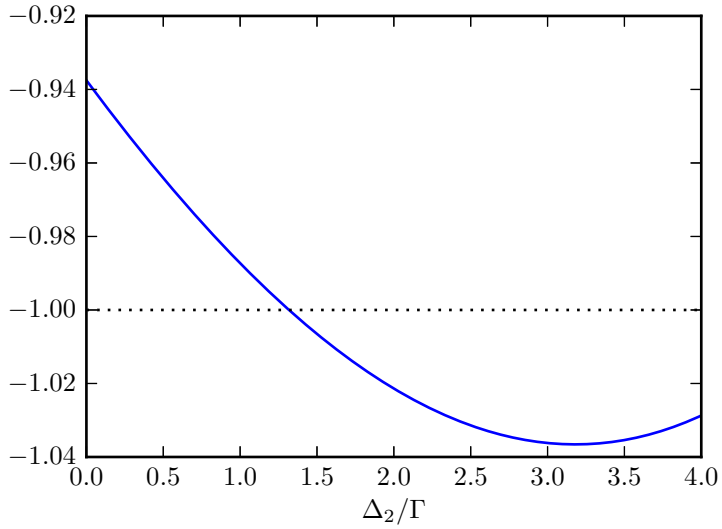

Figure 7.3: Plot of the real value of the expression (7.42) with parameters $N/(k_{\mathrm{w}}L) = 1000$, $\Gamma_{1\mathrm{D}} = 0.5\Gamma$, $\Delta_1 = -\Gamma$.

In the above expression we included the imaginary part of the mass. However, this can cause it to have real value less than -1 (see figure 7.3) which is unphysical. Here it seems that the effective description with an imaginary mass is incorrect when one needs to consider scattering. In the following we shall neglect the imaginary part of the mass in the scattering factor. Thus we assume

$$\frac{1 - i\kappa m/k_{\mathrm{w}}}{1 + i\kappa m/k_{\mathrm{w}}} = \frac{8k_{\mathrm{w}}L\Delta_1(2\Delta_2 + i\Gamma) + i\Gamma_{1\mathrm{D}}^2 N}{8k_{\mathrm{w}}L\Delta_1(2\Delta_2 + i\Gamma) - i\Gamma_{1\mathrm{D}}^2 N}. \tag{7.43}$$

We note that for the absolute value squared of the above expression it holds that

$$\left|\frac{1 - i\kappa m/k_{\mathrm{w}}}{1 + i\kappa m/k_{\mathrm{w}}}\right|^2 = \frac{(16k_{\mathrm{w}}L\Delta_1\Delta_2)^2 + (8k_{\mathrm{w}}L\Delta_1\Gamma + \Gamma_{1\mathrm{D}}^2 N)^2}{(16k_{\mathrm{w}}L\Delta_1\Delta_2)^2 + (8k_{\mathrm{w}}L\Delta_1\Gamma - \Gamma_{1\mathrm{D}}^2 N)^2} < 1 \quad \text{for } \Delta_1 < 0.$$

The requirement $\Delta_1 < 0$ is natural, since it also makes positive values of k_{w} correspond to positive group velocities $v_{\mathrm{g}} = k_{\mathrm{w}} \operatorname{Re}[1/m]$ (see the expression for the mass (7.7)).

We expand the scattering factor (7.43) around the limit

$$\left|i\Gamma_{1\mathrm{D}}^2 N / \left(8k_{\mathrm{w}}L\Delta_1(2\Delta_2 + i\Gamma)\right)\right| \gg 1 \tag{7.44}$$

and find

$$\frac{1 - i\kappa m/k_{\mathrm{w}}}{1 + i\kappa m/k_{\mathrm{w}}} \approx -1 - \frac{16k_{\mathrm{w}}L\Delta_1(2\Delta_2 + i\Gamma)}{i\Gamma_{1\mathrm{D}}^2 N}.$$

We shall also expand the loss term due to the imaginary mass in I_{10} around the limit

$$k_{\mathrm{w}} L\Gamma/\Delta_1 \ll 1. \tag{7.45}$$

Thus

$$\exp\left(k_{\mathrm{w}} L\Gamma/(2\Delta_1)\right) \approx 1 + k_{\mathrm{w}} L\Gamma/(2\Delta_1).$$

Note that (7.44) and (7.45) are not contradictory. The limit (7.44) can still hold even if Γ/Δ_1 is small. We just need bigger $N\Gamma_{1\mathrm{D}}^2/\Gamma^2$ to counteract that.

In I_{11} we shall neglect the phase term $\exp(ia^2 k_{\mathrm{w}} L/8)$ since it depends on a, which was chosen rather arbitrarily. Formally we can say that in the limit of big $k_{\mathrm{w}} L$ we can adjust a slightly to obtain $\exp(ia^2 k_{\mathrm{w}} L/8) = 1$. Experimentally we assume that it should be possible to optimize the loading process such that these kinds of phases are cancelled. In I_{12} we also neglect the corresponding phase factors. In I_{13} we shall neglect the terms $ik_{\mathrm{w}}\mu$, i.e. assume that $k_{\mathrm{w}}^2\sigma^2 \gg k_{\mathrm{w}}\mu$.

Adding contributions of I_{10}, I_{11}, I_{13} and I_{14} we get

$$I_1 = \frac{(-1)}{\sqrt{\mathcal{N}_\phi}}\left[1 + \frac{16k_{\mathrm{w}} L\Delta_1(2\Delta_2 - i\Gamma)}{-i\Gamma_{1\mathrm{D}}^2 N} + \frac{k_{\mathrm{w}} L\Gamma}{2\Delta_1} - \frac{\exp\left(-2(k_{\mathrm{w}}\sigma)^2\right)}{2\sqrt{\pi}k_{\mathrm{w}}\sigma} - \sum_{j=1}^{5} B_j \frac{\exp\left(-D_j(L/\sigma)^2\right)}{L/\sigma}\right]$$

with

$$\left.\begin{aligned} B_1 &= \frac{6}{\sqrt{\pi}a}, D_1 = a^2/16; \\ B_2 &= \frac{2}{\sqrt{\pi}}, D_2 = 1/16; \end{aligned}\right\} \text{ from } I_{10}$$

$$\left.\begin{aligned} B_3 &= \frac{4\sqrt{2}}{\sqrt{\pi}a}, D_3 = \left(\frac{1}{32} + \frac{1}{512}\right)a^2; \end{aligned}\right\} \text{ from } I_{11} \tag{7.46}$$

$$\left.\begin{aligned} B_4 &= 4, D_4 = \left(\frac{1}{32} + \frac{1+a^2}{512}\right); \\ B_5 &= \frac{4}{a}, D_5 = \left(\frac{a^2}{32} + \frac{1+a^2}{512}\right). \end{aligned}\right\} \text{ from } I_{12}$$

In the limit $L/\sigma \gg 1$, the terms $B_j \exp\left(-D_j(L/\sigma)^2\right)/(L/\sigma)$ are dominated by the exponential factor. Thus the biggest contribution comes from the term with the smallest value of D_j, i.e. D_3. The term with D_5 is almost as big (see figure 7.4). To find a crude

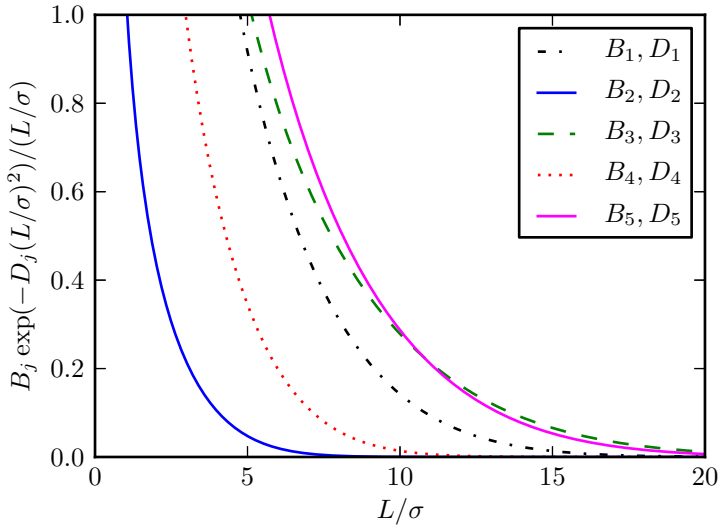

Figure 7.4: Plot of the terms $B_j \exp\left(-D_j(L/\sigma)^2\right)/(L/\sigma)$ with B_j and D_j given by (7.46) ($a = 1/2$). The error term with constants B_2, D_2 (blue solid line) is smaller than the error term with constants B_5, D_5 (magenta solid line).

estimate for the whole sum $\sum_j B_j \exp\left(-D_j(L/\sigma)^2\right)/(L/\sigma)$ we replace it with only the term $B_3 \exp\left(-D_3(L/\sigma)^2\right)/(L/\sigma)$ multiplied by 2 to account for the term with D_5. With these approximations we get

$$I_1 = \frac{(-1)}{\sqrt{\mathcal{N}_\phi}}\left[1 + \frac{16k_{\mathrm{w}}L\Delta_1(2\Delta_2 - i\Gamma)}{-i\Gamma_{1\mathrm{D}}^2 N} + \frac{k_{\mathrm{w}}L\Gamma}{2\Delta_1} - \frac{\exp\left(-2(k_{\mathrm{w}}\sigma)^2\right)}{2\sqrt{\pi}k_{\mathrm{w}}\sigma} - 2B_3\frac{\exp\left(-D_3(L/\sigma)^2\right)}{L/\sigma}\right]$$

In the expression for the fidelity (7.35), the normalization constants $\mathcal{N}_1$ and $\mathcal{N}_2$ account for the errors that happen due to the linear effects: imaginary part of the mass and finite ensemble. Based on the results we have found for so far, we get

$$\frac{1}{\sqrt{\mathcal{N}_1\mathcal{N}_2}} \approx 1 - \frac{k_{\mathrm{w}}L\Gamma}{4\Delta_1} + B_3\frac{\exp\left(-D_3(L/\sigma)^2\right)}{L/\sigma}.$$

We could have taken the normalization factor $\mathcal{N}_\phi$ into account in a similar manner. However, for simplicity we set $\mathcal{N}_\phi = 1$ in the following.

The fidelity (7.35) can be written as

$$F = \frac{1}{4}\left(1 - 2\,\mathrm{Re}\left[\frac{1}{\sqrt{\mathcal{N}_1\mathcal{N}_2}}I_1\right] + \left|\frac{1}{\sqrt{\mathcal{N}_1\mathcal{N}_2}}I_1\right|^2\right).$$

Discarding the cross terms due to different corrections, we get

$$F = 1 + \frac{16k_{\mathrm{w}}L\Delta_1\Gamma}{\Gamma_{1\mathrm{D}}^2 N} + \frac{k_{\mathrm{w}}L\Gamma}{4\Delta_1} - \frac{\exp\left(-2(k_{\mathrm{w}}\sigma)^2\right)}{2\sqrt{\pi}k_{\mathrm{w}}\sigma} - B_3\frac{\exp\left(-D_3(L/\sigma)^2\right)}{L/\sigma} \tag{7.47}$$

The detuning Δ_2 only appears in the second order term that we have already discarded in the above expression. The scattering factor (7.43) suggests that Δ_2 should be as small as possible for it to be closer to the limiting value -1. Hence the implicit assumption $\Delta_2 = 0$ in (7.47) is justified. The remaining parameters Δ_1, σ and k_{w} can be chosen such that the fidelity is maximized. This is what we shall do now.

To find the optimal Δ_1 we only need to consider the first two error terms in (7.47). The optimal value is

$$\Delta_1 = -\frac{\Gamma_{1\mathrm{D}}\sqrt{N}}{8}. \tag{7.48}$$

Inserting this value of Δ_1 back into (7.47), we get

$$F = 1 - \frac{4k_{\mathrm{w}}L\Gamma}{\Gamma_{1\mathrm{D}}\sqrt{N}} - \frac{\exp\left(-2(k_{\mathrm{w}}\sigma)^2\right)}{2\sqrt{\pi}k_{\mathrm{w}}\sigma} - B_3\frac{\exp\left(-D_3(L/\sigma)^2\right)}{L/\sigma}. \tag{7.49}$$

This expression depends on two variables: $k_{\mathrm{w}}\sigma$ and L/σ. To optimize it with respect to them we find the partial derivatives and set them equal to 0. Thus we obtain the equations

$$\frac{L}{\sigma} = \frac{\Gamma_{1\mathrm{D}}\sqrt{N}}{4\Gamma}\left(\frac{2}{\sqrt{\pi}}\exp\left(-2(k_{\mathrm{w}}\sigma)^2\right) + \frac{\exp\left(-2(k_{\mathrm{w}}\sigma)^2\right)}{2\sqrt{\pi}(k_{\mathrm{w}}\sigma)^2}\right),$$

$$k_{\mathrm{w}}\sigma = \frac{\Gamma_{1\mathrm{D}}\sqrt{N}}{4\Gamma}\left(2B_3D_3\exp\left(-D_3(L/\sigma)^2\right) + B_3\frac{\exp\left(-D_3(L/\sigma)^2\right)}{(L/\sigma)^2}\right).$$

We are going to solve these equations under two very crude approximations. First approximation is that the the second terms on the right hand sides of those equations will be discarded, since they are smaller than the first terms. Second approximation is that we shall set the left hand sides to $L/\sigma \approx 1$ and $k_{\mathrm{w}}\sigma \approx 1$. However, we shall not do this approximation on the right hand sides. Under these approximations we get the equations

$$1 = \frac{\Gamma_{1\mathrm{D}}\sqrt{N}}{4\Gamma}\frac{2}{\sqrt{\pi}}\exp\left(-2(k_{\mathrm{w}}\sigma)^2\right), \tag{7.50}$$

$$1 = \frac{\Gamma_{1\mathrm{D}}\sqrt{N}}{4\Gamma}2B_3D_3\exp\left(-D_3(L/\sigma)^2\right). \tag{7.51}$$

We take the logarithm of both sides and rearrange to find

$$k_{\mathrm{w}}\sigma = \sqrt{\frac{1}{2}\ln\left(\frac{\Gamma_{1\mathrm{D}}\sqrt{N}}{4\Gamma}\frac{2}{\sqrt{\pi}}\right)}, \tag{7.52}$$

$$\frac{L}{\sigma} = \sqrt{\frac{1}{D_3}\ln\left(\frac{\Gamma_{1\mathrm{D}}\sqrt{N}}{4\Gamma}2B_3D_3\right)}. \tag{7.53}$$

As we see in figure 7.5(a), a better approximation for $k_{\mathrm{w}}\sigma$ can be obtained, if instead of equation (7.50) we solve the equation

$$\frac{L}{\sigma} = \frac{\Gamma_{1\mathrm{D}}\sqrt{N}}{4\Gamma}\frac{2}{\sqrt{\pi}}\exp\left(-2(k_{\mathrm{w}}\sigma)^2\right)$$

with L/σ on the left hand side given by (7.53). We find

$$k_{\mathrm{w}}\sigma = \sqrt{\frac{1}{2}\ln\left(\frac{\Gamma_{1\mathrm{D}}\sqrt{N}}{4\Gamma}\frac{2}{\sqrt{\pi}}\left(\frac{1}{D_3}\ln\left(\frac{\Gamma_{1\mathrm{D}}\sqrt{N}}{4\Gamma}2B_3D_3\right)\right)^{-1/2}\right)}. \tag{7.54}$$

Thus we can have two different approximations for the optimal fidelity. The first is the most crude one

$$F = 1 - k_{\mathrm{w}}\sigma\frac{L}{\sigma}\frac{4\Gamma}{\sqrt{N}\Gamma_{1\mathrm{D}}} \tag{7.55}$$

with $k_{\mathrm{w}}\sigma$ and L/σ given by (7.52) and (7.53) respectively. The second approximation for the fidelity is (7.49) with $k_{\mathrm{w}}\sigma$ and L/σ given by (7.54) and (7.53) respectively. These two approximations are plotted in figure 7.5(c) and 7.5(d).

The fidelity (7.55) has the same scaling with the parameter $\sqrt{N}\Gamma_{1\mathrm{D}}/\Gamma$ as the expression (6.11). Alternatively, we can write (7.55) in terms of the optical depth $d^{\mathrm{opt}} = 2N\Gamma_{1\mathrm{D}}/\Gamma$ as

$$F = 1 - k_{\mathrm{w}}\sigma\frac{L}{\sigma}\frac{2\sqrt{2}}{\sqrt{d^{\mathrm{opt}}\Gamma_{1\mathrm{D}}/\Gamma}}. \tag{7.56}$$

This expression can be compared with (6.12). The similarity of (6.12) and (7.56) suggests that if we did the fidelity calculation for the gate of section 6.3 in the same way, as we did here, then we would have obtained the same scaling with the optical depth d^{opt} and the parameter $\Gamma_{1\mathrm{D}}/\Gamma$.

From the figure 7.5(c) and figure 7.5(d) we see that to make the gate work with reasonably high fidelity, the values of the optical depth need to be extremely high, which renders the gate impractical. To put this result into perspective, experimentally one was able to

achieve optical depth of $d^{\mathrm{opt}} \sim 66$ in [25]. Increasing the value of $\Gamma_{1\mathrm{D}}/\Gamma$ does help, but at this stage even $\Gamma_{1\mathrm{D}}/\Gamma = 0.5$ in figure 7.5(c) can be considered very optimistic, so we do not try to increase it even more. Among the other parameters it seems that L/σ has the most influence and the values shown in figure 7.5(b) correspond to the initial pulses that hardly have any probabiliy outside of the atomic ensemble. It is probably due to the approximative nature of the fidelity calculation that we obtain so restrictive results. In particular expansions around the limit $k_{\mathrm{w}}\sigma \gg 1$ that we were anticipating may not be valid considering the actual values in figure 7.5(a). Also the value of the arbitrary parameter a can have a noticable effect. Perhaps, if all of these were taken into account, the needed values of d^{opt} could have been reduced by an order of magnitudue, which still puts the gate in the area, where practical implementation is extremely difficult.

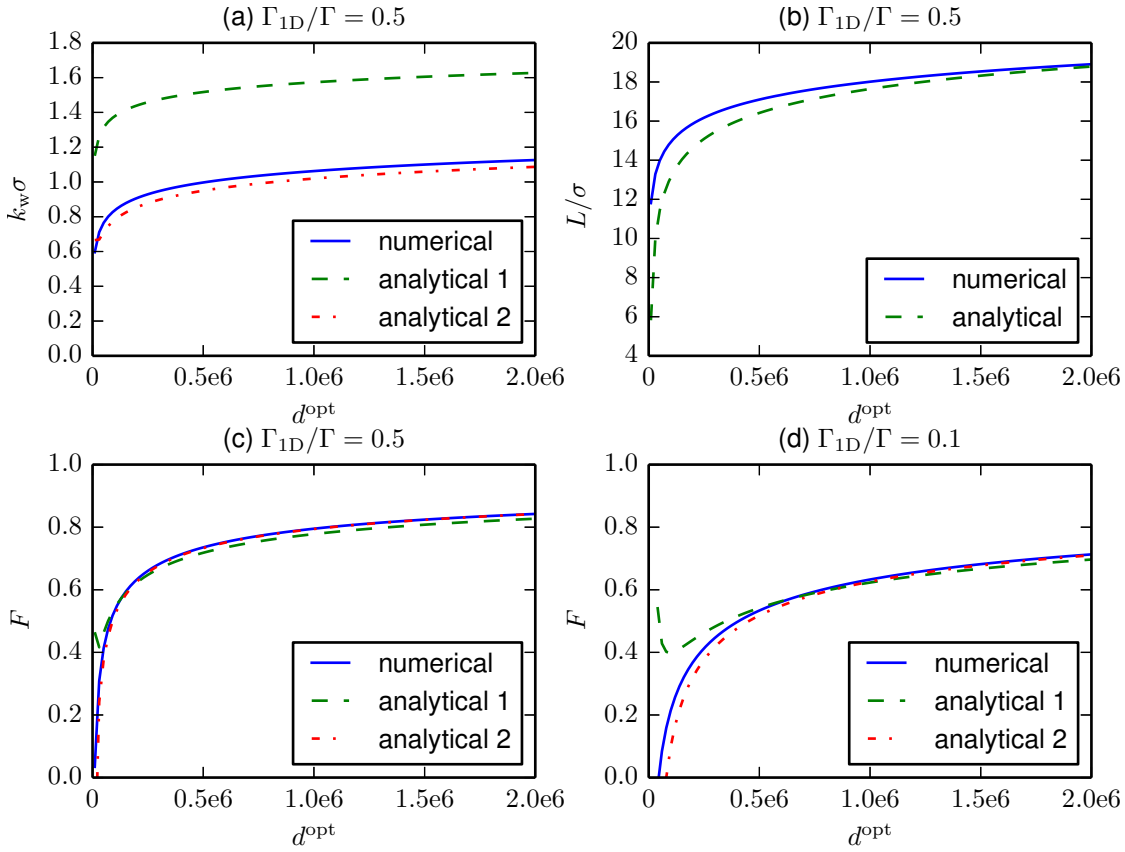

Figure 7.5: Comparison of the numerical and analytical optimization of the fidelity (7.49) ($a = 1/2$). (a) Plot of the optimal $k_w\sigma$ for $\Gamma_{1D}/\Gamma = 0.5$ as a function of optical depth. The plot "analytical 1" is using (7.52), while the plot "analytical 2" is using (7.54). (b) Plot of the optimal L/σ for $\Gamma_{1D}/\Gamma = 0.5$. The analytical plot is using (7.53). (c) and (d) Plot of the fidelity with optimal $k_w\sigma$ and L/σ for (c) $\Gamma_{1D}/\Gamma = 0.5$ and (d) $\Gamma_{1D}/\Gamma = 0.1$. The plot "analytical 1" is using (7.55) with $k_w\sigma$ and L/σ given by (7.52) and (7.53) respectively. The plot "analytical 2" is using (7.49) with $k_w\sigma$ and L/σ given by (7.54) and (7.53) respectively.

Chapter 8

Transfer matrix analysis of the ensemble

8.1 Introduction

In chapter 7 we saw that it is (theoretically) possible to make a phase gate with the counter-propagating classical drives. In the derivation of the final expression for fidelity we needed to make a lot of approximations to keep the analytical calculations tractable. Some of those approximations, such as setting real mass in the scattering coefficient to avoid unphysical values, are difficult to understand from that formalism alone. Even before the derivation of the expression for fidelity was begun, the effective equations of motion themselves, (7.13) and (7.14), were found under a number of approximations (see Appendix A).

If would be very useful if we had a method to simply simulate the whole evolution numerically without needing to make any approximations and see, how well the analytical results reflect the actual processes in the atomic ensemble. This chapter can be thought of as laying the foundation for that goal. Here we shall derive an analytical expression for the dispersion relation, which is essential to be able to choose the parameters of the numerical simulation (for both the linear and nonlinear processes).

8.2 Model

If we look at an ensemble, where atoms have well-defined positions, the counterpropagating classical drives of chapter 7 can look in many different ways. The simplest one that we shall consider here (figure 8.1), is the one where the coherent drives have the same k-vector as the quantum light pulses and we use the distance between the atoms $\lambda/4$ as in section 3.3.2. With this setup every second four-level atom is on the node ($\Omega(z) = 0$) of the standing wave and effectively becomes a two-level atom. From the point of view of section 3.3.1, this can be viewed as extending the setup of figure 3.4. Figure 8.1 is basically

the setup of figure 3.4, but where we put an "impurity" atom between each pair of the two-level atoms. Thus we can think of the setup of figure 8.1 either in terms of the theory of chapter 7 as an ensemble enhancement effect or terms of the theory of section 3.3.1 as a cavity enhancement effect.

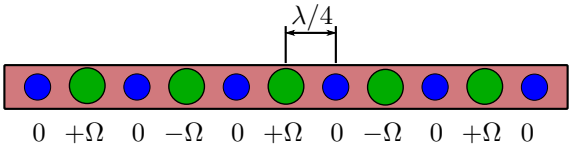

Figure 8.1: The simplest setup with the counterpropagating classical drives. All the atoms in a waveguide (red rectangular background) have four levels and are placed with distance $\lambda/4$ between each other. The classical drive strength at the position of each atom is shown below the waveguide (either $\pm\Omega$ or 0). Since every second atom (small blue) is located on a node of the classical drive, it effectively becomes a two-level atom. The other atoms (big green) are on the antinodes of the classical drive and hence still function as "full" four-level atoms.

We are going to use transfer matrices (see section 3.3.2) to describe the linear processes of figure 8.1. The transfer matrix for the unit cell is $M_{\text{cell}} = M_f(kd)M(\beta_2)M_f(kd)M(\beta_3)$ in terms of the matrices (3.11) and (3.12). The equation for the Bloch vectors K_b is

$$\cos(2K_\text{b}d) = \frac{1}{2}\text{tr}(M_{\text{cell}}) = (1+\beta_2\beta_3)\cos(2kd) - i(\beta_2+\beta_3)\sin(2kd) - \beta_2\beta_3.$$

Choosing $kd = \pi/2$ it reduces to

$$\cos(2K_\text{b}d) = -1 - 2\beta_2\beta_3.$$

Inserting the expressions for β_3 (3.13) and β_2 (β_3 with $\Omega = 0$) into the above equation and rearranging we obtain

$$(\cos(2K_\text{b}d)+1)(\Gamma' - 2i\delta_k)\left((\Gamma' - 2i\delta_k)(\delta_k - \Delta_\text{p}) + 2i|\Omega|^2\right) = -2\Gamma_{1\text{D}}^2(\delta_k - \Delta_\text{p}). \quad (8.1)$$

This equation (cubic in δ_k) can be in principle solved exactly to find δ_k as a function of K_b. However, to obtain simpler expressions, we are going to solve it perturbatively. We are going to expand the cosine on the left hand side around $K_\text{b} = k = \pi/(2d)$. To zeroth order, we have $\cos(2K_\text{b}d) = \cos(2kd) = -1$, so that (8.1) gives zeroth order contribution $\delta_k^{(0)} = \Delta_\text{p}$. The first order term of the cosine is zero, so that $\delta_k^{(1)} = 0$. The expansion of the cosine to second order is $\cos(2K_\text{b}d) + 1 \approx 2(K_\text{b}d - \pi/2)^2$. If we insert this expansion into (8.1) and write $\delta_k = \delta_k^{(0)} + \delta_k^{(2)} = \Delta_\text{p} + \delta_k^{(2)}$, then we end up with

$$2\left(K_\text{b}d - \frac{\pi}{2}\right)^2\left(\Gamma' - 2i\Delta_\text{p} - 2i\delta_k^{(2)}\right)\left(\left(\Gamma' - 2i\Delta_\text{p} - 2i\delta_k^{(2)}\right)\delta_k^{(2)} + 2i|\Omega|^2\right) = -2\Gamma_{1\text{D}}^2\delta_k^{(2)}.$$

If we only keep terms up to first order in $\delta_k^{(2)}$ we get

$$2\left(K_\mathrm{b}d-\frac{\pi}{2}\right)^2\left(\left(\Gamma'-2i\Delta_\mathrm{p}\right)\delta_k^{(2)}+2i|\Omega|^2\left(\Gamma'-2i\Delta_\mathrm{p}-2i\delta_k^{(2)}\right)\right)=-2\Gamma_{1\mathrm{D}}^2\delta_k^{(2)}.$$

From here we can solve for $\delta_k^{(2)}$, so that the final perturbative expression for δ_k becomes

$$\delta_k(K_\mathrm{b})=\Delta_\mathrm{p}+\frac{-4i\left(K_\mathrm{b}d-\frac{\pi}{2}\right)^2|\Omega|^2(\Gamma'-2i\Delta_\mathrm{p})}{2\left(K_\mathrm{b}d-\frac{\pi}{2}\right)^2\left((\Gamma'-2i\Delta_\mathrm{p})^2+4|\Omega|^2\right)+2\Gamma_{1\mathrm{D}}^2} \tag{8.2}$$

Among the three exact analytical solutions to (8.1), only one of them is finite for $K_\mathrm{b}=\pi/(2d)$. It it this solution that the perturbative one approximates. The exact and the perturbative solutions are very close when Ω is small (figure 8.2(a)). For higher values of Ω (figure 8.2(b)), the exact solutions become discontinuous and deviate significantly from the perturbative solutions. Even in this case they agree around $K_\mathrm{b}=\pi/(2d)$, which is the point that we are intersted in.

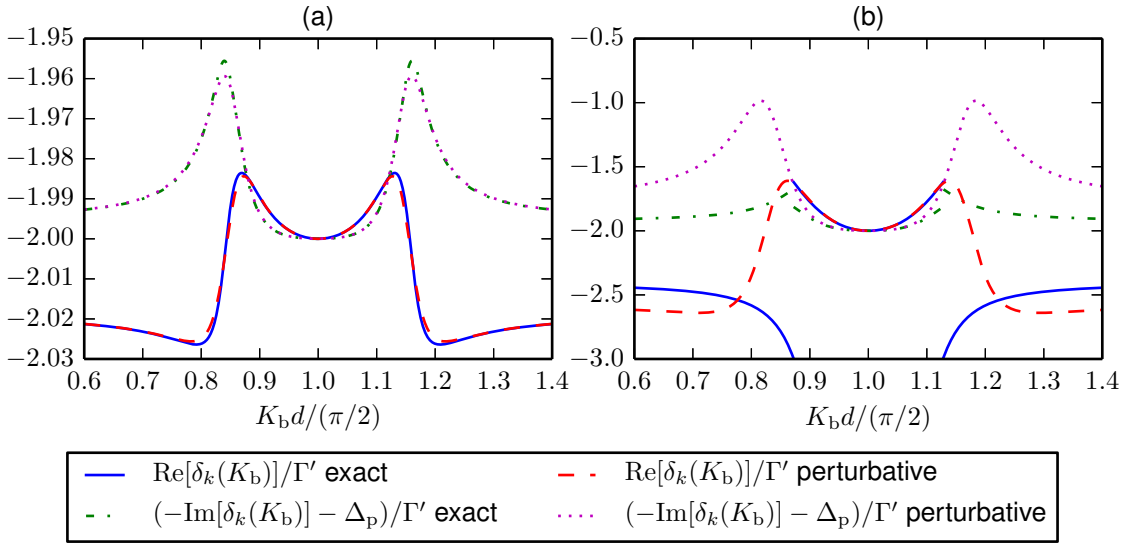

Figure 8.2: Plot of the exact solution of (8.1) and its perturbative approximation (8.2). (a) $\Omega=0.2\Gamma'$, (b) $\Omega=\Gamma'$. For both plots $\Delta_\mathrm{p}=-2\Gamma'$ and $\Gamma_{1\mathrm{D}}=\Gamma'$.

Now that we have an explicit formula for the dispersion relation (8.2), we can use it to expand around arbitrary $K_\mathrm{b}=K_{\mathrm{b}0}$ and obtain the group velocity $v_\mathrm{g}=\frac{\mathrm{d}\delta_k}{\mathrm{d}K_\mathrm{b}}$ and $\alpha=\frac{\mathrm{d}^2\delta_k}{\mathrm{d}K_\mathrm{b}^2}$.

We get

$$v_{\mathrm{g}} = \frac{32(2\Delta_{\mathrm{p}} + i\Gamma')\Gamma_{1\mathrm{D}}^2|\Omega|^2(\pi - 2K_{\mathrm{b}0}d)d}{(-4\Gamma_{1\mathrm{D}}^2 + ((2\Delta_{\mathrm{p}} + i\Gamma')^2 - 4|\Omega|^2)(\pi - 2K_{\mathrm{b}0}d)^2)^2}, \tag{8.3}$$

$$\alpha = -\frac{64(2\Delta_{\mathrm{p}} + i\Gamma')\Gamma_{1\mathrm{D}}^2|\Omega|^2(4\Gamma_{1\mathrm{D}}^2 + 3((2\Delta_{\mathrm{p}} + i\Gamma')^2 - 4|\Omega|^2)(\pi - 2K_{\mathrm{b}0}d)^2)d^2}{(4\Gamma_{1\mathrm{D}}^2 - ((2\Delta_{\mathrm{p}} + i\Gamma')^2 - 4|\Omega|^2)(\pi - 2K_{\mathrm{b}0}d)^2)^3}; \tag{8.4}$$

or approximately

$$v_{\mathrm{g}} \approx -\frac{4(2\Delta_{\mathrm{p}} + i\Gamma')|\Omega|^2d^2}{\Gamma_{1\mathrm{D}}^2}\left(K_{\mathrm{b}0} - \frac{\pi}{2d}\right), \tag{8.5}$$

$$\alpha \approx -\frac{4(2\Delta_{\mathrm{p}} + i\Gamma')|\Omega|^2d^2}{\Gamma_{1\mathrm{D}}^2}. \tag{8.6}$$

From (8.5) and (8.6) we see that, approximatively, this system behaves as if the polaritons had a mass

$$m = -\frac{\Gamma_{1\mathrm{D}}^2}{4(2\Delta_{\mathrm{p}} + i\Gamma')|\Omega|^2d^2}.$$

This mass resembles very much the mass (7.7) that we found in chapter 7 (remember that $d = L/N$, and detunings Δ_{p} and Δ_1 are essentially the same). One notable change is replacement of the total decay rate $\Gamma = \Gamma_{1\mathrm{D}} + \Gamma'$ by only Γ'. The Γ in (7.7) comes from the derivation in Appendix A, which in turn follows [23]. The derivation assumed low $\Gamma_{1\mathrm{D}}$ limit and hence no difference between Γ' and Γ.

As we mentioned earlier, the Bloch vector $K_{\mathrm{b}} = \pi/(2d)$ is the one, where the two counterpropagating drives of equal strength keep the pulse from going anywhere. Alternatively, this is also the vector, for which the reflection from the array of the two-level atoms works most strongly. As soon as we deviate slighly from $K_{\mathrm{b}} = \pi/(2d)$, i.e. acquire a small "bias" k-vector, we get a non-zero group velocity (8.3).

8.3 Simulations

We can use the theory of chapter 4 to simulate the evolution of a given initial state and thereby check the dispersion relation that we found above. The setup is similar to the one in section 4.5. Here, due to use of the counterpropagating classical drives, we need a different initial state. In the language of chapter 7 we need the states of the symmetric mode, i.e. states of the form

$$|\psi\rangle = \int \theta(z,t)\hat{S}^\dagger(z)dz|0\rangle = \int \frac{1}{\sqrt{2}}\left(\hat{\Psi}_+^\dagger(z) + \hat{\Psi}_-^\dagger(z)\right)\theta(z,t)dz|0\rangle.$$

The operators $\hat{\Psi}_\pm$ were defined to be slowly varying in space. Since the theory of chapter 4 deals with states that are not slowly varying in space, we need to explicitly reinstate the corresponding factors of $e^{\pm ik_0 z}$. If the classical drive is turned off, the operators $\hat{\Psi}_\pm$ (7.1) are proportional to the coherences $\hat{\sigma}_{ac}$. In this case $\hat{\Psi}_+ = \hat{\Psi}_-$ and we get a common factor of $(e^{ik_0 z} + e^{-ik_0 z})/\sqrt{2} = \sqrt{2}\cos(k_0 z)$. In terms of the setup of the figure 8.1, this cosine factor ensures that we store our excitations only in the atoms that will have the classical drive present, when the counterpropagating fields are turned on. These considerations lead us to consider the following initial state for the simulations:

$$|\psi_{\text{initial}}\rangle = \sum_{j=0}^{N} \sqrt{2}\cos(k_0 z_j) f(z_j)\sqrt{d}|c_j a\rangle, \tag{8.7}$$

where

$$f(z) = \frac{1}{(2\pi\sigma^2)^{1/4}} \exp\left(-\frac{(z-\mu)^2}{4\sigma^2}\right) e^{i(k_{\text{w}}+\pi/(2d))z}. \tag{8.8}$$

We assume that the k-vectors of the quantum field k_0 and the classical drive k_{p} are equal, so we could have written k_{p} in the argument of the cosine in the initial state (8.7). Also note that (8.8) is different from (3.19) in that the phase factor has k-vector $k_{\text{w}} + \pi/(2d)$, that is different from the central k-vector k_0 of the quantum field. We have shifted k_{w} by $k_0 = \pi/(2d)$ to make it correspond to the k_{w} used in chapter 7.

After evolution for a time t, the final wavefunction will be

$$f(z,t) = \frac{1}{(2\pi\sigma^2)^{1/4}}\sqrt{\frac{1}{1+\frac{i\alpha t}{2\sigma^2}}} \exp\left(-\frac{(z-\mu-v_{\text{g}}t)^2}{4\sigma^2(1+\frac{i\alpha t}{2\sigma^2})}\right) e^{-i\delta_k(k_{\text{w}}+\pi/(2d))t} e^{i(k_{\text{w}}+\pi/(2d))z}. \tag{8.9}$$

Again the only difference from (3.20) is the phase factor: both the original with the argument $(k_{\text{w}} + \pi/(2d))z$ and the one acquired because of the zeroth term of the dispersion relation with the argument $\delta_k(k_{\text{w}} + \pi/(2d))t$. Writing the final wavefunction in this form is slightly deceptive, however. The reason is that here α has an imaginary part, which essentially means that the decay is different for the different Fourier components. This means that the propagation of the wavepacket is *not* simply given by the real value of the group velocity v_{g}. Indeed, by taking the absolute square of (8.9) and defining $v_{\text{gr}} = \text{Re}[v_{\text{g}}]$, $v_{\text{gi}} = \text{Im}[v_{\text{g}}]$, $\alpha_{\text{r}} = \text{Re}[\alpha]$ and $\alpha_{\text{i}} = \text{Im}[\alpha]$ we find

$$\begin{aligned} |f(z,t)|^2 = {} & \frac{1}{\sqrt{2\pi\sigma^2}}\left|\frac{1}{1+\frac{i\alpha t}{2\sigma^2}}\right| e^{2\,\text{Im}[\delta_k(k_{\text{w}}+\pi/(2d))]t} \\ & \times \exp\left(-\frac{\left[2(z-\mu-v_{\text{gr}}t)^2 - 2v_{\text{gi}}^2 t^2\right]\left(1-\frac{\alpha_{\text{i}}t}{2\sigma^2}\right) - 4(z-\mu-v_{\text{gr}}t)\frac{v_{\text{gi}}\alpha_{\text{r}}t^2}{2\sigma^2}}{4\sigma^2\left(\left(1-\frac{\alpha_{\text{i}}t}{2\sigma^2}\right)^2 + \left(\frac{\alpha_{\text{r}}t}{2\sigma^2}\right)^2\right)}\right). \end{aligned} \tag{8.10}$$

To derive the position of the peak of this function is, we find the stationary point of the argument of the exponential by differentiating it with respect to z and setting the derivative equal to zero. Thus we obtain

$$z = \mu + v_{\mathrm{gr}} t + \frac{v_{\mathrm{gi}}\alpha_{\mathrm{r}}}{2\sigma^2 - \alpha_{\mathrm{i}} t} t^2.$$

Here the last term is the nonlinear propagation correction compared to the usual situation with purely real group velocity.

In the simulations we shall initialize the wavepacket with the mean $\mu = L/4$ and let it evolve until the new mean is $3L/4$. To make this happen the evolution time must fulfill

$$v_{\mathrm{gr}} t + \frac{v_{\mathrm{gi}}\alpha_{\mathrm{r}}}{2\sigma^2 - \alpha_{\mathrm{i}} t} t^2 = \frac{L}{2}$$

or

$$(v_{\mathrm{gi}}\alpha_{\mathrm{r}} - v_{\mathrm{gr}}\alpha_{\mathrm{i}})t^2 + (2\sigma^2 v_{\mathrm{gr}} + (L/2)\alpha_{\mathrm{i}})t - L\sigma^2 = 0.$$

We note that if the quadratic dispersion relation is assumed, i.e. $v_{\mathrm{g}} = k_{\mathrm{w}}/m$ and $\alpha = 1/m$, then $v_{\mathrm{gi}}\alpha_{\mathrm{r}} - v_{\mathrm{gr}}\alpha_{\mathrm{i}} = 0$ and the equation above becomes linear in t. However, for the expressions (8.3) and (8.4) this is not the case.

To make the pulses travel from $L/4$ to $3L/4$ we thus need to choose the time

$$t = \frac{1}{2(v_{\mathrm{gi}}\alpha_{\mathrm{r}} - v_{\mathrm{gr}}\alpha_{\mathrm{i}})}(2\sigma^2 v_{\mathrm{gr}} + (L/2)\alpha_{\mathrm{i}}) \left(-1 + \sqrt{1+G}\right)$$

with the parameter

$$G = 4\frac{v_{\mathrm{gi}}\alpha_{\mathrm{r}} - v_{\mathrm{gr}}\alpha_{\mathrm{i}}}{(2\sigma^2 v_{\mathrm{gr}} + (L/2)\alpha_{\mathrm{i}})^2} L\sigma^2, \tag{8.11}$$

which expresses how much the actual dispersion relation deviates from the idealized quadratic dispersion relation.

In figure 8.3 the results of the optimization of the propagation are shown. We optimize with respect to the norm of the final state obtained by the analytical propagation (subplot (e)). This norm is found by multiplying the norm of the initial state (which may have some probability outside of the ensemble) and the norm of the final state (that is found under the assumption that the initial state is normalized). We also calculate the norm of the final state obtained by the numerical propagation with the found values of the optimal parameters (subplot (f)). In this way the value of the numerical norm may deviate from the optimal one. However, still we take this approach because it is faster and because optimizing with respect to the norm obtained by the numerical propagation has a tendency to find a completely different regime, where the pulses do not move at all, and consequently the final norm is very high. There is a noticeble difference between the analytical and the

numerical norm. This is caused by the fact that the boundary conditions make the final state calculated numerically be distorted compared to the analytical solution that was simply cut off at the ensemble boundary (see figure 8.4).

The figure 8.3 can be compared with figure 7.5. The subplots (a) and (b) of both figures plot the same quantities (respectively k_{w} and L/σ). The detining Δ_{p} of the subplot (c) corresponds to the detuning Δ_1 of chapter 7 (see the optimal value (7.48)), however we expect that for the linear processes the optimal Δ_{p} is found under rather different constraints than in the nonlinear processes and hence cannot be directly compared. In the subplot (d) for figure 8.3 we see that the parameter (8.11) for the optimal values starts being bigger than unity for optical depths $d^{\mathrm{opt}} < 100$ and then goes to zero with the increase of d^{opt}. This suggests that the approximation of the dispersion relation by a quadradic one becomes better for big optical depths.

We also remark that in figure 8.3 the difference between the plots $\Gamma_{1\mathrm{D}}/\Gamma = 0.5$ and $\Gamma_{1\mathrm{D}}/\Gamma = 0.1$ in all the subfigures except (c) stems from the fact that the quantities are plotted with respect to the optical depth $d^{\mathrm{opt}} = 2N\Gamma_{1\mathrm{D}}/\Gamma$. If the same quantities were plotted with respect to the parameter $2N\Gamma_{1\mathrm{D}}/\Gamma'$ (i.e. $\Gamma = \Gamma_{1\mathrm{D}} + \Gamma'$ replaced by Γ'), then the respective quantities in the two plots ($\Gamma_{1\mathrm{D}}/\Gamma = 0.5$ and $\Gamma_{1\mathrm{D}}/\Gamma = 0.1$) would have had the same values. Thus it is consistent with the previous statement (see section 3.3.2) that only the quantity $2N\Gamma_{1\mathrm{D}}/\Gamma'$ matters for the linear effects and not the number of atoms N or decay rate ratio $\Gamma_{1\mathrm{D}}/\Gamma'$ separately.

In the context of the fidelity results of figure 7.5, the figure 8.3 shows that it is much easier to achieve good results for the linear effects than nonliner ones in the counterpropagating classical drive setup. However, even for the linear effects, the required values of optical depth above 100 still make it very challenging to realize experimentally [25].

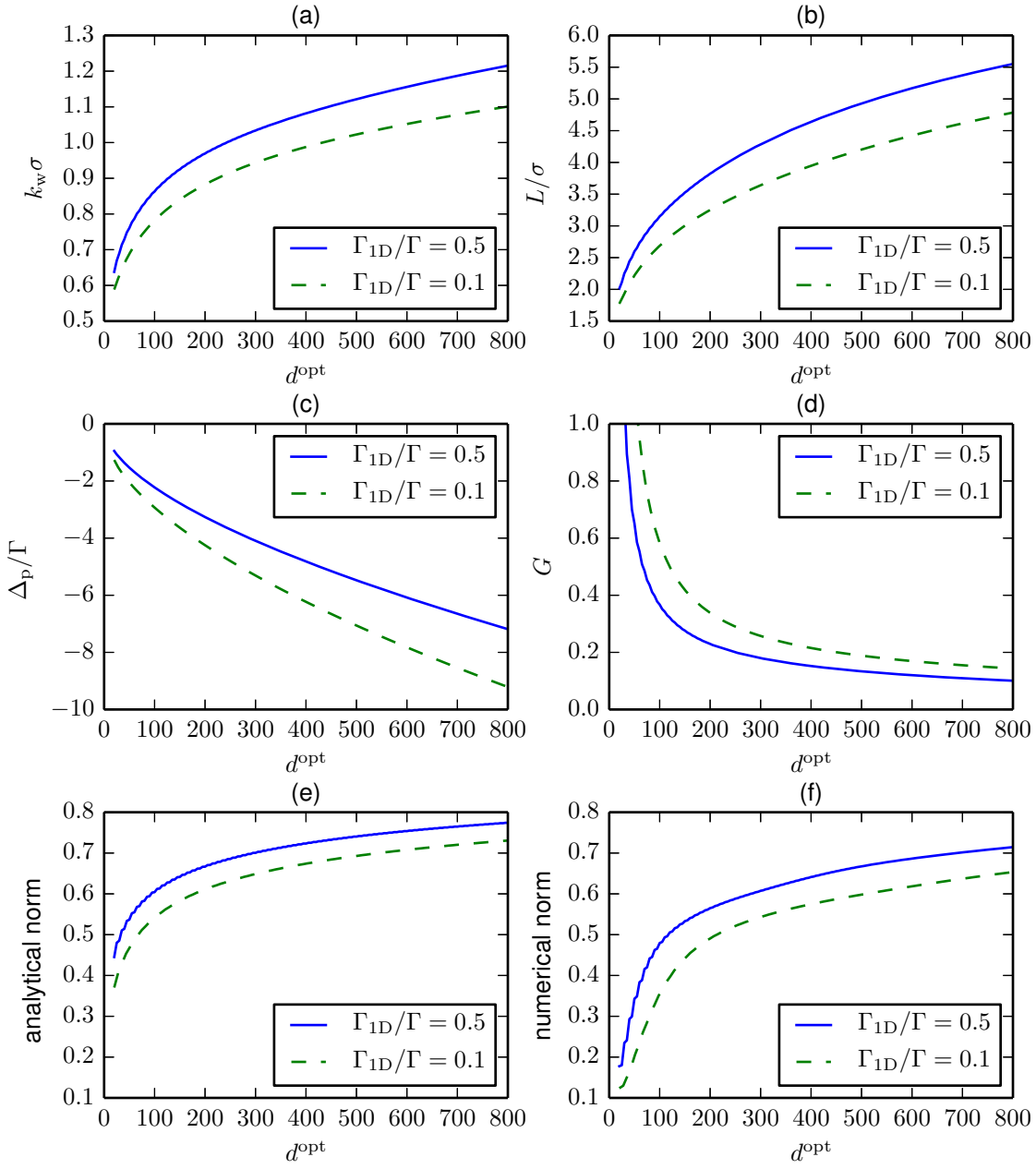

Figure 8.3: Optimization of the process, where the state (8.7) is propagated through the ensemble of figure 8.1 from $\mu = L/4$ to $\mu = 3L/4$. Optimal values of the different parameters are plotted in (a), (b), (c) and (d). The norms for the final states with the optimal parameters are plotted in (e) and (f).

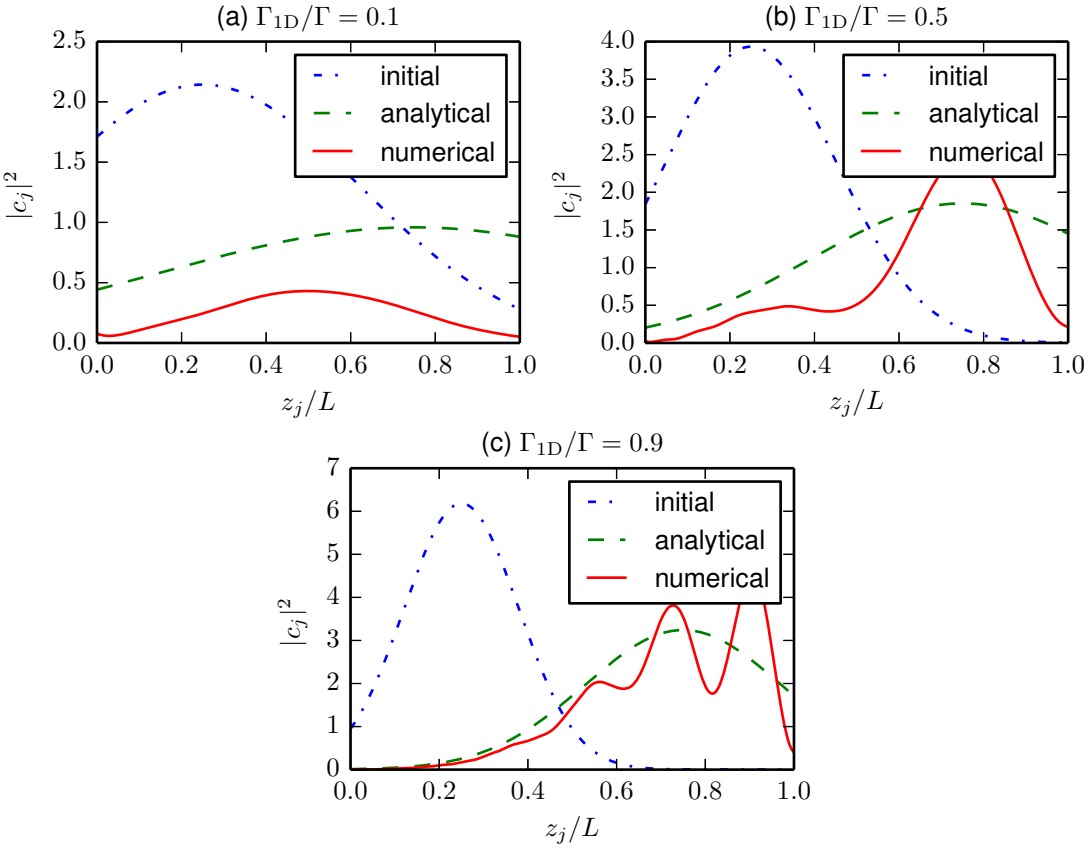

Figure 8.4: The initial state (8.7) is propagated through the ensemble numerically and compared with the analytical solution (with the wavefunction (8.9)). We choose the number of atoms $N = 500$ and (a) $\Gamma_{1D} = 0.1$, (b) $\Gamma_{1D} = 0.5$, (c) $\Gamma_{1D} = 0.9$. All the other parameters are chosen such that the analytical final state has the highest norm.

Chapter 9

Outlook and conclusion

9.1 Outlook

There are several different things, that could be worked on further.

One is to look at, how the photons can be stored as excitations of the symmetric modes. In chapter 7 we just assumed that is was possible to do it and looked at what happened inside the ensemble. A related topic to this one is to find out, how to get the atomic excitations back as photons in the end. Thus ideally we want to be able to describe the whole process of storage, interaction and retrieval and not only the interaction.

A different thing is to use the theory of chapter 8 to do the simulations on the two-excitation manifold. Here the main problem is the computational power. In the limited testing that was perfomed, it seemed possible to simulate atomic ensembles of up to about 500 atoms on the two-excitation manifold. However, the results we got from both chapter 7 and chapter 8 indicate, that a much higher number of atoms is required if Γ_{1D} is low. Perhaps a hybrid approach could be adopted, if one could be sure that the nonlinear part of the effective theory constitutes a good approximation. Then the linear part could be simulated numerically with the analytical corrections to the parameters that the nonlinear part imposes. In particular one could try to use the optimal values of Δ_1 (7.48) found from the analysis of the nonlinear part in the simulations of the linear one.

In the high Γ_{1D} limit we may need to make the corrections to the effective theory of chapter 7. Especially make sure that each time we have a factor of Γ_{1D}/Γ that it should not have been a factor of Γ_{1D}/Γ' instead. As chapter 8 indicates, this is the case at least for the linear effects. In the high Γ_{1D} regime the distinction between Γ_{1D}/Γ and Γ_{1D}/Γ' is very important. For example $\Gamma_{1D}/\Gamma = 0.9$ corresponds to $\Gamma_{1D}/\Gamma' = 9$, which according to the results of chapter 6 and chapter 7 effectively corresponds to increasing the number of atoms N by 81. And this in turn can relaxes the requirement of the unrealistically high optical depth that was found in chapter 7.

Another extension of chapter 8 could be to find out, whether one can make the gate

work even in the case, when the positions of the atoms are random. The effective theory of chapter 7 does not seem to need any particular requirement on the positions of the atoms. On the other hand, results of section 3.3.1 and section 3.3.2 show, that for one-dimensional systems the relative positions of the atoms are extremely important for at least some applications.

Finally, in chapter 6 the scattering of two photons from a single four-level atom does not really have a formal proof. The numerical simulations support it, but even there we did not really simulate the single atom case, but also a small ensemble around it. The hope is that, if a formal proof is done, perhaps using the generalization of the transfer matrices for two-photon processes, then a better understanding of the important assumptions can be reached.

9.2 Conclusion

In this thesis we have considered three different controlled phase gates for photons. All of them could be made to work in a certain limit. One of them needed a big decay rate ratio Γ_{1D}/Γ, where Γ_{1D} is the decay rate into the waveguide, Γ' is the decay rate into other modes, and $\Gamma = \Gamma_{1D} + \Gamma'$. The other two phase gates could use the collective enhancement effects of N atoms to compensate for the low values of Γ_{1D}/Γ. Even for the last two phase gates the ratio Γ_{1D}/Γ proved to be very important. For low values of Γ_{1D}/Γ one would need a prohibitively big N to make the gate work with reasonably high fidelity. Through the analysis of the last two phase gates we learned that compared to the linear phenomena, such as EIT (slow light), which depend on a single parameter which is called optical depth $d^{\mathrm{opt}} = 2N\Gamma_{1D}/\Gamma$, the nonlinear phenomena that make those two phase gates work, rather depend on $d^{\mathrm{opt}}\Gamma_{1D}/\Gamma$. An additional result of the analysis is that in the high Γ_{1D} limit, the parameter $2N\Gamma_{1D}/\Gamma'$ seems to be more relevant than the optical depth – both for the linear and for the nonlinear effects. Considering the current experimentally achievable values of the parameters (Γ_{1D}/Γ and d^{opt}) all three phase gate schemes seem very difficult to implement.

As for the secondary goal to verify the effective theory of the atomic ensembles with the counterpropagating classical drives, we got as far as looking at the linear effects by employing the transfer matrix formalism and numerical simulations. The result of this analysis is that for experimentally achievable values of d^{opt} the dispersion relation can deviate significantly from the purely quadratic one that the effective theory implies. On the other hand, in the limit of very big optical depths, where the ensemble-based phase gates start to work, the approximation of a quadratic dispersion relation is indeed valid. Verification of the nonlinear part would require a generalization of the transfer matrix formalism to nonlinear processes on the analytical side and a significant computational power to be able to simulate states on the two-excitation manifold of the ensemble on the numerical side.

Appendix A

Adiabatic elimination of the four-level atoms

Here we derive the equations (7.3) and (7.4). In the following we shall assume weak excitation limit. I.e. we assume that the ensemble is initialized such that all the atoms are in the state $|a\rangle$. Even when we have (one or two) excitations in the ensemble, they are going to be spread over many atoms, and hence each individual atom is still mostly in the state $|a\rangle$. Thus, when finding the Heisenberg equations of motion for the atom, we shall approximate $\hat{\sigma}_{bb} \approx 0$, $\hat{\sigma}_{aa} \approx 1$ in the equation for the coherence $\dot{\hat{\sigma}}_{ab}$. In the equation for $\dot{\hat{\sigma}}_{ac}$ we shall neglect the coherence $\hat{\sigma}_{bc}$, since it expresses the transitions between two weakly populated states. Similarly, in the equation for $\dot{\hat{\sigma}}_{ad}$ we shall neglect neglect the coherence $\hat{\sigma}_{bd}$. In the equation for $\dot{\hat{\sigma}}_{cd}$ we set $\hat{\sigma}_{dd} = 0$. However, we do *not* set $\hat{\sigma}_{cc} = 0$, since the states $|c\rangle$ are on the second place after states $|a\rangle$ in terms of population, as atomic excitations are stored there and only briefly transition to states $|b\rangle$ and $|d\rangle$. Moreover, as we shall see below, setting $\hat{\sigma}_{cc} = 0$ would have completely decoupled the transition $|c\rangle \leftrightarrow |d\rangle$ from the quantum electric field, which would have made any two excitation interaction impossible.

The Heisenberg equations of motion for the field and the atoms are

$$\left(\frac{\partial}{\partial t} \pm c\,\frac{\partial}{\partial z}\right)\hat{\mathcal{E}}_{\pm} = ig\sqrt{2\pi}(N/L)(\hat{\sigma}_{ab} + \hat{\sigma}_{cd})e^{\mp ik_0 z} \tag{A.1}$$

$$\dot{\hat{\sigma}}_{ab} = (i\Delta_1 - \Gamma/2)\hat{\sigma}_{ab} + ig\sqrt{2\pi}(\hat{\mathcal{E}}_{+}e^{ik_0 z} + \hat{\mathcal{E}}_{-}e^{-ik_0 z}) + i(\Omega_{+}e^{ik_{\mathrm{p}} z} + \Omega_{-}e^{-ik_{\mathrm{p}} z})\hat{\sigma}_{ac} \tag{A.2}$$

$$\dot{\hat{\sigma}}_{ac} = i\Delta_3\hat{\sigma}_{ac} + ig\sqrt{2\pi}(\hat{\mathcal{E}}_{+}^{\dagger}e^{-ik_0 z} + \hat{\mathcal{E}}_{-}^{\dagger}e^{ik_0 z})\hat{\sigma}_{ad} + i(\Omega_{+}^{*}e^{-ik_{\mathrm{p}} z} + \Omega_{-}^{*}e^{ik_{\mathrm{p}} z})\hat{\sigma}_{ab} \tag{A.3}$$

$$\dot{\hat{\sigma}}_{ad} = (i\Delta_2 + i\Delta_3 - \Gamma/2)\hat{\sigma}_{ad} + ig\sqrt{2\pi}(\hat{\mathcal{E}}_{+}e^{ik_0 z} + \hat{\mathcal{E}}_{-}e^{-ik_0 z})\hat{\sigma}_{ac} \tag{A.4}$$

$$\dot{\hat{\sigma}}_{cd} = (i\Delta_2 - \Gamma/2)\hat{\sigma}_{cd} + ig\sqrt{2\pi}(\hat{\mathcal{E}}_{+}e^{ik_0 z} + \hat{\mathcal{E}}_{-}e^{-ik_0 z})\hat{\sigma}_{cc} \tag{A.5}$$

The total spontaneous decay rate $\Gamma = \Gamma' + \Gamma_{1\mathrm{D}}$ from the states $|b\rangle$ and $|d\rangle$ was included "by hand" in the Heisenberg equations of motion. The choice of Γ instead of Γ' was taken to follow [23] most closely. As we discuss in the main text (section 8.2), it appears, that

the choice of Γ' instead would have been more apropriate. However, in the low Γ_{1D} limit this difference is almost purely notational, as $\Gamma' \approx \Gamma$. Also, strictly speaking, we should have also included the noise operator, that is associated with this decay rate.

For the atomic coherences, we assume that

$$\hat{\sigma}_{ab} = \hat{\sigma}^{+}_{ab} e^{ik_0 z} + \hat{\sigma}^{-}_{ab} e^{-ik_0 z}, \tag{A.6}$$

$$\hat{\sigma}_{cd} = \hat{\sigma}^{+}_{cd} e^{ik_0 z} + \hat{\sigma}^{-}_{cd} e^{-ik_0 z}. \tag{A.7}$$

This is effectively a Fourier expansion of the coherences in up to the lowest order. The assumption here is that $\hat{\sigma}^{\pm}_{ab}$ and $\hat{\sigma}^{\pm}_{cd}$ should correspond to the slowly varying components of the electric field $\hat{\mathcal{E}}_{\pm}$. The higher order Fourier components of the atomic coherences are thus neglected. The reason is that, in practice one expects the higher orders to be destroyed by atomic motion and collisions [23].

We use (A.6) and (A.7) to approximate equations (A.1), (A.2) and (A.5). The procedure is the same: insert (A.6) and (A.7), discard the terms that rotate with phase factors $e^{\pm 2ik_0 z}$ and write the remaining phase factors in terms in terms of the relative momenta $\Delta k = k_{\mathrm{p}} - k_0$. The equations for the field (A.1) are also written in terms of $\hat{\Psi}_{\pm}$ (7.2). Thus we find

$$\left(\frac{\partial}{\partial t} \pm c\,\frac{\partial}{\partial z}\right)\hat{\Psi}_{\pm} = i\frac{2\pi g^2}{\Omega_{\pm}}\frac{N}{L}\sqrt{\frac{N}{L}}(\hat{\sigma}^{\pm}_{ab} + \hat{\sigma}^{\pm}_{cd}), \tag{A.8}$$

$$\dot{\hat{\sigma}}^{\pm}_{ab} = (i\Delta_1 - \Gamma/2)\hat{\sigma}^{\pm}_{ab} + ig\sqrt{2\pi}\hat{\mathcal{E}}_{\pm} + i\Omega_{\pm}\hat{\sigma}_{ac}e^{\pm i(\Delta k)z}, \tag{A.9}$$

$$\dot{\hat{\sigma}}^{\pm}_{cd} = (i\Delta_2 - \Gamma/2)\hat{\sigma}^{\pm}_{cd} + ig\sqrt{2\pi}\hat{\mathcal{E}}_{\pm}\hat{\sigma}_{cc}. \tag{A.10}$$

We solve (A.9) and (A.10) adiabatically by assuming $\dot{\hat{\sigma}}^{\pm}_{ab} = \dot{\hat{\sigma}}^{\pm}_{cd} = 0$. The solutions written in terms of $\hat{\Psi}_{\pm}$ are

$$\hat{\sigma}^{\pm}_{ab} = \frac{\Omega_{\pm}}{-i\Delta_1 + \Gamma/2}\left(i\sqrt{\frac{L}{N}}\hat{\Psi}_{\pm} + i\hat{\sigma}_{ac}e^{\pm i(\Delta k)z}\right), \tag{A.11}$$

$$\hat{\sigma}^{\pm}_{cd} = -\frac{i\Omega_{\pm}}{i\Delta_2 - \Gamma/2}\sqrt{\frac{L}{N}}\hat{\Psi}_{\pm}\hat{\sigma}_{cc}. \tag{A.12}$$

Now we find an expression for $\hat{\sigma}_{ac}$. First we set $\dot{\hat{\sigma}}_{ad} = 0$ in (A.4), which gives

$$\hat{\sigma}_{ad} = \frac{g\sqrt{2\pi}}{-\Delta_2 - \Delta_3 - i\Gamma/2}(\hat{\mathcal{E}}_{+}e^{ik_0 z} + \hat{\mathcal{E}}_{-}e^{-ik_0 z})\hat{\sigma}_{ac}$$

Using the this expression together with (A.6) and (A.11), we can write (A.3) (discarding the quickly rotating terms) as

$$\dot{\hat{\sigma}}_{ac} = A\hat{\sigma}_{ac} + \hat{\mathcal{E}}\hat{\sigma}_{ac} - \hat{f}, \tag{A.13}$$

where

$$A = i\Delta_3 - \frac{|\Omega_-|^2}{-i\Delta_1 + \Gamma/2} - \frac{|\Omega_+|^2}{-i\Delta_1 + \Gamma/2}, \quad \hat{\mathcal{E}} = \frac{2\pi i g^2}{-\Delta_2 - \Delta_3 - i\Gamma/2}(\hat{\mathcal{E}}_+^\dagger \hat{\mathcal{E}}_+ + \hat{\mathcal{E}}_-^\dagger \hat{\mathcal{E}}_-),$$
$$\hat{f} = \frac{|\Omega_+|^2 e^{-i(\Delta k)z}}{-i\Delta_1 + \Gamma/2}\sqrt{\frac{L}{N}}\hat{\Psi}_+ + \frac{|\Omega_-|^2 e^{i(\Delta k)z}}{-i\Delta_1 + \Gamma/2}\sqrt{\frac{L}{N}}\hat{\Psi}_-.$$

Now we can solve (A.13):

$$\hat{\sigma}_{ac} = (A + \hat{\mathcal{E}})^{-1}(\dot{\hat{\sigma}}_{ac} + \hat{f}) = \frac{1}{A}\left(1 + \frac{\hat{\mathcal{E}}}{A}\right)^{-1}(\dot{\hat{\sigma}}_{ac} + \hat{f}) \approx \frac{1}{A}\dot{\hat{\sigma}}_{ac} + \left(\frac{1}{A} - \frac{\hat{\mathcal{E}}}{A^2}\right)\hat{f}$$

The above equation is to the first order (and we have neglected the higher order correction term $\hat{\mathcal{E}}\dot{\hat{\sigma}}_{ac}/A^2$). We shall also use the same equation to the zeroth order, i.e. $\hat{\sigma}_{ac} \approx \hat{f}/A$. In fact, we shall use the zeroth order equation to approximate the $\dot{\hat{\sigma}}_{ac}$ in the first order equation. Thus

$$\hat{\sigma}_{ac} \approx \frac{1}{A^2}\dot{\hat{f}} + \left(\frac{1}{A} - \frac{\hat{\mathcal{E}}}{A^2}\right)\hat{f}. \tag{A.14}$$

Assume that the classical drives have equal strength, i.e. $|\Omega_+| = |\Omega_-| = \Omega$. Also define an operator $\hat{\Phi}_\pm = \hat{\Psi}_\pm e^{\mp i(\Delta k)z}$ and a constant $B = \Omega^2/(-i\Delta_1 + \Gamma/2)$. Then $\hat{f} = B\sqrt{L/N}(\hat{\Phi}_+ + \hat{\Phi}_-)$. Using the the new definitions and (A.14) to the zeroth and first order we can rewrite (A.11) and (A.12). We insert (A.14) to first order into (A.11) and to zeroth order into (A.11) (note that $\hat{\sigma}_{cc} = \hat{\sigma}_{ca}\hat{\sigma}_{ac}$). Thus we obtain

$$\hat{\sigma}_{ab}^{\pm} = \frac{\Omega}{-i\Delta_1 + \Gamma/2}\left(i\sqrt{\frac{L}{N}}\hat{\Phi}_\pm + i\left(\frac{1}{A^2}\dot{\hat{f}} + \left(\frac{1}{A} - \frac{\hat{\mathcal{E}}}{A^2}\right)\hat{f}\right)\right)e^{\pm i(\Delta k)z},$$
$$\hat{\sigma}_{cd}^{\pm} = -\frac{i\Omega}{i\Delta_2 - \Gamma/2}\sqrt{\frac{L}{N}}\hat{\Phi}_\pm \frac{1}{A^2}\hat{f}^\dagger \hat{f} e^{\pm i(\Delta k)z}.$$

Insert these equations into (A.8) and get

$$\left(\frac{\partial}{\partial t} \pm c\,\frac{\partial}{\partial z} + i(\Delta k)\right)\hat{\Phi}_\pm = -\xi\left(\hat{\Phi}_\pm + \sqrt{\frac{N}{L}}\left(\frac{1}{A^2}\dot{\hat{f}} + \left(\frac{1}{A} - \frac{\hat{\mathcal{E}}}{A^2}\right)\hat{f}\right)\right)$$
$$- 4i\frac{N}{L}\Delta_n \hat{\Phi}_\pm \frac{1}{A^2}\hat{f}^\dagger \hat{f}$$

If we set $\Delta_3 = 0$ in the above equations (so that $A = -2B$), neglect the $i(\Delta k)$ term on the left hand side, simplify the equations and call $\hat{\Phi}_\pm$ by $\hat{\Psi}_\pm$, then we find (7.3) and (7.4).

Appendix B

NLSE for wavefunctions

First we verify that Hamiltonian (7.11) gives equation (7.6). The Heisenberg equation is

$$\begin{aligned} i\,\frac{\partial \tilde{S}(z)}{\partial t} &= -\frac{1}{\hbar}\left[\hat{H}_{\mathrm{NLSE}}, \tilde{S}(z)\right] \\ &= -\frac{1}{L}\int\left(\frac{1}{2m}\left[\tilde{S}^{\dagger}(z'), \hat{S}(z)\right]\frac{\partial^2 \tilde{S}(z')}{\partial z'^2} + \frac{\kappa}{L}\left[(\tilde{S}^{\dagger}(z'))^2, \hat{S}(z)\right](\tilde{S}(z'))^2\right)dz' \\ &= -\frac{1}{L}\int\left(\frac{1}{2m}L\delta(z-z')\frac{\partial^2 \tilde{S}(z')}{\partial z'^2} - \frac{\kappa}{L}\tilde{S}^{\dagger}(z')L\delta(z-z')(\tilde{S}(z'))^2\right)dz' \\ &= -\frac{1}{2m}\frac{\partial^2 \tilde{S}(z)}{\partial z^2} + \frac{\kappa}{L}\tilde{S}^{\dagger}(z)(\tilde{S}(z))^2 \end{aligned}$$

Now we find the equation for the coefficients (wavefunctions) ϕ and θ of the state (7.9). Using (7.12) and (7.11) we can write

$$\begin{aligned} i\,\frac{\partial}{\partial t}\,|\psi(t)\rangle =& \frac{1}{2mL}\iiint \phi(z_1, z_2, t)\tilde{S}^{\dagger}(z)\,\frac{\partial^2 \tilde{S}(z)}{\partial z^2}\,\tilde{S}^{\dagger}(z_1)\tilde{S}^{\dagger}(z_2)|0\rangle dz_1 dz_2 dz \\ &+ \frac{\kappa}{L^2}\iiint \phi(z_1, z_2, t)(\tilde{S}^{\dagger}(z))^2(\tilde{S}(z))^2\tilde{S}^{\dagger}(z_1)\tilde{S}^{\dagger}(z_2)|0\rangle dz_1 dz_2 dz \\ &+ \frac{1}{2mL}\iint \theta(z', t)\tilde{S}^{\dagger}(z)\,\frac{\partial^2 \tilde{S}(z)}{\partial z^2}\,\tilde{S}^{\dagger}(z')|0\rangle dz' dz \\ &+ \frac{\kappa}{L^2}\iint \theta(z', t)(\tilde{S}^{\dagger}(z))^2(\tilde{S}(z))^2\tilde{S}^{\dagger}(z')|0\rangle dz' dz. \end{aligned}$$

Rewriting the operators in the integrands we obtain

$$\begin{aligned}
&\tilde{S}^\dagger(z)\,\frac{\partial^2\tilde{S}(z)}{\partial z^2}\,\tilde{S}^\dagger(z_1)\tilde{S}^\dagger(z_2)|0\rangle = \tilde{S}^\dagger(z)\,\frac{\partial^2}{\partial z^2}\left[\tilde{S}(z),\tilde{S}^\dagger(z_1)\tilde{S}^\dagger(z_2)\right]|0\rangle \\
&= \tilde{S}^\dagger(z)\,\frac{\partial^2}{\partial z^2}\left(\left[\tilde{S}(z),\tilde{S}^\dagger(z_1)\right]\tilde{S}^\dagger(z_2)+\tilde{S}^\dagger(z_1)\left[\tilde{S}(z),\tilde{S}^\dagger(z_2)\right]\right)|0\rangle \\
&= \tilde{S}^\dagger(z)\,\frac{\partial^2}{\partial z^2}\left(L\delta(z-z_1)\tilde{S}^\dagger(z_2)+\tilde{S}^\dagger(z_1)L\delta(z-z_2)\right)|0\rangle
\end{aligned}$$

and

$$\begin{aligned}
&(\tilde{S}^\dagger(z))^2(\tilde{S}(z))^2\tilde{S}^\dagger(z_1)\tilde{S}^\dagger(z_2)|0\rangle = (\tilde{S}^\dagger(z))^2\left[(\tilde{S}(z))^2,\tilde{S}^\dagger(z_1)\tilde{S}^\dagger(z_2)\right]|0\rangle \\
&= (\tilde{S}^\dagger(z))^2\left(\left[(\tilde{S}(z))^2,\tilde{S}^\dagger(z_1)\right]\tilde{S}^\dagger(z_2)+\tilde{S}^\dagger(z_1)\left[(\tilde{S}(z))^2,\tilde{S}^\dagger(z_2)\right]\right)|0\rangle \\
&= 2(\tilde{S}^\dagger(z))^2\left(\tilde{S}(z)L\delta(z-z_1)\tilde{S}^\dagger(z_2)+\tilde{S}^\dagger(z_1)\tilde{S}(z)L\delta(z-z_2)\right)|0\rangle \\
&= 2(\tilde{S}^\dagger(z))^2L\delta(z-z_1)\left[\tilde{S}(z),\tilde{S}^\dagger(z_2)\right]|0\rangle = 2(\tilde{S}^\dagger(z))^2L^2\delta(z-z_1)\delta(z-z_2)|0\rangle.
\end{aligned}$$

Rewriting of the single excitation integrands is similar.

Hence

$$\begin{aligned}
i\,\frac{\partial}{\partial t}\,|\psi(t)\rangle =& \frac{1}{2m}\iint\left(\frac{\partial^2}{\partial z_1^2}+\frac{\partial^2}{\partial z_2^2}\right)\phi(z_1,z_2,t)\tilde{S}^\dagger(z_1)\tilde{S}^\dagger(z_2)|0\rangle dz_1dz_2 \\
&+2\kappa\iint\phi(z_1,z_2,t)\delta(z_1-z_2)(\tilde{S}^\dagger(z))^2|0\rangle dz_1dz_2 \\
&+\frac{1}{2m}\int\frac{\partial^2}{\partial z^2}\,\theta(z,t)\tilde{S}^\dagger(z)|0\rangle dz.
\end{aligned}$$

Taking inner products of the above and using (7.10), we obtain equations (7.13) and (7.14) in the main text.

Bibliography

[1] Gordon E. Moore. Readings in computer architecture. chapter Cramming more components onto integrated circuits, pages 56–59. Morgan Kaufmann Publishers Inc., San Francisco, CA, USA, 2000.

[2] International Technology Roadmap for Semiconductors – 2012 Overview. `http://www.itrs.net/Links/2012ITRS/2012Chapters/2012Overview.pdf`, 2012.

[3] Adam Mann. High-temperature superconductivity at 25: Still in suspense. *Nature*, 475(7356):280–2, 2011.

[4] J. Ignacio Cirac and Peter Zoller. Goals and opportunities in quantum simulation. *Nat Phys*, 8(4):264–266, Apr 2012.

[5] P.W. Shor. Algorithms for quantum computation: discrete logarithms and factoring. In *Foundations of Computer Science, 1994 Proceedings., 35th Annual Symposium on*, pages 124–134, 1994.

[6] David P. DiVincenzo. The physical implementation of quantum computation. *Fortschritte der Physik*, 48(9-11):771–783, 2000.

[7] J. I. Cirac and P. Zoller. Quantum computations with cold trapped ions. *Phys. Rev. Lett.*, 74:4091–4094, May 1995.

[8] Jeremy L. O'Brien. Optical quantum computing. *Science*, 318(5856):1567–1570, 2007.

[9] C. Monroe and J. Kim. Scaling the ion trap quantum processor. *Science*, 339(6124):1164–1169, 2013.

[10] H.-J. Briegel, W. Dür, J. I. Cirac, and P. Zoller. Quantum repeaters: The role of imperfect local operations in quantum communication. *Phys. Rev. Lett.*, 81:5932–5935, Dec 1998.

[11] W. Dreves, H. Jänsch, E. Koch, and D. Fick. Production of atomic alkali-metal beams in single hyperfine sublevels. *Phys. Rev. Lett.*, 50:1759–1762, May 1983.

[12] Nicolas Gisin, Grégoire Ribordy, Wolfgang Tittel, and Hugo Zbinden. Quantum cryptography. *Rev. Mod. Phys.*, 74:145–195, Mar 2002.

[13] Adriano Barenco, Charles H. Bennett, Richard Cleve, David P. DiVincenzo, Norman Margolus, Peter Shor, Tycho Sleator, John A. Smolin, and Harald Weinfurter. Elementary gates for quantum computation. *Phys. Rev. A*, 52:3457–3467, Nov 1995.

[14] P. Oscar Boykin, Tal Mor, Matthew Pulver, Vwani Roychowdhury, and Farrokh Vatan. On universal and fault-tolerant quantum computing. In *Proc. 40th FOCS*, pages 486–494. Society Press, 1999.

[15] Darrick E. Chang, Anders S. Sørensen, Eugene A. Demler, and Mikhail D. Lukin. A single-photon transistor using nanoscale surface plasmons. *Nat Phys*, 3(11):807–812, Nov 2007.

[16] D E Chang, L Jiang, A V Gorshkov, and H J Kimble. Cavity QED with atomic mirrors. *New Journal of Physics*, 14(6):063003, 2012.

[17] Klemens Hammerer, Anders S. Sørensen, and Eugene S. Polzik. Quantum interface between light and atomic ensembles. *Rev. Mod. Phys.*, 82:1041–1093, Apr 2010.

[18] D E Chang, A H Safavi-Naeini, M Hafezi, and O Painter. Slowing and stopping light using an optomechanical crystal array. *New Journal of Physics*, 13(2):023003, 2011.

[19] M. Fleischhauer and M. D. Lukin. Dark-state polaritons in electromagnetically induced transparency. *Phys. Rev. Lett.*, 84:5094–5097, May 2000.

[20] Jean Dalibard, Yvan Castin, and Klaus Mølmer. Wave-function approach to dissipative processes in quantum optics. *Phys. Rev. Lett.*, 68:580–583, Feb 1992.

[21] Alexey V. Gorshkov, Johannes Otterbach, Michael Fleischhauer, Thomas Pohl, and Mikhail D. Lukin. Photon-photon interactions via rydberg blockade. *Phys. Rev. Lett.*, 107:133602, Sep 2011.

[22] C. L. Hung, S. M. Meenehan, D. E. Chang, O. Painter, and H. J. Kimble. Trapped atoms in one-dimensional photonic crystals, 2013. arXiv:1301.5252.

[23] Mohammad Hafezi, Darrick E. Chang, Vladimir Gritsev, Eugene Demler, and Mikhail D. Lukin. Quantum transport of strongly interacting photons in a one-dimensional nonlinear waveguide. *Phys. Rev. A*, 85:013822, Jan 2012.

[24] David Griffiths. *Introduction to Quantum Mechanics*. 2nd edition edition, 2005.

[25] A. Goban, K. S. Choi, D. J. Alton, D. Ding, C. Lacroûte, M. Pototschnig, T. Thiele, N. P. Stern, and H. J. Kimble. Demonstration of a state-insensitive, compensated nanofiber trap, 2012. arXiv:1203.5108.